

NONIONIC SURFACTANT PERFORMANCE IN HIGH-TEMPERATURE

EAGLE FORD RESERVOIR

A Thesis

by

ELSIE BAHATI LADAN

Submitted to the Graduate and Professional School of  
Texas A&M University  
in partial fulfillment of the requirements for the degree of

MASTER OF SCIENCE

Chair of Committee, David Schechter  
Committee Members, Ibrahim Yucel Akkutlu  
Mukul Bhatia

Head of Department, Jeff Spath

December 2021

Major Subject: Petroleum Engineering

Copyright 2021 Elsie Ladan

## ABSTRACT

The focus of this study was the use of nonionic surfactants and novel nonionic-ionic surfactant blends for enhanced oil recovery in high-temperature liquid-rich unconventional reservoirs. Through cloud point, wettability, IFT, and spontaneous imbibition experiments, 23 industrial surfactants samples (individual and blends) were investigated in an effort to design surfactant systems which could withstand temperature and pressure conditions from atmospheric up to 350°F and 5000 psi.

Although surfactants have proven successful and cost-effective in enhancing production from conventional and unconventional reservoirs, studies that used nonionic surfactants have been limited to reservoirs with temperatures below 200°F due to the temperature-dependent physiochemical properties of these surfactants. Therefore, this study aims at designing surfactant blends for reservoirs like the Eagle Ford and Monterey formation in the US and the Embla field in Norway, whose reservoir temperature is above 300°F. The effectiveness of the surfactants in reducing the interfacial tension (IFT) at the oil-brine boundary and restoring contact angle (CA) to water-wet ( $\Theta < 75^\circ$ ) were the critical factors in choosing the most appropriate systems.

Results showed that the amount of ionic cosurfactant used affected thermal stability, with increasing concentration leading to increasing cloud point temperature (CPT). Wettability alteration was seen to be dependent not only on temperature but on the class of ionic cosurfactant. Cationic cosurfactants were observed to be better at improving the thermal stability of the nonionic surfactant. However, they resulted in oil-wet contact

angles with increasing temperature. On the other hand, anionic cosurfactants displayed better synergy in terms of wettability alteration, creating strongly water-wet and intermediate contact angles at high temperatures. Therefore, focus was placed on nonionic-anionic surfactant blends for the reservoir sample used in this study.

In the end, stable surfactant blends with cloud point temperatures from 316°F to 348°F were created for EOR applications in high-temperature conditions. Spontaneous imbibition studies using these blends indicated an improved recovery of up to 173%. Therefore, this work was successful in providing novel and cost-effective surfactant solutions for EOR in high-temperature conditions. This study ergo serves as a template for the surfactant screening and selection process to be undertaken when considering nonionic surfactants. And, valuable insight on the mechanisms of nonionic surfactant blends is provided to help in further design and application situations. The surfactant solutions designed for the reservoir under investigation produced tight emulsions, implying surface treatment will be required in some fields to deal with possible emulsions problems.

## DEDICATION

I dedicate this to

my loving, ever-present, ever-faithful heavenly Father for bringing this far,

my Lord Jesus for loving me,

and the gracious and kind Holy Spirit for helping me grow through this journey.

Also,

my parents, James, and Marie, for loving, teaching, and supporting me at every

stage. And finally,

the love of my life, Raymond, for never giving up on me and has chosen me above

every other.

## ACKNOWLEDGEMENTS

I would like to express my sincere appreciation to my advisor, Dr. David Schechter, for providing the opportunity to learn and conduct such engaging research. The time and resources provided were instrumental in ensuring my success.

I would like to thank the other committee members, Dr. Akkutlu and Dr. Bhatia, for their support and contribution to my learning experience.

I would also like to thank Conoco Phillips for the immense support and funding that came along with the chance to be a part of this study.

Thanks also go to the members of the research group who were supportive and encouraging friends, I.W.R. Saputra, Stefano Tagliaferri, Tobi Adebisi, Abhishek Sarmah, Isaiah Ataceri, Rohan Vijapurapu, Aashrit Bagareddy, Jingjing Zhang, Omar Abdelwahab, and Kemi Olofinnika.

Finally, thanks to my friends and colleagues and the department faculty and staff for making my time at Texas A&M University a great experience.

## CONTRIBUTORS AND FUNDING SOURCES

### **Contributors**

This work was supervised by a thesis committee consisting of Professors David Schechter and Ibrahim Yucel Akkutlu of the Department of Petroleum Engineering and Professor Mukul Bhatia of the Geology and Geophysics Department.

All work conducted for this thesis was completed by the student independently.

### **Funding Sources**

Graduate study was supported by a research assistantship from Harold Vance Department of Petroleum Engineering and Texas Engineering Experimental Station (TEES) at Texas A&M University.

Conoco Phillips funded the student through a period of this study.

## NOMENCLATURE

Bopd	Barrels of oil per day
B	Betaine
CA	Contact angle
CAP	Cocoamidopropyl
CMC	Critical Micelle Concentration
CP	Cloud point
CPT	Cloud point temperature
CT	Computed tomography
D	Days
DAC	Dimethyl Ammonium Chloride
DI	Deionized water
EIA	Energy Information Administration
EO	Ethylene oxide
EOR	Enhanced oil recovery
EUR	Estimated ultimate recovery
gpt	Gallon per thousand gallons
h	Hours
IFT	Interfacial tension
IOS	Internal Olefin Sulfonate
mN/m	Millinewton per meter

MW	Makeup water
OOIP	Original oil in place
Pc	Capillary pressure
POS	Propylene Oxide Sulphate
PW	Produced water
SASI	Surfactant assisted spontaneous imbibition
TAC	Trimethyl Ammonium Chloride
TDS	Total dissolved solids
ULR	Unconventional reservoir
wt%	Weight percent



## TABLE OF CONTENTS

	Page
ABSTRACT .....	ii
DEDICATION .....	iv
ACKNOWLEDGEMENTS .....	v
CONTRIBUTORS AND FUNDING SOURCES.....	vi
NOMENCLATURE.....	vii
TABLE OF CONTENTS .....	ix
LIST OF FIGURES.....	xi
LIST OF TABLES .....	xxi
CHAPTER I INTRODUCTION .....	1
Enhanced Oil Recovery.....	2
Chemical EOR.....	4
Scope and Objectives of Research .....	6
CHAPTER II LITERATURE REVIEW .....	8
Surfactants.....	8
Surfactant Classification.....	8
Surfactant Cloud Point .....	12
Wettability.....	24
Wettability and Interfacial Tension (IFT) .....	24
Wettability Classification .....	25
Measurement of Wettability .....	26
Mechanism of Wettability .....	33
Wettability Alteration.....	37
CHAPTER III METHODOLOGY .....	46
Materials.....	47
Rock Sample Description .....	47
Cleaning and Aging.....	48

Oil Sample.....	50
Surfactant and Brine.....	50
High-Pressure Cloud Point.....	55
Contact Angle and Interfacial Tension.....	56
High-Pressure High-Temperature Contact Angle and IFT .....	58
Spontaneous Imbibition.....	59
CHAPTER IV CLOUD POINT .....	62
Low-Pressure Test.....	62
High-Pressure Test .....	66
Effect of Ethylene Oxide Number.....	67
Effect of Ionic Surfactant .....	68
Effect of Salinity .....	73
Effect of Alcohols .....	75
CHAPTER V CONTACT ANGLE AND INTERFACIAL TENSION .....	78
Low-Pressure Tests .....	78
Contact Angle.....	78
Interfacial Tension.....	89
High-Pressure Tests.....	93
Contact Angle.....	93
Interfacial Tension.....	121
CHAPTER VI SPONTANEOUS IMBIBITION .....	127
Recovery Factor .....	127
Computerized Tomography Scan Results .....	136
Surfactant Adsorption .....	141
CHAPTER VII CONCLUSIONS .....	147
Cloud Point.....	147
Contact Angle and IFT .....	148
Spontaneous Imbibition.....	149
Recommendations .....	150
REFERENCES .....	152

## LIST OF FIGURES

	Page
Figure 1: Summary of enhanced oil recovery techniques. ....	3
Figure 2: Illustration of fluid distribution based on influence of pore walls leading to nanoconfinement effects (Akkutlu 2019) .....	6
Figure 3: Surfactant chemical structure. Image culled from Wikipedia. ....	8
Figure 4: Surfactant classification. ....	9
Figure 5: Increasing salinity shown to result in decrease in cloud point of nonionic surfactant. Where salinity is fixed, increasing surfactant concentration also results in lower cloud point temperature. (Curbelo, 2013). ....	15
Figure 6: Effect of ionic surfactant on cloud point of nonionic surfactant Triton X-100. Increasing ionic surfactant ratio results in improved cloud point. (Sadaghiana and Khan, 1990).....	17
Figure 7: Surface tension as a function of surfactant concentration. Increasing surfactant concentration reduces interfacial tension up to the CMC. Beyond CMC, surfactant molecules form micelles and IFT remains constant. Culled from Dataphysics-instruments. ....	20
Figure 8: Illustration of micelle formation. Surfactant molecules orient at interface (left), with increased concentration, molecules aggregate to form micelles with tailgroups interacting with the apolar phase (right). ....	21
Figure 9: Schematic diagram of adsorption mechanism of (a) cationic surfactant on clean quartz, (b) anionic surfactant on quartz, (c) cationic surfactant on quartz (double layer formation), d) anionic surfactant on calcite, e) cationic surfactant on calcite, and f) anionic surfactant on calcite (Zhou et al., 2016)..	23
Figure 10: Illustration of contact angle in a rock-oil-brine system .....	24
Figure 11: Illustration of a sessile drop (Lee and Zhao, 2015) .....	29
Figure 12: Illustration of the interface between oil and water due to wettability preference of the tube wall (Glover, 2002). ....	32
Figure 13: Illustration of water-wet rock and interactions influencing its activity. Left: Wettability of the rock surface influenced by the interaction between the brine/oil and the brine/rock. Increase and stability in brine film thickness (h)	

leads to water-wet surface. Right: Attractive interactions result in decrease in brine film thickness and create oil-wet clay surface. (Myint and Firoozabadi, 2015) .....	34
Figure 14: The (a) initial configuration and (b) equilibrium configuration of (I) decane-water (II) methyl benzene-water (III) pyridine-water (IV) acetic acid-water on silica surface. Polar compounds pyridine and acetic acid penetrate through the water film and adsorb onto the silica surface while apolar components (methyl benzene and decane) do not. (Zhong et al., 2013).....	35
Figure 15: Density distribution of different oil components. Peaks of polar molecules..	37
Figure 16: Change in air-water contact angle with varying mineralogy, (Borysenko et al. 2009) .....	45
Figure 17: Flow chart explaining systematic workflow of the study. ....	46
Figure 18: Mineral composition of Eagle Ford rock sample .....	48
Figure 19: Aging study data showing contact angles measured in formation brine at 170°F. CAs show shift towards oil-wet with increasing aging time.....	49
Figure 20: Aging study data showing contact angles measured in DI water at 170°F. CAs show shift towards oil-wet with increasing aging time. ....	50
Figure 21: Ion concentration of the makeup and produced water with TDS of 0.18% and 2.5% respectively. ....	54
Figure 22: Image showing change in turbidity noted after variation of bicarbonate concentration.....	54
Figure 23: Setup for high-pressure cloud point measurement. ....	56
Figure 24: Setup for contact angle measurement on the Dataphysics OCA 15 Pro.....	57
Figure 25: Setup for interfacial tension measurement on the Dataphysics OCA 15 Pro. ....	58
Figure 26: Setup for the high-pressure high-temperature study on the Biolin Theta Flex. ....	59
Figure 27: Setup for spontaneous imbibition experiment. ....	61
Figure 28: Cloud points of various samples of nonionic surfactant. The increment in CPT occurs with an increase in EO groups. (N1, N2, N3 < 30 EOs ≥N5, N6, N9, N11) Note: concentration of surfactant was 0.4 wt% .....	63

Figure 29: Image of surfactant samples during cloud point tests at low-pressure conditions before heating (left) and above the cloud point (right). .....	64
Figure 30: Cloud point of single surfactant N2 (left) and blends containing anionic, cationic, and zwitterionic surfactants. Note: Main surfactant N2 is at a concentration of 0.2 wt%, and ionic surfactants at a concentration of 0.02 wt%. .....	65
Figure 31: Cloud point of surfactant blends showing increase in CPT with increasing co-surfactant concentration. For ternary mixture, change in CPT is between those observed with single ionic co- surfactant. Main surfactant, N2 at concentration of 0.2 wt%. Aqueous phase used produced water. ....	66
Figure 32: Effect of EO number on cloud point. Single surfactants (X, Y, Z) display lower CPT compared to mixtures containing ionic co-surfactant. Note: Nonionic surfactant used is at 0.2 wt% and stabilizing ionic surfactant C1 is at 0.02 wt%. .....	68
Figure 33: Cloud point temperature of nonionic surfactants N4, N8, and N12 at a concentration of 0.2 wt% and ionic stabilizer C1 at 0.1wt%. Increasing the concentration of ionic co-surfactant leads to varying increments on the CPT for the different classes of nonionic surfactant with similar number of EOs. ...	69
Figure 34: Cloud point temperature recorded during heating of solutions containing ionic stabilizers at varying concentrations. Increasing hydrophobicity and concentration of the ionic stabilizers leads to improved CPT. Note: Nonionic surfactant used N4 at a concentration of 0.2 wt%. ....	70
Figure 35: Cloud point temperature recorded during cooling of solutions containing ionic stabilizers at varying concentrations. Anionic surfactants are observed to remain turbid during cooling. Note: Nonionic surfactant used N4 at a concentration of 0.2 wt%. ....	70
Figure 36: Improvement in cloud point temperature of ternary surfactant blends compared to binary blends (grey). Increment in CPT is higher with the introduction of co-surfactant A2 compared to Z1. Note: Nonionic surfactant used N4 at a concentration of 0.2 wt%, ionic-cosurfactants, A1, A2, A4 and Z1 at concentration of 0.1 wt%. .....	72
Figure 37: Effect of salinity on cloud point temperature. For nonionic surfactant N,4 with no ionic co-surfactant to serve as thermal stabilizer, and surfactant systems with C1 and A3 as co-surfactant, increasing brine salinity leads to decrease in CPT. With exception of FF:2.4% in the mixed surfactant system which performs better than the DI case. Note: Main surfactant used N4 (0.2 wt%). .....	74

Figure 38: Laptop view during cloud point experiment on the Trombone for solution with methanol. The photos show at 399°F on the RHS the solution shows slight change in turbidity compared to the clear solution on the LHS, i.e., turbidity is not distinct during heating.....	76
Figure 39: Change in cloud point temperature (heating) due to addition of methanol. Data is grouped based on co-surfactant and shows better improvement with the more hydrophobic stabilizer A4. Note Main surfactant used N4 (0.2 wt%), ionic surfactant (0.2 wt%).....	76
Figure 40: Change in cloud point temperature (heating) due to addition of isopropanol. Data is grouped based on co-surfactant and it shows increase in CPT with increasing concentration of isopropanol. Note Main surfactant used N4 (0.2 wt%), ionic surfactant (0.2 wt%).....	77
Figure 41: Oil droplets deposited on rock-chips from varying depths of the Eagle Ford a. before aging and b. at the 7-week mark of the aging process.....	79
Figure 42: Contact angle measurements on aged rock-chips (base case) using single surfactants to prove wettability alteration potential of nonionic surfactants. Note: concentration of surfactant used was 0.2 wt%.....	80
Figure 43: Effect of cosurfactant as thermal stabilizer C1 on the contact angle of S2 chips measured at 170°F. Note: Base represents the contact angle after the aging 125.3° (oil-wet). Numbers 1 to 7 represent the sequence in the bar chart. CA decrease significantly in the presence of nonionic surfactant and increases when cationic-co-surfactant C1 is included.....	82
Figure 44: Effect of cosurfactant as thermal stabilizer C3 on the contact angle of S2 chips measured at 170°F. Note: Base represents the contact angle after the aging 125.3° (oil-wet). Numbers 1 to 6 represent the sequence in the bar chart. ....	84
Figure 45: Effect of cosurfactant as thermal stabilizer A3 on contact angles measured on S2 chips at 170°F. Note: Base represents the contact angle after the aging 125.3° (oil-wet). Numbers 1 to 5 represent the sequence in the bar chart. Surfactant blends with anionic co-surfactant A3 produced water-wet CAs.....	84
Figure 46: Wettability alteration by surfactant N4 (0.2wt%) as single surfactant and in combination with thermal stabilizers on rock chips from S2. No clear trend in CA was observed for the mixed surfactants at room conditions. Note: temperature is 70°F.....	86
Figure 47: Wettability alteration by surfactant N4 (0.2wt%) as single surfactant and in combination with thermal stabilizers on rock chips from S2. Cationic co-	

surfactants perform poorly when compared to anionic and zwitterionic at low concentrations at elevated temperature. Note temperature is 170°F.....	87
Figure 48: Wettability alteration of binary surfactant blend N4 (0.2 wt%) and ionic cosurfactant (0.2 wt%) in aqueous solution containing isopropanol as cosolvent. Increasing concentration of co-solvent increase CA which is more prominent in co-surfactant system with A1.....	88
Figure 49: Images showing wettability alteration of binary surfactant blend N4 (0.2 wt%) and ionic cosurfactant (0.2 wt%) in aqueous solution containing isopropanol as cosolvent.....	89
Figure 50: IFT of main surfactant N4 at concentrations of 0.1, 0.2 and 0.4 wt% at atmospheric pressure and with increasing temperature. Higher IFT is observed at room temperature with higher surfactant concentration, however, IFT declines with increasing temperature to result in similar IFT at 170°F.....	90
Figure 51: Images of oil drop in surfactant solution N4 at 0.1 wt%, 0.2 wt%, and 0.4 wt%.....	91
Figure 52: Interfacial tension of surfactant blends containing N4 (0.2wt%) as a single surfactant and in combination with thermal stabilizers at 70°F at atmospheric pressure. Presence of ionic co-surfactant leads to decrease in IFT, with increasing concentration generally leading to further reduction. ....	92
Figure 53: Interfacial tension of surfactant blends containing N4 (0.2wt%) as a single surfactant and in combination with thermal stabilizers at 170°F at atmospheric pressure. ....	93
Figure 54: Contact angle data from HPT on aged rock sample. (a) Increasing temperature, (b) increasing and decreasing pressure, do not alter wettability in the absence of surfactant. Note: Aqueous phase was produced water with no surfactant.....	95
Figure 55: Images of the oil drop on aged rock chip in the presence of produced water with no surfactant. Note: wettability remained constant on the strongly oil-wet surface.....	95
Figure 56: Influence on wettability alteration of changing main surfactant (N4) concentration from 0.2 wt% to 0.4 wt% to 0.8 wt%. Increasing ratio of nonionic concentration creates stronger water-wet CAs. Note: Thermal stabilizer used is cationic sample C3 at 0.1 wt%.....	96

Figure 57: Plot of contact angle against temperature for binary surfactant N4 (0.2 wt%) and cationic thermal stabilizer C1 (0.1 wt%). CA remains water-wet at temperature below 212°F.....	98
Figure 58: Images showing wettability observed with binary surfactant N4 (0.2 wt%) and cationic thermal stabilizer C1 (0.1 wt%). .....	99
Figure 59: Images of the rock surface at the start of experiment(left) and at the end (right) in N4 (0.4 wt%) + C3 (0.2 wt%) showing degradation of the rock surface.....	99
Figure 60: Plot of contact angle against temperature for binary surfactant N4 (0.2 wt%) and anionic thermal stabilizer A3 (0.1 wt%). Main surfactant causes a decrease in solubility with increasing temperature which forces the surfactant to the interface and improves wettability.....	100
Figure 61: Images showing wettability alteration observed with binary surfactant N4 (0.2 wt%) and anionic thermal stabilizer A3 (0.1 wt%).....	101
Figure 62: Plot of contact angle against temperature for binary surfactant N4 (0.2 wt%) and zwitterionic thermal stabilizer Z1 (0.1 wt%).....	102
Figure 63: Images showing wettability alteration observed with binary surfactant N4 (0.2 wt%) and amphoteric thermal stabilizer Z1 (0.1 wt%).....	102
Figure 64: Influence on wettability alteration of increasing concentration of thermal stabilizer. Increasing ratio of co-surfactant to create 1:1 Surfactant blends leads improved CPT and very water-wet CAs for mixture with A1. Shift to intermediate CAs for the combination with Z1. While the mixture with A2 displays a more erratic trend decreasing CAs followed by a sharp increase. Note: Main surfactant used is N4 at 0.2 wt%.....	103
Figure 65: Contact angle hysteresis observed for surfactant N4+A1 (1:1) as temperature is lowered at constant pressure. ....	105
Figure 66: Images of oil drop on aged rock surface: a) Increasing temperature and pressuring during heating. b) Decreasing temperature and constant pressure during cooling for N4+A1 (2:1). ....	107
Figure 67: Contact angle hysteresis observed for surfactant N4+Z1 (1:1) as temperature is lowered at constant pressure. ....	108
Figure 68: Images of oil drop on aged rock surface: a) Increasing temperature and pressuring during heating. b) Decreasing temperature and constant pressure during cooling, for surfactant N4+Z1 (1:1). ....	109



Figure 69: Plot of contact angle against temperature showing wettability alteration for surfactant N4+A4 (1:1) total surfactant concentration of 0.2 wt% in solution with 5 wt% isopropanol. ....	110
Figure 70: Images of an oil drop on aged rock surface showing contact angle with increasing temperature and pressuring during heating for surfactant N4+A4 (1:1) total surfactant concentration of 0.2 wt% in solution with 5 wt% isopropanol. ....	111
Figure 71: Plot of contact angle against temperature showing wettability alteration for surfactant N4+A1 (1:1) total surfactant concentration of 0.2 wt% in solution with 5 wt% isopropanol. ....	112
Figure 72: Images of an oil drop on aged rock surface: a) Increasing temperature and pressuring during heating. b) Decreasing temperature and constant pressure during cooling; for surfactant N4+A1 (1:1) with total surfactant concentration of 0.2 wt% in solution with 5 wt% isopropanol. ....	113
Figure 73: Plot of contact angle against temperature showing wettability alteration for surfactant N4+A1 (1:1) with total surfactant concentration of 0.4 wt% in solution with 5 wt% isopropanol. ....	114
Figure 74: Images of an oil drop on aged rock surface: a) Increasing temperature and pressure during heating. b) Decreasing temperature and constant pressure during cooling; for surfactant N4+A1 (1:1) with total surfactant concentration of 0.4 wt% in solution with 5 wt% isopropanol. ....	115
Figure 75: Plot of contact angle against temperature showing wettability alteration for surfactant N4+A4 (1:1) with total surfactant concentration of 0.4 wt% in solution with 5 wt% isopropanol. ....	116
Figure 76: Images of an oil drop on aged rock surface: a) Increasing temperature and pressure during heating. b) Decreasing temperature and constant pressure during cooling; alteration for surfactant N4+A4 (1:1) with total surfactant concentration of 0.4 wt% in solution with 5 wt% isopropanol.....	117
Figure 77: Wettability alteration with surfactant N4 and two ionic thermal stabilizers. Note: Total surfactant concentration 0.4 wt%. ....	118
Figure 78: Images showing a change in contact angle of an oil drop on aged rock in ternary surfactant blend containing N4:A4:A3 (2:1:1). Note: Total surfactant concentration is 0.4 wt%.....	119
Figure 79: Wettability alteration using ternary blend N4+A4+A2 varying anionic surfactant ratios from 1:1 to 3:1.....	120

Figure 80: IFT Eagle Ford oil in make-up water with no surfactant.....	121
Figure 81: Interfacial tension of N4+A1 surfactant blends under high-pressure high temperature conditions. Note: IFT observed to decrease and then increase with increasing temperature and pressure.....	122
Figure 82: Interfacial tension of N4+A4 surfactant blends under high-pressure high temperature conditions. Note: IFT observed to decrease and then increase with increasing temperature and pressure.....	123
Figure 83: Interfacial tension of ternary surfactant blend: N4(0.1)+A1(0.2).....	123
Figure 84: Interfacial tension of ternary surfactant blend: N4(0.2)+A1(0.2).....	124
Figure 85: Images of oil drops during IFT experiment using surfactant blends of N4 and A1 in ratio 1:1 showing a decrease in IFT followed by an increase. ....	124
Figure 86: Interfacial tension of ternary surfactant blend: N4(0.1) + A1(0.05) + A2(0.05).....	125
Figure 87: Interfacial tension of ternary surfactant blend: N4(0.2)+A1(0.1)+A2(0.1)..	125
Figure 88: Images of oil drops during IFT experiment using surfactant blends of N4 and A2 in ratio 1:1 showing a decrease in IFT followed by an increase. ....	126
Figure 89: Oil recovery factor for novel nonionic systems developed. ....	128
Figure 90: Images showing recovery (left) and effluent from HPHT Imbibition cell (right) using surfactant N4+A1.....	130
Figure 91: Wax produced during HPHT SASI experiment with surfactant system N4(0.1)+A1(0.05)+A2(0.05). ....	130
Figure 92: Wax produced during HPHT SASI experiment with surfactant system N4(0.2)+A4(0.1)+A2(0.1). ....	131
Figure 93: Correlation between contact angle and recovery factor. ....	133
Figure 94: Correlation between interfacial tension and recovery factor. ....	133
Figure 95: Correlation between capillary pressure and recovery factor. ....	134
Figure 96: Images of surfactant solutions collected during the life cycle of the HPHT SASI study. From left to right: 1. Fresh surfactant sample, 2. Effluent from imbibition cell, and 3. Sample recovered from accumulator (after heating). Surfactant: a. N4+A2 (0.4 wt%), b. N4+A1+A2 (0.2 wt%), c. N4+A1+A2	

(0.4 wt%), d. N4+A4+A2 (0.2 wt%), e. N4+A4+A2 (0.4 wt%), f. N4+A1+A2 (4:3:1, 0.4 wt%).	135
Figure 97: CT images of core plug which imbibed surfactant N4(0.2)+A1(0.2). Post-imbibition CT numbers are lower, implying higher oil saturation which is unlikely.	137
Figure 98: CT images of core plug which imbibed surfactant N4(0.1)+A1(0.05)+A2(0.05). Post-imbibition CT numbers are lower, implying higher oil saturation which is unlikely.	137
Figure 99: CT images of core plug which imbibed surfactant N4(0.1)+A4(0.05)+A2(0.05). Post-imbibition CT numbers are higher, implying increased water saturation.	138
Figure 100: CT images of core plug which imbibed surfactant N4(0.2)+A1(0.1)+A2(0.1). Post-imbibition CT numbers were lower in a few regions, implying increased water saturation.	138
Figure 101: CT images of core plug which imbibed surfactant N4(0.2)+A4(0.1)+A2(0.1). Post-imbibition CT numbers are lower, implying increased oil saturation.	139
Figure 102: CT images of core plug which imbibed surfactant N4(0.2)+A2(0.15)+A2(0.05). Post-imbibition CT numbers appear similar indication little oil saturation.	139
Figure 103: Correlation between average CT number difference and recovery factor.	140
Figure 104: Surfactant adsorption curves showing interfacial tension of effluent compared to surfactant concentrations not in contact with core plug. Note: surfactant system N4+A1 (1:1) in aqueous solution of 0.2 TDS.	143
Figure 105: Surfactant adsorption curves showing interfacial tension of the effluents from the surfactants with total wt% of 0.2 and 0.4, compared to surfactant concentrations not in contact with core plug. Note: surfactant system N4+A1+A2 (2:1:1) in aqueous solution of 0.2 TDS.	144
Figure 106: Surfactant adsorption curves showing interfacial tension of the effluents from the surfactants with total wt% of 0.2 and 0.4, compared to surfactant concentrations not in contact with core plug. Note: surfactant system N4+A4+A2 (2:1:1) in aqueous solution of 0.2 TDS.	145
Figure 107: Surfactant adsorption curves showing interfacial tension of the effluents from the surfactants with total wt% of 0.4 compared to surfactant	

concentrations not in contact with core plug. Note: surfactant system  
N4+A1+A2 (4:3:1) in aqueous solution of 0.2 TDS. .... 146

## LIST OF TABLES

	Page
Table 1: Types of nonionic surfactant.....	11
Table 2: Eagle Ford SARA composition.....	50
Table 3: Molecular structure of surfactants tested in the study.....	51
Table 4: Effect of surfactant ratio on cloud point temperature for ternary surfactant blends.....	104
Table 5: Summary of spontaneous imbibition experiments showing recovery factors and improvement in recovery compared to the base case. ....	131
Table 6: Estimated capillary pressure at 320°F.....	132
Table 7: Average CT numbers for each core sample. ....	140

## CHAPTER I

### INTRODUCTION

As the demand for energy increases so does the search for new reserves. This search drives exploration farther and deeper, resulting in increasing exploration costs, added job complexity, and the demand for better technology. These, in addition to the low oil prices, are a few reasons technology that can improve or enhance the life of mature fields has gained popularity in recent times.

The EIA estimates that 65% of oil production in the United States, 2.67 billion barrels (approximately 7.31 million barrels per day) of crude oil were produced directly from tight oil resources in 2020. A large amount of the estimated production came from Shale reservoirs which are known for their low porosity, ultra-low permeability, and low recovery factors. For these resources to be effective, enhanced oil recovery methods must be deployed. Gas injection has been used in several shale reservoirs with some success; however, the use of surfactants has been identified as another cost-effective method of improving oil recovery in resource shales.

The addition of surfactant in completion fluids has gained in popularity, with the belief that it improves on both initial production and ultimate oil recovery (EUR) by changing the capillary forces within the reservoir and altering wettability which ultimately results in better productivity via surfactant-assisted spontaneous imbibition (SASI). Although surfactant molecules are sensitive to temperature and pressure, there has been little work done at temperatures above 200°F to prove the efficiency of this EOR

technique. This work aims to explore the use of nonionic surfactants to enhance oil recovery from shales at high temperatures between 170°F up to 320°F.

### **Enhanced Oil Recovery**

In conventional reservoirs, oil recovery has typically been divided into three main stages, primary, secondary, and tertiary recovery. Primary recovery referring to the production of the reservoir by its internal energy (gas or liquid expansion, water influx from an aquifer), while secondary recovery involves techniques that supplement original reservoir energy (water or gas injection)

Tertiary recovery, also known as Enhanced recovery, is defined as additional recovery obtained from a petroleum reservoir that could not be obtained via traditional primary or secondary methods (Haynes et al., 1967). EOR is more concerned with affecting the mobility of the oil and can result in 30 - 60% of more of the reservoir's original oil being extracted, compared to just 20 - 40% using primary or secondary recovery methods. Mobility of the oil is influenced by two major factors: Capillary Number and Mobility Ratio. Capillary Number is defined as  $N_c = v\mu/\sigma$ , where  $v$  is the Darcy velocity (m/s),  $\mu$  is the displacing fluid viscosity (Pa.s), and  $\sigma$  is the interfacial tension (N/m). Mobility ratio is defined as  $M = \lambda_{ing}/\lambda_{ed}$ , where  $\lambda_{ing}$  is the mobility of the displacing fluid (e.g., water), and  $\lambda_{ed}$  is the mobility of the displaced fluid (oil). ( $\lambda = k/\mu$ , where  $k$  is the effective permeability, (m<sup>2</sup>) and  $\mu$  is the viscosity (Pa.s) of the fluid concerned).

The primary techniques of EOR include gas injection, thermal injection, and chemical injection, as seen in Figure 1. It is important to note that the selection of an EOR technique is dependent on the price of oil, as the price must exceed the cost of the injecting plus operating costs by a sizeable margin for an EOR process to be considered economical (Masoud 2015).

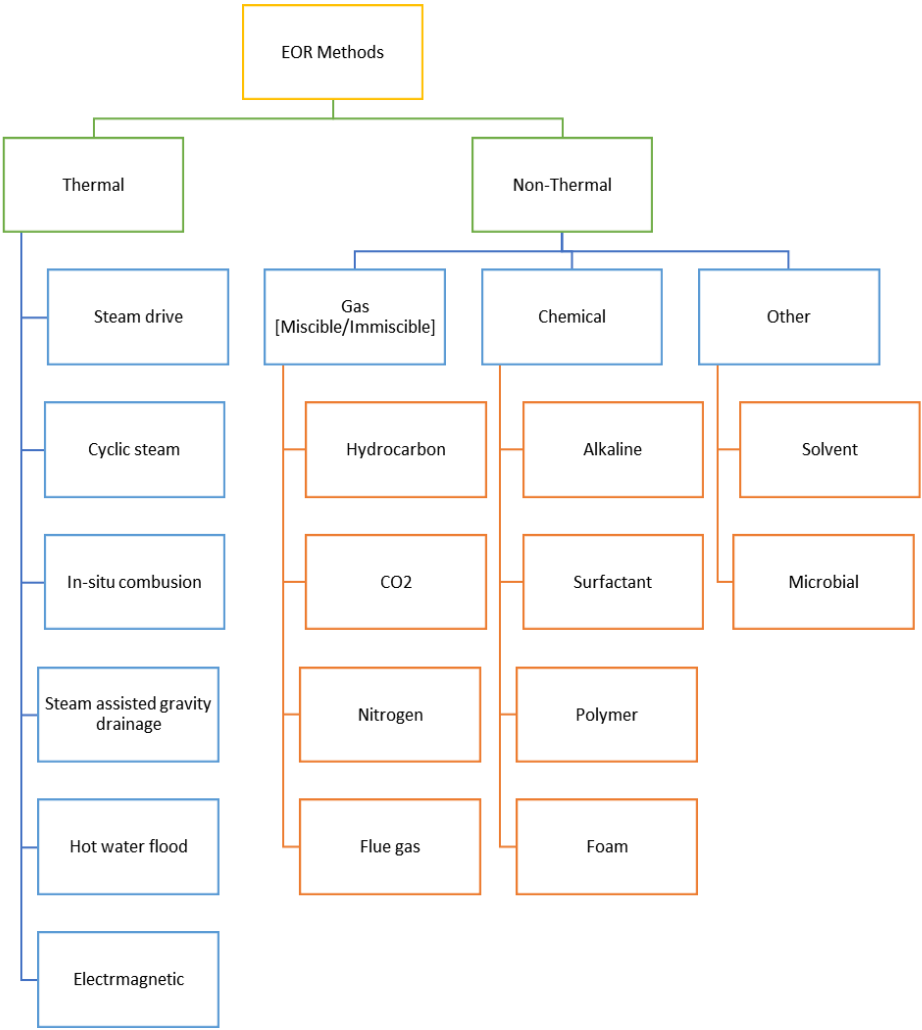


**Figure 1: Summary of enhanced oil recovery techniques.**



## **Chemical EOR**

Among the various EOR techniques, chemical EOR has been adjudged as the most promising because of its higher efficiency, technical and economic feasibility, and reasonable capital cost (Gbadamosi et al., 2019). Chemical EOR methods increase oil recovery by increasing the effectiveness of water injected into the reservoir to displace the oil. The chemical formulation deployed is tailored to decrease the mobility ratio and/or increase the capillary number.

Decreasing mobility is possible where polymers are deployed; the high molecular weight water-soluble polymers increase the injectant's viscosity. The incremental viscosity of the injectant improves the mobility and conformance control of the injected slug. Increasing the capillary number can be achieved by reducing IFT, which can be achieved using a suitable surfactant.

The use of surfactants generally improves oil recovery by altering the fluid/fluid interaction by reducing IFT between the oil and brine, and fluid/rock properties via wettability alteration of the porous medium. Where IFT between the crude and water is high, the oil forms large spherical globules which possess cross-sectional areas that make flow through the pore throats extremely difficult. A decrease in IFT reduces the differential pressure, which allows distortion of the oil drop, resulting in a subsequent decrease in capillary pressure, then allowing the flow of the oil through the pore throats (Wilson et al., 2019, Sheng 2013). In conventional reservoirs, the surfactants' ability to lower- water-oil interfacial tension, which reduces residual oil saturation, is captured by

the capillary number ( $N_c = \frac{u \mu}{\sigma}$

Equation 1).

$$N_c = \frac{u \mu}{\sigma}$$

**Equation 1**

Where  $\mu$  is the displacing fluid,  $u$  is the displacing Darcy velocity, and  $\sigma$  is the interfacial tension between the displacing fluid and the displaced fluid (oil). The decrease in IFT can increase the capillary number by up to 1000 times as IFT between brine and oil reduces from 20 - 30 mN/m to  $10^{-3}$  mN/m (Sheng 2015).

In comparison, in unconventional reservoirs the reduction in IFT to ultra-low values is often insufficient to dislodge oil drops from the nanoporous shale reservoir which is known to exhibit nanoconfinement effects. Nanoconfinement is the existence of compositional variability observed in the lower end of the pore size distribution; heavier oil components are located near the pore walls where they are preferentially adsorbed while molecules like methane are located towards the center of the pore where they exist as free fluid in the bulk phase.

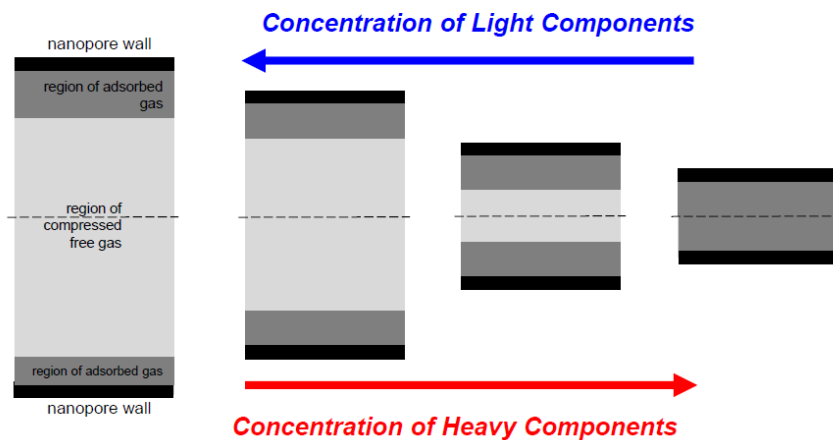


**Figure 2: Illustration of fluid distribution based on influence of pore walls leading to nanoconfinement effects (Akkutlu 2019)**

With these forces on a molecular scale alongside the presence of organic matter (kerogen) a system of organic and inorganic pores exists within shale, filled with moveable hydrocarbon. For these oil-wet shale reservoirs, the oil is trapped in the smaller pores while the brine is located in the larger pores. This distribution means the injected fluid must overcome negative capillary pressure to invade the matrix and displace oil. Wettability alteration with the aid of surfactant shifts the capillary pressure to positive, allowing spontaneous imbibition of the aqueous solution into the matrix, promoting oil recovery (Singh 2020).

### **Scope and Objectives of Research**

The scope of this study is to investigate the potential use of nonionic surfactants in ULR of high-temperature to improve fracturing treatments. Given that no one surfactant is designed for all EOR applications, this study was performed using samples from a specific window of the Eagle Ford. The specific objectives include:

- Restore reservoir rock samples to reservoir wettability and determine its impact on oil recovery.
- Determine what surfactants are suitable for high-temperature reservoirs by conducting high-pressure cloud point studies to identify thermal stability limits.
- Evaluation of different surfactants' ability to alter the wettability and IFT in oil shale cores by conducting contact angle and IFT measurement experiments at reservoir conditions.

- Analysis of the impact of wettability and IFT alteration on recovery of hydrocarbons from ULR cores via spontaneous imbibition experiments.
- Study the relation and trade-off between wettability alteration and IFT and determine the more influential factor for higher oil recovery factor.
- Provide recommendations for the screening of surfactants for high-temperature reservoirs.

CHAPTER II  
LITERATURE REVIEW

**Surfactants**

The word surfactant is short for surface-active agent; it refers to an amphiphilic organic compound with a chemical structure composed of two parts, a hydrophilic group, and a hydrophobic group. The hydrophile exhibiting a strong affinity for polar solvents, particularly water, forms the 'head'. The 'tail' is made of the hydrophobe or lipophile, which is apolar.

Because of its amphiphilic nature, the surfactant molecule migrates to an interface where it orients with the polar group lying in water, and the apolar group out of it. This reorientation reduces the surface tension between a solid and a liquid or the interfacial tension between two liquids.

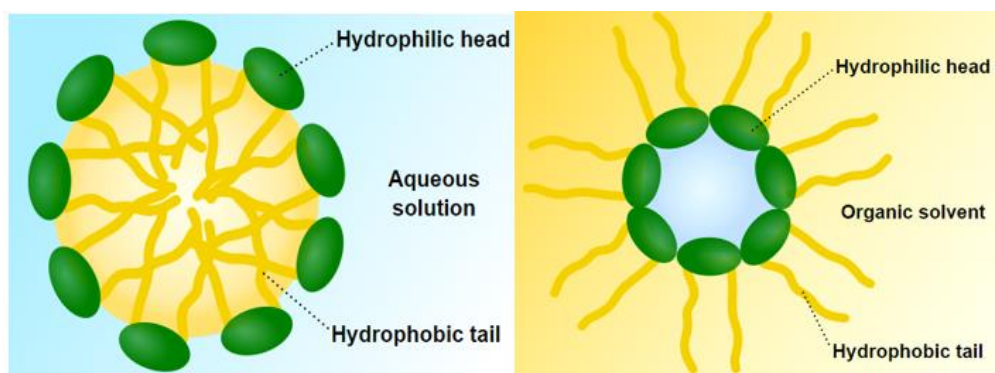


**Figure 3: Surfactant chemical structure. Image culled from Wikipedia.**

**Surfactant Classification**

Surfactants are classified based on the ionic nature of the head group; anionic, cationic, nonionic, and zwitterionic (or amphoteric). Ionic surfactants possess a head

group that carries a charge, negative for the anionic and positive for the cationic. Non-ionic surfactants carry no charged group, and Zwitterionic carry both positive and negative charges in the head group. Based on the charges carried by the head group, the surfactant interaction with a surface and its efficiency in promoting oil recovery vary as adsorption at the interface occurs.

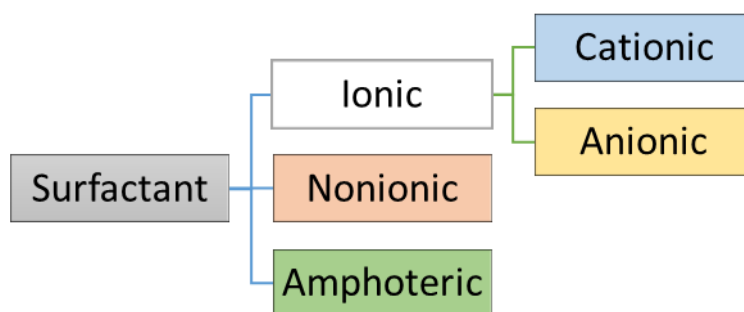


**Figure 4: Surfactant classification.**

### **Anionic Surfactant**

Anionic surfactants are the most used surfactants, accounting for about 50% of the world production (Salager 2002). In solution, they dissociated in water in an amphiphilic anion and a cation, which is, in general, an alkaline metal ( $\text{Na}^+$ ,  $\text{K}^+$ ) or a quaternary ammonium. This class includes alkylbenzene sulfonates (detergents), (fatty acid) soaps, lauryl sulfate (foaming agent), di-alkyl sulfosuccinate (wetting agent), lignosulfonates (dispersants) etc. Anionic surfactants are known to be high and stable foaming agents; however, they do have the disadvantage of being sensitive to the presence of minerals in water (water hardness) or pH changes. It is observed that an increase in calcium and magnesium molecules in the water results in the deactivation of the anionic surfactant

system. To prevent this, the anionic surfactants need help from other ingredients such as builders (Ca/Mg sequestrants), and more detergent should be dosed in hard water.

### **Cationic Surfactant**

Cationic surfactants dissociate in water into an amphiphilic cation and an anion, most often of the halogen type. These surfactants are, in general, more expensive than anionic surfactants because of the high-pressure hydrogenation reaction required during their synthesis. Cationic surfactants are often of great commercial importance, such as in corrosion inhibition, bactericides, and anti-fungal. In laundry detergents, cationic surfactants improve the packing of anionic surfactant molecules at the stain/water interface. This helps to reduce the dirt/water interfacial tension in a very efficient way, leading to a more robust dirt removal system. While in disinfectant and sanitizing fluids they disrupt cell membranes of bacteria and viruses.

### **Amphoteric Surfactant**

These surfactants exhibit anionic, cationic, or nonionic dissociations depending on the acidity or pH of the water. The anionic part can be sulfonates, such as in the sultaines CHAPS (3-[(3-Cholamidopropyl)dimethylammonio]-1-propanesulfonate), or betaines such as cocamidopropyl betaine. The cationic part is made of primary, secondary, or tertiary amines or quaternary ammonium cations. Zwitterionic surfactants are mild, making them suited for use in personal care and household cleaning products. However, because these surfactants are expensive, their use is typically limited. Examples of

amphoteric/zwitterionic surfactants include alkyl betaine, sulfobetaines, and natural substances such as amino acids and phospholipids.

### **Nonionic Surfactant**

Nonionic surfactants are the second most used surfactants, with about 45% of the overall industrial production. They do not ionize in an aqueous solution because their hydrophilic group is of a non-dissociable type, such as alcohol, phenol, ether, ester, or amide. While some nonionic surfactants, polyethoxylated nonionic, become hydrophilic via polycondensation of ethylene oxide to form polyethylene glycol chains. Typically, the lipophilic group of the nonionic surfactant consists of the alkyl or alkylbenzene type, which comes from naturally occurring fatty acids.

Depending on the head group, this surfactant can be classified into different groups.

**Table 1: Types of nonionic surfactant**

<b>Surfactant Type</b>	<b>Total (%)</b>
Ethoxylated Linear Alcohols	40
Ethoxylated Alkyl Phenols	15
Fatty Acid Esters	20
Amine and Amide Derivatives	10
Alkylpolyglucosides	-
Ethyleneoxide/Propyleneoxide Copolymers	-
Polyalcolols and ethoxylated polyalcohols	-



Thiols (mercaptans) and derivatives	-
-------------------------------------	---

### **Surfactant Cloud Point**

Surfactant solubility is a reflection of the surfactant's activity in brine and affects its imbibition into the reservoir matrix (Mirchi 2017). Solubility of nonionic surfactants, which is a result of hydrogen bonds, is strongly dependent on temperature and can impact interfacial properties. Cloud point is the temperature above which surfactant loses sufficient water solubility, creating a cloudy dispersion, with phase separation into a surfactant rich phase and a brine rich phase. With increasing temperature, the degree of hydration of the hydrophilic portion is insufficient to solubilize the remaining hydrocarbon portion (Sharma 2003). The cloud point is an essential factor to consider when choosing to deploy nonionic surfactants because, above the cloud point, the surfactant ceases to perform some or all its normal detergency, wettability, and IFT alteration functions (Huibers et al., 1997).

### **Factors Affecting Cloud Point**

Studies have shown that the cloud point is dependent on factors including surfactant molecular structure, concentration, presence of additives.

#### *Surfactant Structure*

The cloud point temperature is highly dependent on the hydrophobic and hydrophilic arrangement of a surfactant. This is mostly because the physical

characteristics of surfactant molecules and rock properties vary as the temperature and pressure conditions of a system are altered.

Gu and Sjoblom (1992) demonstrated a linear relationship between the cloud point and the logarithm of ethylene oxide number for alkyl ethoxylates, alkyl phenyl ethoxylates and methyl capped alkyl ethoxylates esters, as well as a linear relationship between the cloud point and alkyl carbon number. They found that although a higher percentage of oxyethylene led to higher cloud points, the relationship between polyoxyethylene (POE) percentage and CP is not linear (Sharma 2003).

Mirchi (2017) noted that surfactants with EO values between 2.5 and 3 form turbid solutions at ambient conditions due to the short polar heads, limiting dissolution in water. It was observed during the study that by sequentially lengthening the PEO chain, the cloud point for different alkyl chains was successfully increased. In contrast, increasing the alkyl chain length slightly reduced the CP.

### *Additives*

#### *a. Ions*

The cloud point of non-ionic surfactants is also highly influenced by the addition of electrolytes. These additives modify surfactant interactions, change CMC, size of the micelles, and phase behavior in the surfactant solutions (Sharma 2003).

Investigation of the influence of ions showed that for monovalent anions, it is expected that  $F^- > Cl^- > Br^- > I^-$  in decreasing CP. This is because the ionic sizes increase along the periodic group, consequently decreasing the formal charge density on anion,

thus lowering the attraction on anion, and lowering water attraction. Implying that NaF, NaCl, NaBr cause a decrease in CP while NaI, which is considered a water-structure breaker, results in an increase in CP (Sharma 2003). In a similar study, trivalent and divalent anions  $\text{PO}_4^{3-}$  and  $\text{SO}_4^{2-}$  were found to lead to more dramatic decreases CP of nonionic surfactants when compared to  $\text{F}^-$ ,  $\text{Cl}^-$ , and  $\text{I}^-$ ; in that order (Li 2009).

The presence of ions in a solution can also improve cloud point. Ions with the effect of enhancing the solvent property of water can increase the solubility of surfactants, increasing cloud points. These kinds of ions are termed water structure-breaking ions. The presence of structure-breaking ions can hinder the self-association of water molecules and lead to an increasing amount of hydrogen bond formation between water molecules and ether groups in nonionic surfactants. Ions with this positive influence include  $\text{Cl}^-$ ,  $\text{Br}^-$ ,  $\text{I}^-$  and  $\text{NO}_3^-$ .

Curbelo (2013) showed that by increasing the salinity of the aqueous phase, the CP of four polyoxyethylene surfactants with varying EOs (9.5, 12, 15, and 20) were decreased, thereby demonstrating the influence on the ionic fluid on the POE chains solubility.

The overall effect of the salt on CP is dependent on the cations and anion. However, it has been noted that the effect of cations is relatively smaller, especially with large polyatomic anions (Li 2009).

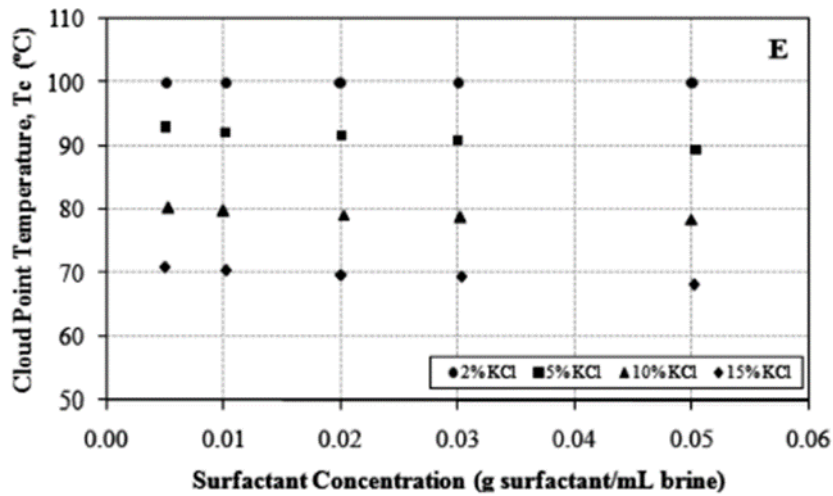


**Figure 5: Increasing salinity shown to result in decrease in cloud point of nonionic surfactant. Where salinity is fixed, increasing surfactant concentration also results in lower cloud point temperature. (Curbelo, 2013).**

*b. Oilfield Chemicals*

Nonionic surfactants are often deployed during acid stimulations activities to help lower IFT and keep the reservoir matrix water-wet, which helps penetration the acid into the formation. Nasr-El-Din et al. (1996) investigated the effect of acid and other chemicals on cloud point and noted an increase in CP with increasing acid concentration. They tested HCl, Formic, Acetic, and Citric acid and noted concentrations greater than 2 wt% led to a notable increase in CP, especially with HCl. This increase in CP is tied to the increasing concentration of hydrogen ions supplied by the acids in the aqueous phase, which enhances solubility via the formation of hydrogen bonds. The effect of alcohols used during stimulation was also investigated, and it was observed that increasing alcohol content also increased CP with the shorter chain alcohols acting similar to the acids,

increasing hydrogen bonding. Longer chain alcohols like decanol have low solubility and have been observed to depress CP (Sadaghiana and Khan 1990, Li 2009).

*c. Ionic Surfactants*

The use of two surfactants with different hydrophilic groups is common practice in the industry as it is aimed at enhancing the properties of the surfactant. Studies have shown that the addition of small amounts of cationic and anionic surfactants increases the CP of nonionic surfactants, with the effect in alteration increasing as the ionic surfactants approach CMC.

Gu (1989) investigated the effect of electrolytes on the cloud point of mixed solutions of ionic and nonionic surfactants. The results of his study showed a significant change in cloud point with the addition of small amounts of ionic surfactants. Gu attributed the observation to work done by Valaulikar and Manohar (1985), who suggested that the rise in the cloud point was due to the formation of mixed micelles which changed the nature of the micelle surface by a small amount of ionic surfactant. "As the ionic surfactant molecules are added to the system, most of them go into the nonionic micelles and charge the surface of the micelle. This added surface charge increases the repulsion between micelles and makes it harder for them to cross the potential barrier, and correspondingly the cloud point is raised."

Sadaghiana and Khan (1990) noted the introduction of sodium dodecyl sulfate, magnesium dodecyl sulfate, cetyltrimethylammonium bromide, or cetyltrimethylammonium sulfate, to 1 wt% micellar solution of Triton X-100 drastically increased the CP.

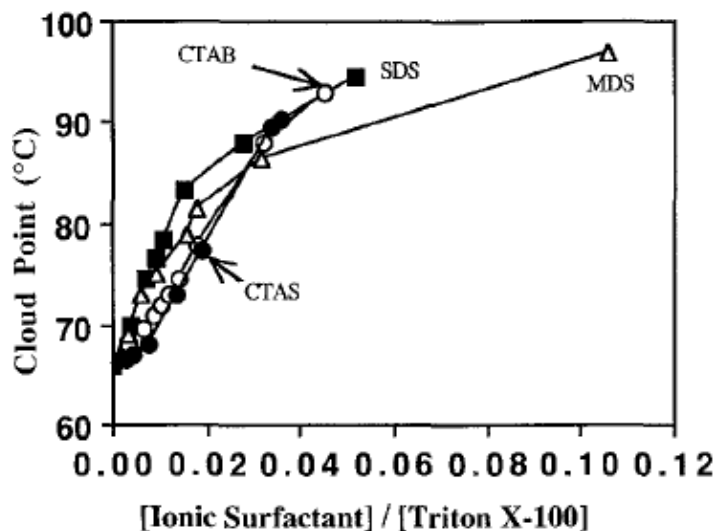


**Figure 6: Effect of ionic surfactant on cloud point of nonionic surfactant Triton X-100. Increasing ionic surfactant ratio results in improved cloud point. (Sadaghiana and Khan, 1990).**

Nasr-El-Din et al. (1996) showed that the addition of an increasing concentration of Sodium Dodecyl Sulfate (SDS), an anionic surfactant, resulted in an increasing CP of TX-100. For phase separation to occur, interactions must take place between the nonionic micelles. The blend of anionic and nonionic surfactant leads to the formation of mixed micelles which possess negative charges. The charge on the micelle thereby creates electrostatic repulsion between micelles in solution, resulting in higher CP. However, where the aqueous phase is an ionic solution, ions can interact with the charged micelles, e.g., sodium or magnesium ions shield the negative charges of the mixed micelles, reducing electrostatic repulsion and causing a decrease in CP (Nasr-El-Din 1996).

Where nonionic surfactants are blended with two ionic surfactants or other nonionic surfactants to create ternary/binary mixtures respectively, CP of the mixture is between those of the individual component surfactants. Sadaghiana and Khan in 1990

carried out cloud point studies using TX-100 in combination with equimolar ratios of cationic and anionic surfactant (catanionic surfactant). The catanionic surfactants, octylammonium octanoate (C8-C8) and dodecyl ammonium dodecanoate (C12-C12), were noted to be uncharged with chemical behavior similar to that of zwitterionic phospholipids. CP was observed to increase minutely at a low concentration of C8-C8, after which it remains constant. Compared to C8-C8, the heavier C12-C12, which was insoluble in all but micellar concentration above 20 wt% TX-100, had no effect on CP. The poor performance of the catanionic surfactant results from the formation of mixed micelles that do not alter the inter-and intra-micellar interactions existing with the pure TX-100 solution.

Li et al. (2009) performed cloud point studies on a combination of nonionic surfactants. Tergitol 15-S-7 (secondary ethoxylated alcohols with 11–15 carbons on the hydrophobic alkyl chain and ethylene oxide (EO) number of 7) was mixed with Tergitol 15-S-9 and Neodol 25-7 (linear primary alcohol ethoxylate with 12-15 carbons on the hydrophobic tail and EO number of 7). The study showed that the resultant mixed surfactant solution CPT could be estimated based on a linear relationship established with the concentration of the nonionic surfactant. This was because no synergism between the nonionic surfactants was attained, and the CP was between those of the single surfactants. As in other studies, the use of ionic surfactants (SDS and CTAB) to boost CPT of the nonionic surfactant proved significant, with more noticeable increase observed when the ionic surfactants approached their critical micelle concentration.

### *Surfactant Concentration*

A surfactant's cloud point is also noted to vary with concentration, decreasing with increasing surfactant concentration. This is because the decrease results from the increasing number density of micelles present in the surfactant solution, which increases interaction between micelles. Therefore, the lowest CP attainable for a pure surfactant will depend on the surfactant CMC, as a low CMC will imply that more of the surfactant molecules exist as micelles than as free molecules within the solution.

Sadaghiana and Khan (1990) observed increasing CP with an increase in the concentration of Triton X-100, a nonionic surfactant with an average EO of 9.5. Similar results were observed by Li (2009) for linear and secondary alcohol ethoxylates Tergitol 15-S\_X, where X represented the number of EOs, 7, 9, and 12. A decrease in CP was observed with increasing surfactant concentration, followed by an increase after reaching a minimum value.

## **Surfactant EOR**

### *Surfactant-Solution Interactions*

Once introduced in a solution, surfactant molecules migrate to the interface and are absorbed where they find the energetically most favorable condition due to their two-art structure. This leads to a decrease in interfacial tension, as seen in

Figure 7. Adsorption at the interface continues until the surface area covered by the surfactant is saturated. At this point, the surfactant molecules do not decrease the interfacial tension further, and rather than exist as free dispersed monomers in the bulk solution, these molecules begin to aggregate into micelles. The point at which micelle



formation begins is referred to as the critical micelle concentration (CMC). Beyond this concentration, further addition of surfactant will form aggregates while the surfactant monomer concentration remains constant. Micelles can incorporate insoluble substances in the bulk liquid, e.g., oil in water or water in oil as shown in Figure 8. Therefore, after reaching the CMC, the system's free energy is reduced by minimizing the area of the hydrophobic parts of the surfactant in contact with the solution.

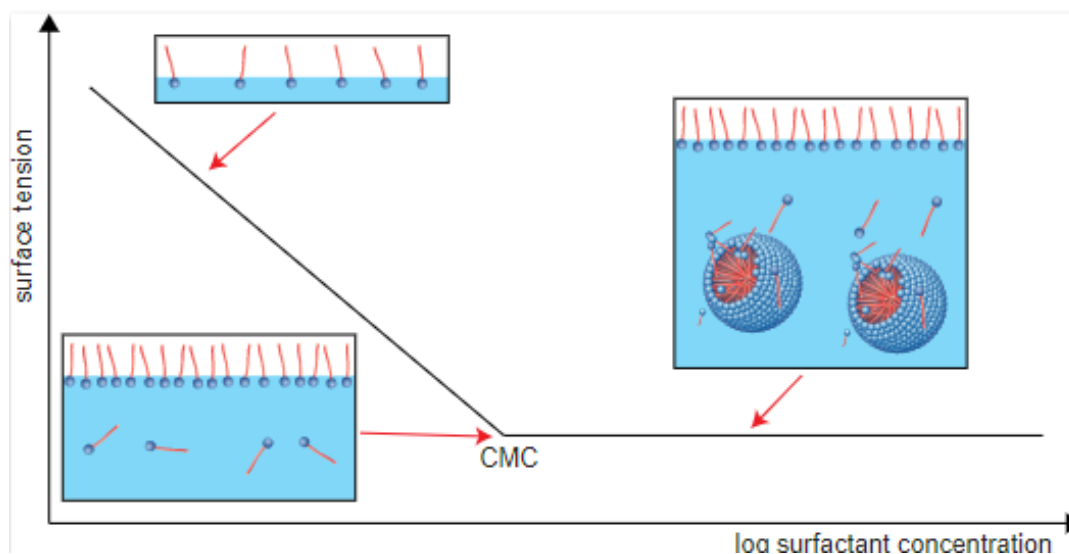


**Figure 7: Surface tension as a function of surfactant concentration. Increasing surfactant concentration reduces interfacial tension up to the CMC. Beyond CMC, surfactant molecules form micelles and IFT remains constant. Culled from Dataphysics-instruments.**

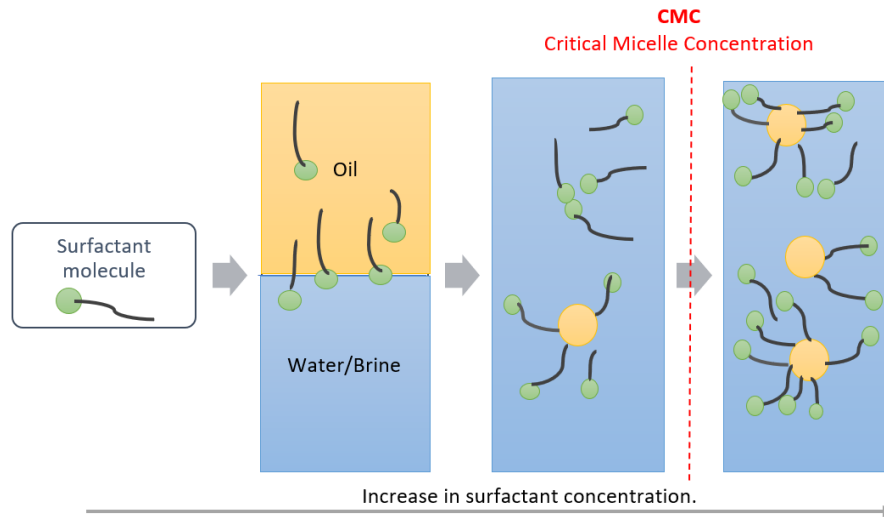


**Figure 8: Illustration of micelle formation. Surfactant molecules orient at interface (left), with increased concentration, molecules aggregate to form micelles with tailgroups interacting with the apolar phase (right).**

### *Surfactant-Rock Interactions*

Based on the nature of the rock, temperature, pH, and other factors, surfactant molecules adsorb onto rock surfaces and cause modification of the hydrophobicity, surface charge, and other key processes that govern interfacial processes (Zhang and Somasundaran 2006). The surfactant molecules adsorb on the rock surface in the form of the layer due to rock-surfactant interactions resulting from forces like covalent bonding, electrostatic attraction, hydrogen bonding, or non-polar interactions between the adsorbed species.

Adsorption is the retention at the interface of solid, liquid, or gas molecules, atoms, or ions by a solid or a liquid. Adsorption of components of crude (polar compounds) or the deposition of organic matter is believed to alter reservoir wettability to oil-wet

conditions. Similarly, the adsorption of chemicals such as surfactant and polymer can alter reservoir wettability back to a water-wet state. Therefore, the theory of adsorption is of importance in understanding wettability as well as altering it. When dealing with surfactants, the adsorption causes a partitioning of the molecules between the interface and the bulk solution because the interface is energetically more favorable when compared to the bulk (Mazen and Radzuan 2008).

Studies suggest that at low concentrations, adsorption is dominated by electrostatic interactions between the charged surfactant head group and the charged mineral sites on the rock surface. Most natural surfaces are negatively charged under naturally occurring conditions. As a result, anionic surfactants will experience a repulsive electrostatic interaction with most surfaces; this in turn decreases the amount of adsorption when compared to nonionic surfactants. In contrast, the positively charged ions in the cationic surfactant adsorb on the negatively charged substrate, such as quartz, forming a monolayer of surfactant ions which orient such that the polar heads face the substrate, and the hydrocarbon tails protrude out into the bulk aqueous phase. A double adsorption layer is formed where the hydrocarbon tails of the oncoming surfactant ions are mutually attracted to the hydrocarbon tails of the adsorbed ions. The bilayer formation neutralizes the surface charge, changing its sign to the same sign as the surfactant ions.

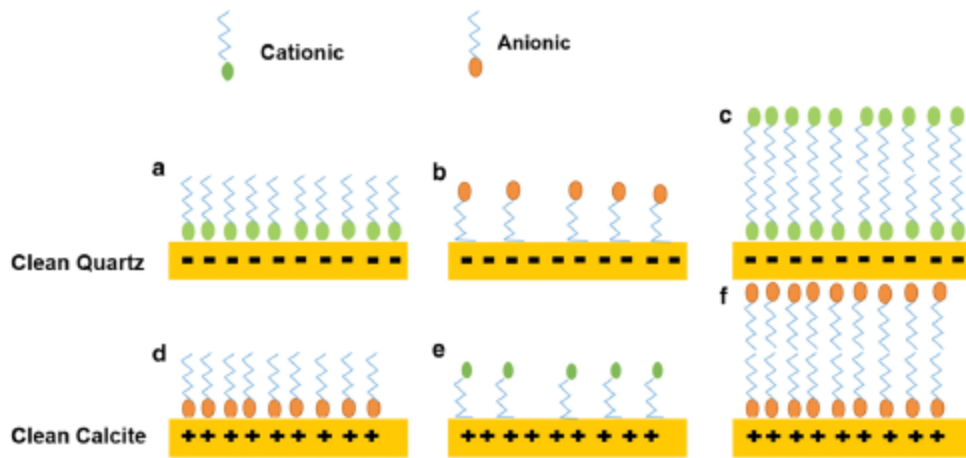


**Figure 9: Schematic diagram of adsorption mechanism of (a) cationic surfactant on clean quartz, (b) anionic surfactant on quartz, (c) cationic surfactant on quartz (double layer formation), d) anionic surfactant on calcite, e) cationic surfactant on calcite, and f) anionic surfactant on calcite (Zhou et al., 2016).**

Adsorption of a nonionic surfactant involves hydrogen bonding where the bonds are formed between the surfactant hydrocarbon chain and the oxygen atoms on the surface of the mineral. For surfactants containing hydroxyl, phenolic, carboxylic and amine groups, adsorption via hydrogen bonding is also possible. It should be noted that hydrogen bonding is weaker than electrostatic interactions, therefore, for adsorption to occur due to hydrogen bonding, the bond formed between the surfactant functional groups and mineral surfaces must be stronger than that formed between the mineral and interfacial water molecules (Zhang and Somasundaran, 2006).

Hydrophobic bonding can also be important for adsorption on solids that possess a fully or partially hydrophobic surface. In this case, surfactant molecules can adsorb flat on the hydrophobic sites on the solid due to the interactions between the alkyl chain and the hydrophobic sites. Such adsorption can also take place on other types of solids that are

originally hydrophilic but that have acquired some hydrophobicity owing to reaction with organic species in solutions (Somasundaran and Huang, 2000).

In addition to the primary and secondary adsorption mechanisms identified, further studies into the nature of adsorption of nonionic surfactants reveal that surfactant structure impact the amount of adsorption. Where nonionic surfactants are concentrated above CMC as is the case during wettability alteration, surfactants with lower EO groups have been observed to absorb more leading to better wettability alteration. This is because the reduced ability of the surfactant-water interaction due to dehydration of the EO group at higher temperature, coupled with increasing hydrophobic interactions, makes surface aggregation more favorable, leading to higher adsorption at higher temperatures (Das et al., 2020).

### **Wettability**

Wettability is a vital rock petrophysical quantity that has been defined as the tendency of one fluid to adhere to or spread on a solid surface in the presence of other immiscible fluids (Anderson 1986). It develops as liquid and solid particles interact through adhesion due to Van der Waals forces' action and ionic bonding.

### **Wettability and Interfacial Tension (IFT)**

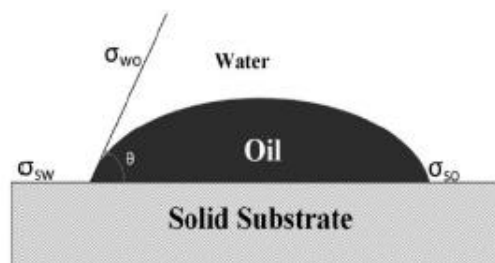


**Figure 10: Illustration of contact angle in a rock-oil-brine system**

The wettability of a solid surface relates directly to the solid–fluid and fluid–fluid interactions. In a rock-oil-brine system, three interfaces exist: rock-oil, rock-water, and the water-oil. These phases experience interfacial tension which results from the attractive and repulsive forces possessed by each phase. The attraction between the substrates causes lower interfacial energy, and repulsion forces result in a higher energy surface (Owen et al., 2012). A liquid that exhibits higher adhesive strength than cohesive strength is called the wetting phase and will typically form a contact angle with the surface less than 90°; ( $\theta < 90^\circ$ ). A non-wetting fluid conversely exhibits a larger cohesive strength, forming a contact angle with the surface which is greater than 90°; ( $\theta > 90^\circ$ ). This distinction in behavior allows for the quantification and characterization of wettability based on contact angle.

The Young equation relates the interfacial forces in a rock/oil/brine system,

$$\cos \theta = \frac{\sigma_{sw} - \sigma_{so}}{\sigma_{wo}} \quad \text{Equation 2}$$

where  $\theta$  is contact angle and  $\sigma$  values indicate the interfacial tensions between solid–water ( $\sigma_{sw}$ ), solid–oil ( $\sigma_{so}$ ), and water–oil ( $\sigma_{wo}$ ).

### **Wettability Classification**

A rock surface is said to be water-wet when the contact angle of the water phase is less than 75°, intermediate-wet for contact angles between 75° - 105°, and oil-wet and when it is greater than 105° (Anderson 1986). An intermediately wet system assumes that all

portions of the rock surface have a slight but equal preference to being wetted by water or oil. While a mixed wet system is one in which the oil-wet surfaces form continuous paths through the larger pores, while the smaller pores remain water-wet, creating strongly oil-wet and strongly water-wet regions.

Treiber and Owens (1972) used the water advancing contact angle to examine the wettability of 55 oil reservoirs with contact angle as criterion of wettability. They observed most carbonate reservoirs were oil-wet. Similarly, studies by Chilingar and Yen (1993) via contact-angle measurements also arrived at the same conclusions that most carbonate reservoirs range from intermediate-wet to oil-wet.

Understanding the wettability preference of a reservoir is of great importance where it directly impacts the driving forces in hydrocarbon recovery (Anderson, 1986; Morrow et al., 2006).

### **Measurement of Wettability**

There are several methods of evaluating wettability; Anderson (1986) in an extensive literature survey described some quantitative and qualitative methods. Among the methods, the Amott-Harvey index, U.S. Bureau of Mines (USBM), and contact angle method are the most celebrated method for quantitative wettability measurements used in the petroleum industry.

#### **Amott Test**

The Amott or the Amott–Harvey method measures the “overall or average” wettability of the core. The test allows for the determination of the average wettability

through the study of spontaneous imbibition and displacement of liquid (water and oil) through the rock samples.

This test is usually carried out in five steps.

- i. The test begins at the residual oil saturation; therefore, the fluids are reduced to  $S_{or}$  ( $S_{or}$  residual oil saturation) by forced displacement of the oil.
- ii. The core is immersed in oil for 20 hours, and the amount of water displaced by the spontaneous imbibition of oil.
- iii. The water is displaced to the residual water saturation ( $S_{wi}$ ) with oil, and the total amount of water displaced (by the imbibition of oil and by forced displacement).
- iv. The core is immersed in brine for 20 hours, and the volume of oil displaced, if any, by spontaneous imbibition of water.
- v. The oil remaining in the core is displaced by water to  $S_{or}$  and the total amount of oil displaced (by the imbibition of water and by forced displacement).

The Amott index for water and oil can be determined from the following formulas.

$$I_o = \frac{\Delta S_{oi}}{1 - S_{wi} - S_{or}} \quad \text{Equation 3}$$

$$I_w = \frac{\Delta S_{wi}}{1 - S_{wi} - S_{or}} \quad \text{Equation 4}$$

where:  $I_o$  – the displacement-by-oil ratio,  $I_w$  – the displacement-by-water ratio,  $\Delta S_{os}$  – the volume of water displaced by the spontaneous imbibition of oil,  $\Delta S_{ws}$  – the volume of oil displaced by the spontaneous imbibition of water,  $S_{wi}$  – irreducible water saturation, and  $S_{or}$  – residual oil saturation.



Cuiec (1984) in studies of wettability index said that the rock is hydrophilic when  $0.3 \leq I_w \leq 1.0$ ; neutral rock wettability, respectively ( $-0.3 \leq I_w \leq 0.3$ ) and hydrophobic rock, where  $-1 \leq I_w \leq -0.3$ .  $I_w = 0$  is usually observed in the case of cores with a neutral wettability, which indicates a lack of spontaneous imbibition of both oil and brine or equal amounts of the two liquids to be imbibed spontaneously.

For the Amott method and Amott–Harvey method, one problem is that the spontaneously imbibed volume depends on imbibition time. Spontaneous imbibition in shale or tight cores is very slow. Therefore, these two methods are not practical to measure shale or tight rock wettability.

### **Contact Angle**

As previously described, the contact angle a fluid makes with a substrate is an indication of the substrate's basic wettability characteristic.

Contact angles can be measured in:

- i. Air i.e., air-water-rock and air-oil-rock system
- ii. Oil-water-rock system

The air-water-rock and air-oil-rock contact measurements are performed using a Sessile drop test. A droplet is deposited by a syringe which is positioned above the rock surface, and a high-resolution camera captures the image from the profile or side view. The image can then be analyzed either by eye (with a protractor) or more often using Drop shape analysis software. This type of measurement is referred to as a static contact angle measurement. In the Oil-water-rock system, contact angle measurement is performed using the Pendant drop technique. A needle is utilized to dispense as well as position oil drop to the bottom-facing surface of the sample surface which has been submerged in

brine. Images of the drop are recorded, and the contact angles are extracted from these images.

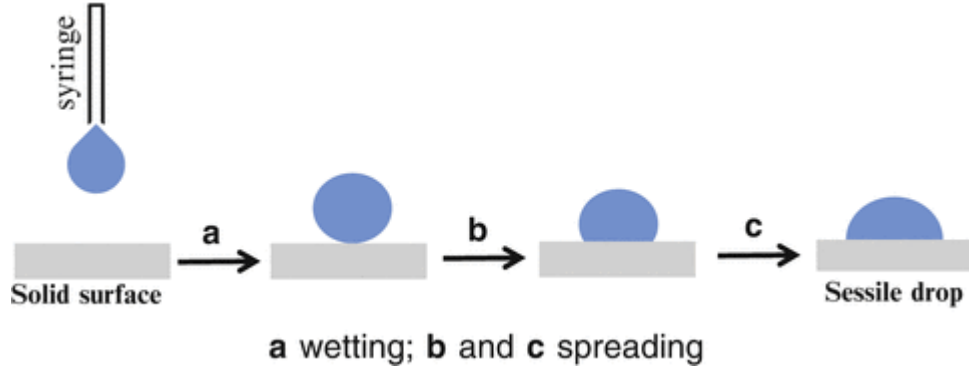


**Figure 11: Illustration of a sessile drop (Lee and Zhao, 2015)**

Siddiqui et al. (2018) recently opined in their comprehensive review that CA-based wettability estimated in an oil-water system is consistent rather than in an air-water system. They thus proposed an equation via which contact angles measured in air could be converted given the interfacial tension data to represent in situ conditions.

$$\theta_{ow} = \cos^{-1} \left( \frac{\gamma_{sw} - \gamma_{so}}{\gamma_{ow}} \right) = \cos^{-1} \left( \frac{\gamma_{oA} \cos \theta_{oA} - \gamma_{wA} \cos \theta_{wA}}{\gamma_{ow}} \right) = 180^\circ - \theta_{wo} \quad \text{Equation 5}$$

where,  $\theta$  is the contact angle formed in water (w) or air (A) and  $\gamma$  is the surface tension at the interface of the two fluids (oil-water, ow; oil-air, oA; water-air, wA; solid-water, sw; or solid-oil, so).

In performing contact angle measurements, accuracy and repeatability of the study is achieved by:

- Taking measurements once the drops had reached a stable state.
- Making two or more droplets and using the average values measured.
- Ensuring average surface roughness by using a considerably flat surface.

- Cleaning the surface, removing traces of oil, and displacing water. This can be achieved using by rinsing with isopropanol followed by 24 hours of vacuuming and oven drying. Isopropanol is used because it displaces water, dissolves oil, and dries quickly. It also washes away any residue and does not alter the surface wettability after rinsing due to its nonreactivity with most minerals.

Contact angle measurement is thought of as an accurate descriptor of wettability because it often gives repeatable results. However, CA measurement, which has wide applicability in the evaluation of the wettability of conventional reservoirs, becomes useless or even misleading in determining shale wettability due to the problems of surface contamination, surface roughness, and compositional heterogeneity (Morrow, 1990). Some studies have also made observations in which shales with the same mineralogy (and from the same formation in a well), but from different depths, exhibited different wetting affinities (Elgmati et al., 2011) or CAs did not correlate with total organic content in some studies (Engelder et al., 2014), that is, while other studies demonstrated a clear correlation with total organic content (Arif et al., 2017; Pan et al., 2018). Considering the tight and complex nature of shale formations, displacement techniques like the Amott wettability and USBM are not applicable to shale reservoirs and contact angle measurement remains the most used method of characterizing shale wettability (Liu et al., 2019).

### **Spontaneous Imbibition (SI)**

SI test measures the ability of the wetting phase to displace the nonwetting phase. The relationship between capillary pressure, IFT, contact angle, and pore radius is given by the Young-Laplace equation.

$$P_c = P_{nw} - P_w = P_0 - P_w = \frac{2\gamma\cos\theta}{r} \quad \text{Equation 6}$$

where:  $P_c$  is capillary pressure,  $P_{nw}$  is non-wetting phase pressure,  $P_w$  is wetting phase pressure,  $\gamma$  is IFT,  $\theta$  is contact angle, and  $r$  is pore radius of the rock.

The imbibed fluid volume or imbibition slope is often used as the main parameter in assessing wettability. In hydrophilic samples, the rate of spontaneous imbibition is high and limited by the permeability of the porous medium. On the other hand, if the sample is strongly hydrophobic, then very little water will enter the sample, and consequently, only a small amount of oil will be recovered. Behavior between these two extreme limits indicates an intermediate wetting state.

The capillary forces that exist within the rock's pore throats provide the dominant driving force for spontaneous imbibition in unconventional reservoir systems. Wettability is one of the two essential factors that determine the magnitude of the capillary forces, as the wettability preference of the surface determines the shape of the oil-water interface. This phenomenon is illustrated in Figure 12 where the fluid of which exhibits the greatest attraction towards the porous medium will displace the other fluid. Consequently, the pressure will always be lower in the fluid phase that occupies the concave side of the interface.

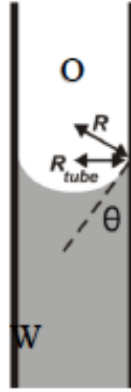


**Figure 12: Illustration of the interface between oil and water due to wettability preference of the tube wall (Glover, 2002).**

Because the capillary pressure is inversely proportional to the tube radius, it signifies that higher capillary pressures are needed to invade the smallest pores in the reservoir. Hence the desire to alter wettability and reduce IFT to allow imbibition of water into the tight unconventional pore system during EOR.

Gravitational and viscous forces also contribute to the imbibition and drainage process, and these can be related to capillary forces by the inverse bond number shown in Equation 7.

$$N_B^{-1} = C \frac{\sigma \sqrt{\frac{\phi}{k}}}{(\Delta\rho)gh} \quad \text{Equation 7}$$

where C is a constant related to pore geometry,  $\sigma$  is IFT,  $\phi$  is porosity, k permeability,  $\Delta\rho$  density difference of the immiscible fluids, g the gravitational acceleration and h the length of the studied core. Schechter et al. (1994) concluded for low IFT imbibition that when  $N_B^{-1}$  is bigger than 5, capillary forces are responsible for imbibition with a countercurrent flow. Conversely, when  $N_B^{-1}$  is smaller than 1, gravitational forces govern with a co-

current flow. Finally,  $N_B^{-1}$  numbers between 1 and 5 have contribution of both capillary and gravitational forces.

### **Zeta Potential**

The measurement of zeta-potential can be used to evaluate wettability alteration and determine the stability of surfactant-solution films on the rock surface.

Zeta-potential is the electrical potential on the double layer. It indicates the strength of surface charges on a solute particle as well as the nature of the charge. A large positive or negative value of zeta potential of nanocrystals indicates good physical stability of nanosuspensions due to electrostatic repulsion of individual particles (Joseph and Singhvi, 2019). Unstable-solution films may be an indication of an oil-wet system, while stable-solution films indicate an increase of electrical-double-layer repulsion, which will help oil detach from the rock surface and alter wettability toward water-wet (Alvarez and Schechter, 2016).

### **Mechanism of Wettability**

Historically, all petroleum reservoirs were believed to be strongly water-wet given they were deposited in aqueous environments where the presence of connate creates a thin stable film of brine that coats the rock surface and prevents oil from adhering to the rock surface. The following interactions influence the film's stability.

- a. Electrostatic interactions between charged groups at the brine/oil interface and the brine/rock interface.
- b. Hydrogen bonding between polar functional groups in the crude oil.

- c. Lewis acid/base interactions between basic oil groups and negatively charged groups at the rock surface.
- d. Formation of organometallic complexes between charged acidic groups on the oil surface and divalent cations absorbed to the rock surface.

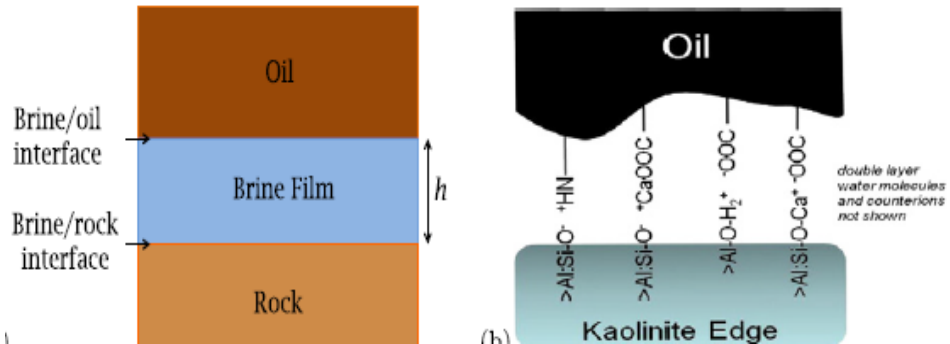


**Figure 13: Illustration of water-wet rock and interactions influencing its activity. Left: Wettability of the rock surface influenced by the interaction between the brine/oil and the brine/rock. Increase and stability in brine film thickness (h) leads to water-wet surface. Right: Attractive interactions result in decrease in brine film thickness and create oil-wet clay surface. (Myint and Firoozabadi, 2015)**

These interactions contribute to the disjoining pressure  $\Pi(h)$  in the film. Attractive interactions between the two interfaces produce negative contributions to  $\Pi$  that cause the film to collapse, decreasing  $h$ . Repulsive interactions produce positive contributions to  $\Pi$  that stabilize the film and increase  $h$ . Stable, thick brine films are indicative of a water-wet state.

Double layer expansion (DLE) is one mechanism believed to enhance wettability towards a water-wet state. With low salinity brines, there is less ionic strength, which implies fewer counter ions shielding the negatively charged brine/oil and brine/rock interfaces. This leads to greater electrostatic repulsion, a thicker brine film, and a more

water-wet surface. Alotaibi et al. (2011) and Nasralla et al. (2014) visualized DLE by increasingly negative zeta potential, with Nasaralla et al. also noting that at higher pH where the sandstone surface becomes more negative there is enhanced DLE leading to better recovery.

The literature shows that to convert a water-wet surface to an oil-wet, either adsorption of polar components of crude oil or deposition of organic matter occurs. These compounds contain polar and hydrocarbon moieties, and the polar end adsorbs on the rock surface, exposing the hydrocarbon end rendering the surface more oil-wet.

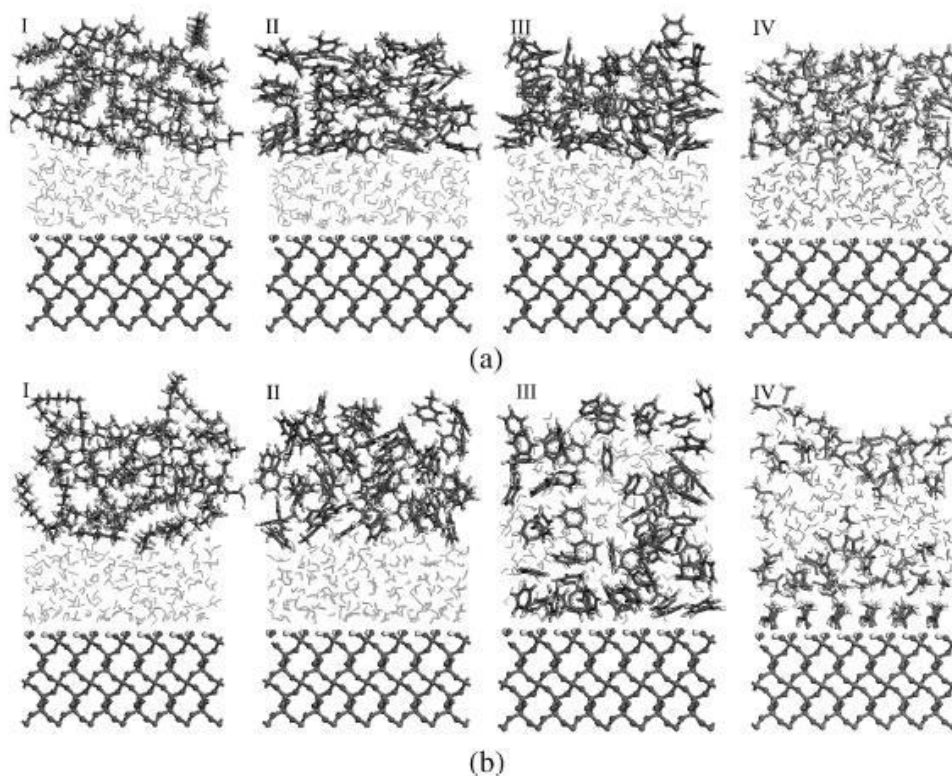


**Figure 14: The (a) initial configuration and (b) equilibrium configuration of (I) decane-water (II) methyl benzene-water (III) pyridine-water (IV) acetic acid-water on silica surface. Polar compounds pyridine and acetic acid penetrate through the water film and adsorb onto the silica surface while apolar components (methyl benzene and decane) do not. (Zhong et al., 2013)**



Zhong et al. (2013) performed an investigation into the adsorption behavior of the different components of crude oil using molecular simulation. The study revealed that the apolar components (e.g., methylbenzene and decane) could not penetrate through the water film and were not adsorbed. However, polar components (e.g., acetic acid and pyridine) penetrated through the water film and adsorbed on the silica surface. The acetic acid molecules displaced water molecules completely and formed a self-assembled monolayer on the silica surface, while the pyridine molecules only co-adsorbed, indicating that they partially displaced the water molecules. The density distribution profiles reflected these observations, with polar molecules, especially the acetic acid, peaking close to the mineral surface while the apolar molecules were concentrated farther away. From the simulation results by Zhong et al., a two-step adsorption mechanism in the formation of an oil reservoir was proposed. Firstly, the polar oil components would adsorb preferentially on the mineral surface, relying on its large diffusion coefficient and strong interaction with the mineral surface. Secondly, these adsorbed polar molecules, playing the role of anchor, would promote the adsorption of the apolar components.

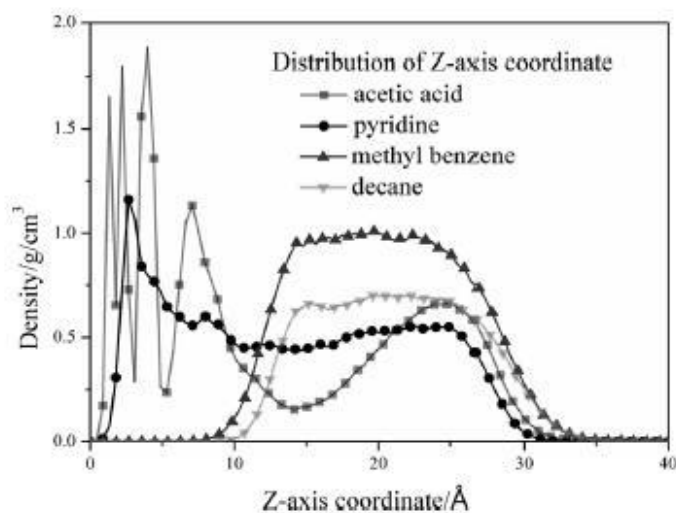


**Figure 15: Density distribution of different oil components. Peaks of polar molecules (pyridine and acetic acid) are close to the mineral surface which indicates that most of acetic acid molecules penetrated through water film and adsorbed on mineral surface. While apolar molecules (methyl benzene and decane) peaks are in the range of 15 - 25 Å, which indicates that these apolar molecules could not penetrate through the water film. (Zhong et al., 2013)**

The wettability mechanisms mentioned above are believed to be active in shales with the addition of strong affinity for crude at the naturally hydrophobic or lipophilic sites, the kerogen surfaces.

### Wettability Alteration

Wettability of the reservoir changes when the water layer is destabilized as a result of oil/water/rock interaction, thereby making it oil-wet. Studies have also shown that the water-wet state of a reservoir rock is affected by oil composition, pressure, temperature, mineral surface, and brine chemistry, including ionic composition and pH (Anderson, 1986a).

Therefore, wettability alteration in the context of this work refers to the restoration of the original water-wet state to promote oil recovery by reducing the affinity of the rock to oil. The introduction of new fluid into the oil/brine/rock system can change IFT and, hence, alter the wettability of the system.

### **Factors Affecting Wettability and Wettability Alteration**

Studies have shown that any surface's wettability depends on a range of factors, including surface chemistry, ionic concentration, pressure, temperature, pH (and surface charge), clay content, and pore structure/connectivity.

#### *Oil Composition*

Changes in the wettability of surfaces from hydrophilic to hydrophobic have been observed and investigated over the years. These studies have found that the polarity of oil components profoundly affects crude oil adsorption onto a reservoir surface.

Morrow et al. (1986) performed tests on aged glass slides and discovered that the extremely clean slides (no oil residue from aging) were water-wet. Depending on the amount of trace oil and ions in the system however, the glass-isooctane-distilled water system tended to be more oil-wet. Attempts at explaining the adsorption phenomenon have revealed that adsorption is affected by factors, such as the interaction strength between oil components and silica surface, the penetration capability of oil components in water film, competitive adsorption capability between oil components and water molecules. It was observed that the apolar molecules interact weakly with the silica surface because their interaction is based on Van der Waals forces, which are attractive yet weak. In contrast, polar molecules display strong electrostatic interactions with the silica surface. Depending

on the interaction between the oil components and silica surface penetration of the water film by the oil components can occur; the larger interaction energy, the stronger of penetration capability and adsorption (Zhong et al. 2013).

### *Total Organic Carbon*

An increase in contact angle with TOC can be attributed to the rock being more hydrophobic and having more affinity for oil due to the presence of high organic matter. This is the case in mature and over mature shales, where pore volume within the organic matter may be a substantial fraction of the entire porosity of the resource shale system.

Oduşina et al. (2011), during an NMR study of shale wettability; using Woodford, Barnett, Floyd, Eagle Ford samples, correlated the amount of oil imbibed with the TOC content and observed a positive correlation between the amount of oil imbibed and the TOC content, with an overall  $R^2=0.55$ . This is because higher TOC provides a higher specific surface area (Zhu et al., 2016), leading to higher oil adsorption on the surface of organic matter (Wang et al., 2015) and higher oil imbibition by organic pores.

Sulucarnain (2012) conducted a wettability study using NMR on Ordovician shale samples rich in organic matter, with TOC values ranging between 0.3% and 5.8% with an average of  $3\% \pm 1.8\%$ . The study showed that the source rock samples are of mixed wettability with a correlation between oil wetting and TOC content. Tinni (2017) stated that hydrocarbon-wet pores are essentially contained within the organic matter and require a minimum amount of total organic carbon (TOC), about 3 wt%, to form a connected network of hydrocarbon-wet pores. However, his study also concluded that although 3

wt% of TOC is necessary, it is not sufficient to develop connectivity throughout organic bodies.

### *Pore Connectivity*

Resource shales have a well-developed network of nanometer-sized organic pores and some inorganic pores, unlike conventional reservoir rocks containing large pore sizes and dominant inorganic pores (Loucks et al., 2009, 2012). The co-existence of oil-wet and water-wet pores in shale complicates its wettability. It is important to note that the connectivity of the pore system (organic or inorganic) matters in characterizing shale wettability. The water-wet, hydrocarbon-wet, and mixed flow paths could be independent or dependent on each other. When the different wettability-system flow paths are independent, fluids can flow in one system without entering the other ones. In contrast, in the case in which the wettability-system flow paths are dependent on each other, fluids will flow from one system to another and will have to overcome barriers caused by different capillary pressures; (Tinni 2017). This explains the different results obtained by Dehghanpour (2012) and Xu and Dehghanpour (2014), where core samples from the Horn River displayed water-wet properties, but later tests on crushed samples showed great oil imbibition rates suggesting oil we-properties.

Lan (2014) investigated the wettability of tight rocks and shale formations using the Montney and Horn River samples. The imbibition results showed the oil-wet property of Montney intact samples and water-wet characteristics of Horn River intact samples. The contact angle measurements indicated the strong oil-wet property of both Montney and Horn River samples. The insignificant oil uptake observed by the Horn River samples

suggests that the connected pore network of the rock is strongly hydrophilic. SEM images proved this, showing the organic matter located in different regions with poor connection, leading to the poorly connected oil-wet pore network.

Gao and Hu (2016), during an investigation of pore structure in American and Chinese shales, observed wettability differences between Longmaxi and Yanchang samples and concluded that these differences were closely related to their pore structure difference, which was caused by their different thermal maturities and compaction/diagenetic stages. Longmaxi samples had organic pores with smaller pore sizes that were more developed, and inorganic pores were largely absent due to the strong compaction at its overmature stage. The Yanchang sample, on the other hand, had developed inorganic pores with larger pore sizes with less developed organic pores. Attributes of the relatively weak compaction and low thermal maturity of the shale.

#### *Brine Salinity*

Salinity has been noted to affect contact angle and imbibition wettability studies, generally decreasing water affinity as observed by larger water contact angles and lower imbibition rates (Anderson, 1986; Alotaibi et al., 2011; Lu et al. 2017; Haagh et al., 2018).

Mirchi et al. (2015) investigated the effect of surfactants on shale wettability performed contact angle measurements for an oil-drop-in-distilled-water configuration at two different salinities (0.1M and 5M) at both ambient and reservoir conditions. It was found that the contact angle increased with salinity i.e., it was 27.04° at 0.1M and 69.94° at 5M in reservoir conditions. Roshan et al. (2015) examined the contact angle of air/DI water and several ionic solutions on Evergreen shale sample. Although Evergreen shale is

not a source rock, it has a significant level of TOC of 1.935 wt.%. The sample was composed of 19.8 wt.% kaolinite and 12.8 wt.% illite. The equilibrium contact angle of DI water, 5 wt.%, and 10 wt.% NaCl solutions were measured as 26°, 30°, and 45° showing that the higher ionic solution leads to a higher contact angle. Xie et al. (2016) measured liquid/liquid contact angles at various salinities for oil/brine/rock on surfaces of individual minerals (quartz, dolomite, calcite, pyrite, albite, and K-feldspar) found in shales instead of using intact core samples. It was found that, in general, contact angle increases with salinity up to a certain concentration then decreases thereafter.

Literature has also indicated that the type of ions present in the brine plays a role in wettability and wettability alterations. For instance, the divalent ions,  $\text{Ca}^{2+}$  and  $\text{Mg}^{2+}$ , have been known to be strongly adsorbed on clay surfaces (part of the shale) and reduce the surface potential. Their increased concentration is believed to increase contact angle towards more oil-wet conditions. For example, Roshan et al. (2016) observed that divalent ionic solutions ( $\text{MgCl}_2$  and  $\text{CaCl}_2$ ) have higher contact angles than monovalent ionic solutions ( $\text{NaCl}$  and  $\text{KCl}$ ) at the same concentrations.

### *pH*

It is known that the surface charge of materials is a strong function of pH i.e., the higher the pH higher the negative surface charge is observed.

Schramm et al. (1990) investigated the electrokinetic properties (surface charge behavior) of rock surfaces as pH and electrolyte concentration functions. A negative surface charge at neutral pH in the NaCl and synthetic brine solutions was observed with Berea sandstone, but this reversed to a positive charge in the  $\text{CaCl}_2$  solution. It was also

observed that the negative charge reverts to a positive in brine at pH above 9, indicating adsorption of oppositely charged ions. For Indiana limestone, which is almost pure calcite, and Baker dolomite, the surface charge was observed to change based on the brine solutions. Divalent cations produced a positively charged limestone and dolomite surface across pH range of 6 to 12, however, the reversal to negative is more abrupt for dolomite in synthetic brine at pH below 10.5. This implies that ionic composition and pH play an important role in determining the wettability of a surface.

Takahashi and Kavscek (2010) conducted spontaneous countercurrent imbibition experiments on siliceous shale core sample observed oil could not be expelled spontaneously from the shale sample in the neutral pH water as contact angle increased with pH reaching a peak at pH 4-6, which indicated an intermediate to oil-wet property of this siliceous shale sample. In low- and high-pH brines, oil recovery was observed. The high pH brine led to the greatest final oil recovery as contact angle then decreases attaining a value of near-zero at pH 7-8, which indicated the wettability of this shale sample changed to greater water-wetness due to the interaction between the shale sample and high-pH brines.

### *Temperature*

The effect of temperature is seen to vary across the literature. Elevated temperature is mainly seen to improve the wettability alteration of carbonate or carbonate-rich rock. At the same time, it varies for quartz-rich surfaces.

Wang & Gupta (1995) investigated the effect of pressure and temperature on wettability using an oil/brine/quartz system at pressures ranging 200-3000 psi and



temperatures from room temperature to 200°F. Their study revealed that contact angles are not very sensitive to pressure; less than 5% increase was observed for a 3000 psi increase in pressure. While the system was more strongly water-wet  $\Theta = 22^\circ$  (at room conditions), but as the temperature increased, the contact angles went through a maximum of  $34^\circ$  at approximately 130°F and a minimum of  $27^\circ$  at approximately 180°F.

Mirchi et al. (2014) observed oil/water (brine) contact angles increase at a higher temperature (80°C) i.e., contact angle increases from  $21^\circ$  to  $45^\circ$  at 0.01 wt. % surfactant in 5M brine and at a constant pressure of 3000 psi. Roshan et al. (2016) observed that temperature increase from 35 °C to 70 °C led to a gradual increase in advancing and receding contact angles for 0.1 and 0.5 M salt concentrations at 20 MPa pressure. An increase in salinity magnified the temperature effect, causing a sudden jump in contact angle, in contrast to the gradual increase seen at the relatively lower salt concentrations. Although the experiments mentioned above all showed an increase in contact angle with temperature, the literature does suggest that temperature can increase or decrease the contact angle on shales depending on physical parameters such as pressure, surface charge, and pH.

### *Clay*

The mineralogical nature of the constituents of shale rocks may govern the wettability directly by speeding - or slowing down- the adsorption of polar molecules on their surface. Due to the variability in the behaviors of different clay species, no trend has been identified as regards clay content in shales.

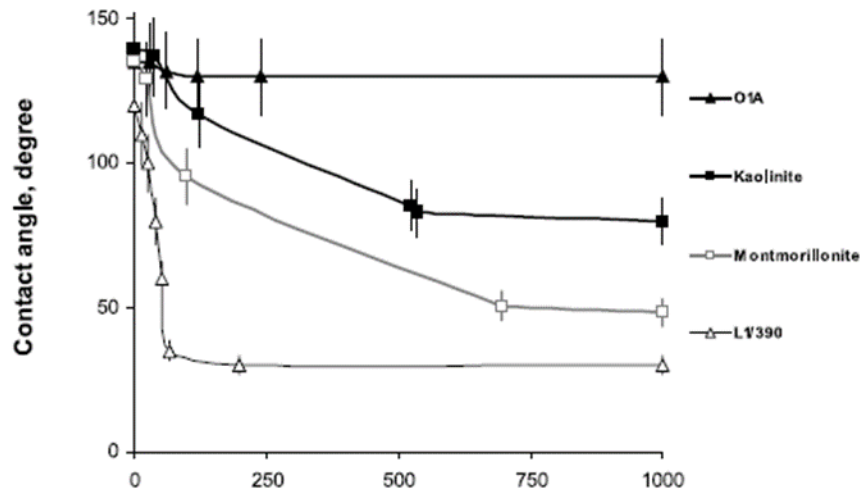


**Figure 16: Change in air-water contact angle with varying minerology, (Borysenko et al. 2009)**

Borysenko et al. (2009) recorded contact angles on Kaolinite and Montmorillonite surfaces which investigating the wettability of clays and shales. They found Montmorillonite clay to be more hydrophilic than Kaolinite, and shale from the Officer Basin in Western Australia, which was rich in illite was more hydrophilic than shale from the Bass basin which was rich in quartz and kaolin. They concluded, illitic and smectitic shales are more hydrophilic and have higher surface activity whereas kaolinitic shales are preferentially oil-wet. Dehghanpour et al. (2012) did observe that the amount of water imbibed was positively related to Illite content and negatively related to quartz content. Illite-rich samples were observed by Siddiqui et al. (2019) to cause Shale swelling by hydration and form structural damage to the sample during wettability studies by SI. Hydration of clay minerals along weak planes generates sufficiently strong stresses to fracture the rock when it is not countered.

CHAPTER III  
METHODOLOGY

The selection of surfactants for wettability alteration was achieved via a systematic study of the interactions between the aqueous phase, oil, and rock samples, as presented in Figure 17.

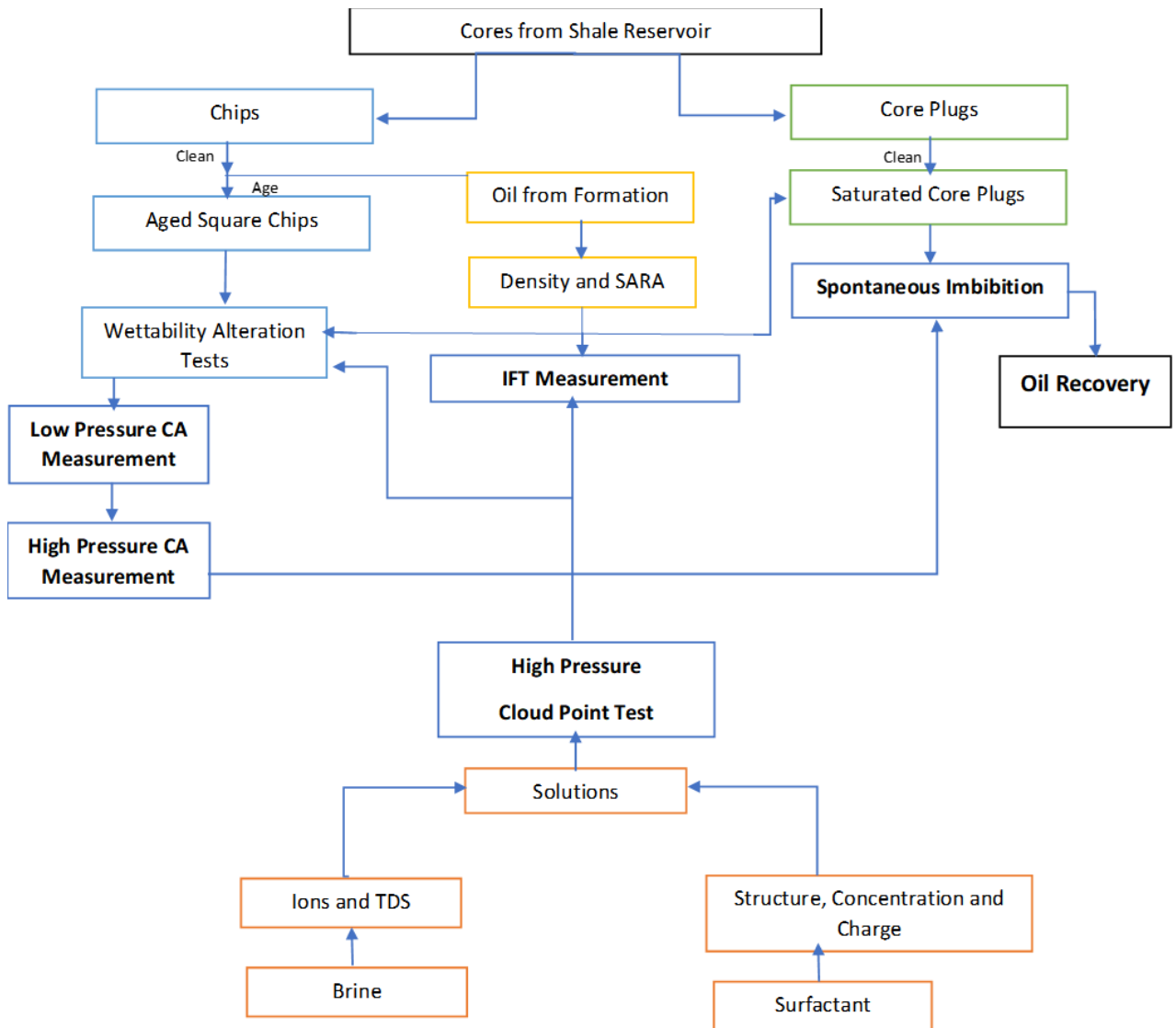


**Figure 17: Flow chart explaining systematic workflow of the study.**

First, high-pressure cloud point tests were run to evaluate the thermal stability of the surfactant solutions, taking into consideration the effects of brine composition and the surfactant properties. Low-pressure contact angle and IFT tests were then run to determine the influence of the surfactant solutions on the brine/rock/oil system. For solutions that showed favorable wettability alteration and low IFT, high-pressure tests were performed to validate the use of the solution in high-temperature shale reservoirs.

## **Materials**

### **Rock Sample Description**

Sidewall cores from varying depths of the Eagle Ford were used in all contact angle and spontaneous imbibition experiments. Cores were received in a preserved state with a thick layer of wax encasing each core plug. X-ray diffraction (XRD) was performed on the rock to determine the mineral composition. As seen in Figure 18, the samples were classified as carbonate-rich due to the prevailing amount of calcite, 61.9%.

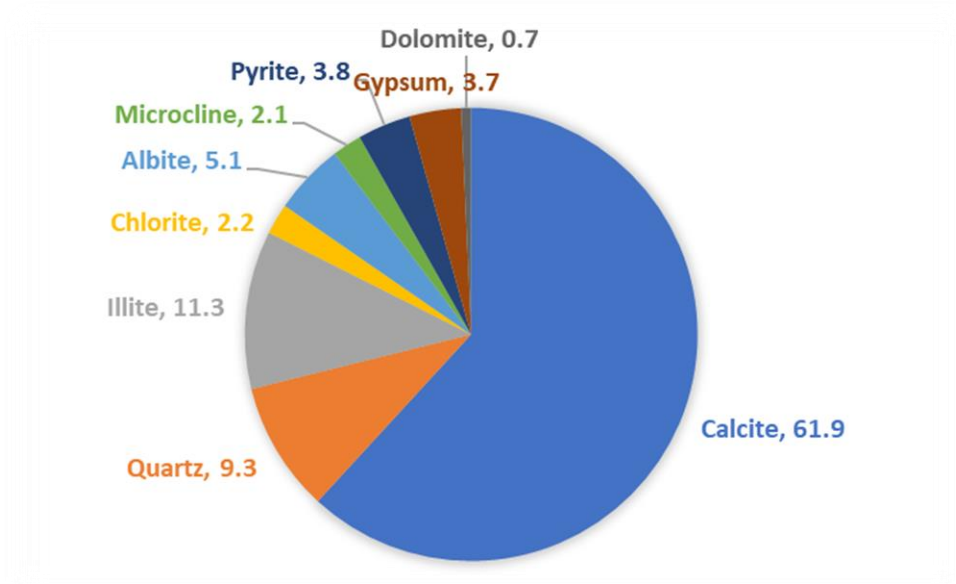


**Figure 18: Mineral composition of Eagle Ford rock sample**

### **Cleaning and Aging**

CA tests run on freshly cut chips indicated that the cores preserved in wax did not retain original wettability (oil-wet). Therefore, before the start of experimentation, all rock chips and core plugs were cleaned, dried, and aged in oil from the formation to restore reservoir wettability. Cleaning the rock chips was performed by soaking in toluene for two days, followed by soaking in methanol for one day. Likewise, the core plugs were boiled for two weeks in toluene and one week in a methanol extraction in a Dean-Stark apparatus. The rock chips were aged by submerging in the Eagle Ford crude oil at 90°C for an optimum aging period of 7 weeks. Figure 19 shows the CA measurements taken during the aging period to monitor the changing wettability. Formation brine and DI without any chemical additives were used as the aqueous phase for these measurements, hence the

determination of the optimum aging time and base case or reference wettability for the surfactant study.

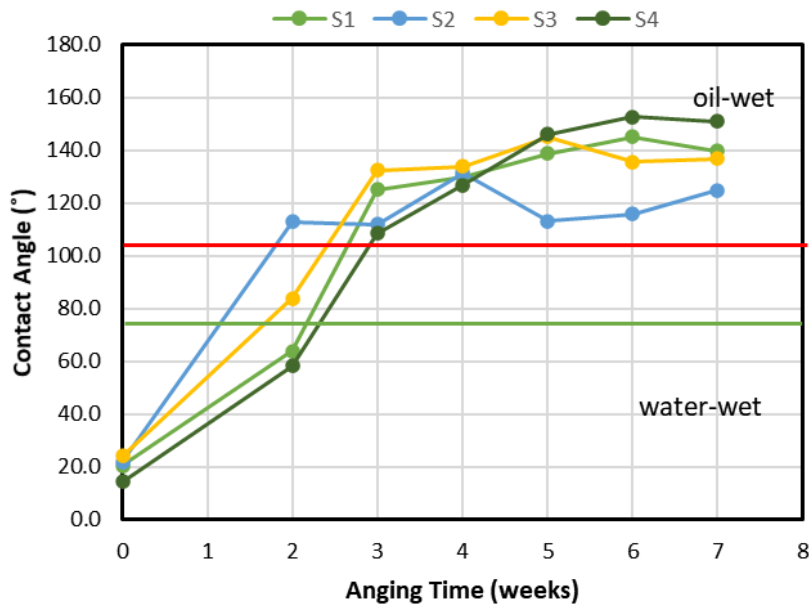


**Figure 19: Aging study data showing contact angles measured in formation brine at 170°F. CAs show shift towards oil-wet with increasing aging time.**

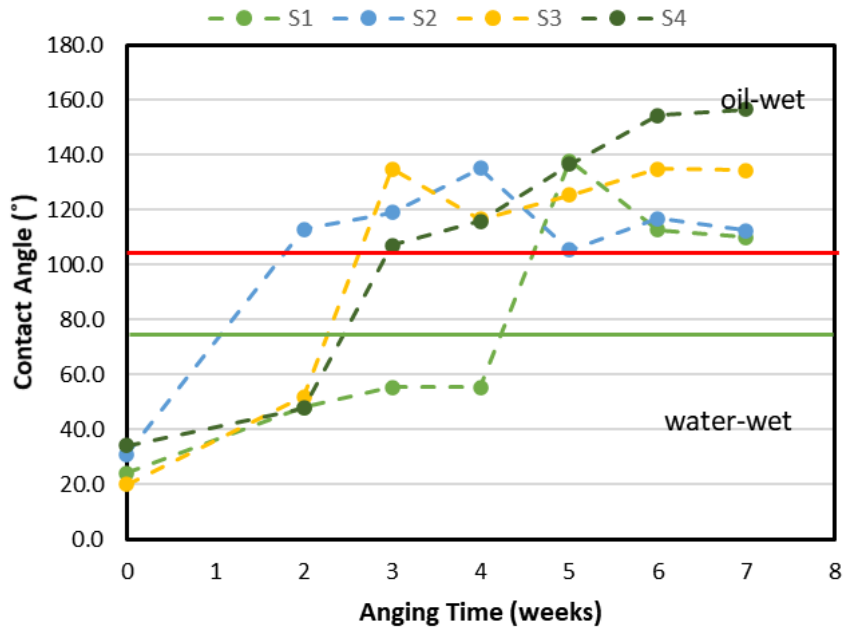


**Figure 20: Aging study data showing contact angles measured in DI water at 170°F. CAs show shift towards oil-wet with increasing aging time.**

### **Oil Sample**

The oil sample used in this study was from the Seidel Unit intervals of the Eagle Ford reservoir. The oil was centrifuged and vacuumed before the start of experiments to remove trace amounts of solids and residual gas, respectively. Using the Anton Paar's DMA 4100M, density was then measured at approximately 0.78 g/cc at 60°F and 49.1 °API which indicates light oil. The low-pressure CA and IFT measurements were performed at 170°F, at which the oil density was approximately 0.74 g/cc, while at reservoir temperature of 325°F, oil density is 0.67 g/cc. SARA analysis was also conducted on the sample, and the results are tabulated below:

**Table 2: Eagle Ford SARA composition**

<C15	56.41
Saturates (%)	88.41
Aromatics (%)	7.88
Nitrogen, Oxygen and Sulphur (NSO) (%)	3.71
Asphaltene (%)	0.00
Sat./Aro.	11.23

### **Surfactant and Brine**

This study, as mentioned previously, aimed to investigate the use of nonionic surfactants at high-temperature reservoir conditions. To achieve this, nonionic surfactants with different head groups and hydrocarbon tail groups were first screened using the high-

pressure cloud point tests to determine thermal stability. Next, the surfactants were used in the CA and IFT tests to investigate the wettability altering behavior.

The nonionic surfactants are characterized by the Ethylene Oxide (EO) group, which serves as the hydrophilic head group, allowing for solubility via the formation of hydrogen bonds with the water molecules. The EO number of the nonionic surfactants used in this study ranged between 5 and 40, with tail groups of Tridecanol, Alcohol Ethoxylate, and Nonylphenol. To improve thermal stability of the nonionic surfactants, ionic surfactants were blended in at lower concentrations to induce synergistic effects on the surfactant cloud point. Functional groups of the cationic surfactant used included Trimethyl Ammonium Chloride (TAC) and Dimethyl Ammonium Chloride (DAC); while those of the anionic surfactant was Internal Olefin Sulfonate (IOS) and Propylene Oxide Sulphate (POS).

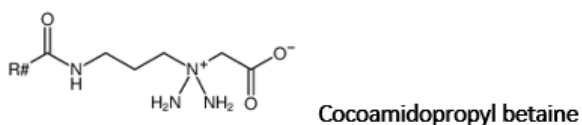
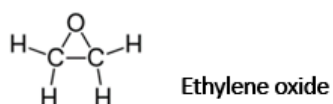
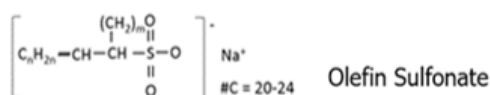
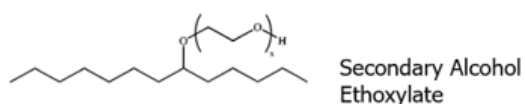
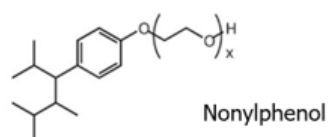
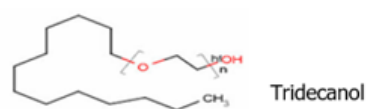
**Table 3: Molecular structure of surfactants tested in the study.**

<b>Surfactant Alias</b>	<b>Head Group</b>	<b>Tail Group</b>
<b>N1</b>	5 EO	Alcohol Ethoxylate
<b>N2</b>	7 EO	
<b>N3</b>	12 EO	Tridecanol
<b>N4</b>	18 EO	
<b>N5</b>	30 EO	
<b>N6</b>	50 EO	



<b>Surfactant Alias</b>	<b>Head Group</b>	<b>Tail Group</b>
<b>N7</b>	12 EO	Nonylphenol
<b>N8</b>	20 EO	
<b>N9</b>	30 EO	
<b>N10</b>	40 EO	
<b>N11</b>	55 EO	
<b>N12</b>	20 EO	Secondary Alcohol Ethoxylate
<b>N13</b>	30 EO	
<b>N14</b>	40 EO	
<b>C1</b>	TAC	C18
<b>C2</b>	TAC	C12
<b>C3</b>	DAC	2 x C10
<b>A1</b>	OS	C15 – C18
<b>A2</b>	OS	C20 – C24
<b>A3</b>	7 PO + AS	C12 – C13
<b>A4</b>	S	C12
<b>Z1</b>	B	12 CAP
<b>EO</b>	Ethylene Oxide	
<b>OS</b>	Olefine Sulfonate	
<b>PO</b>	Propylene Oxide	

<b>AS</b>	Alkoxy Sulfate
<b>TAC</b>	Trimethyl Ammonium Chloride
<b>DAC</b>	Dimethyl Ammonium Chloride
<b>B</b>	Betaine
<b>S</b>	Sulfate
<b>CAP</b>	Cocoamidopropyl



The surfactants concentration was measured in wt%, with a brine formulation representing typical makeup water (MW) obtainable at the well location. The selected surfactants were then tested in the produced water (PW) from the corresponding well. The makeup and produced water contain total dissolved solids (TDS) of approximately 0.18% and 2.5%, with the ion concentrations varying as seen in Figure 21. The final brine

formulation used was modified to correct for turbidity, resulting from bicarbonate anions with magnesium and calcium cations.

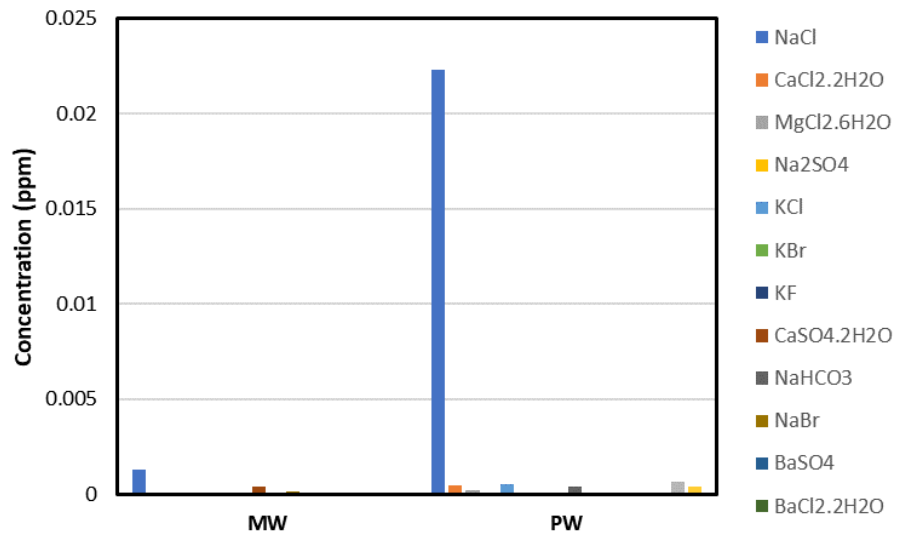
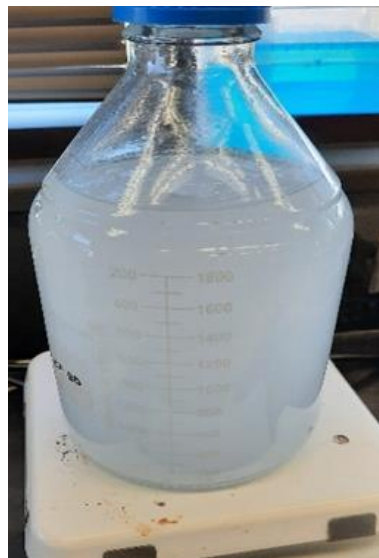


**Figure 21: Ion concentration of the makeup and produced water with TDS of 0.18% and 2.5% respectively.**



Original formulation of produced water      Modified formulation of produced water

**Figure 22: Image showing change in turbidity noted after variation of bicarbonate concentration.**

## **High-Pressure Cloud Point**

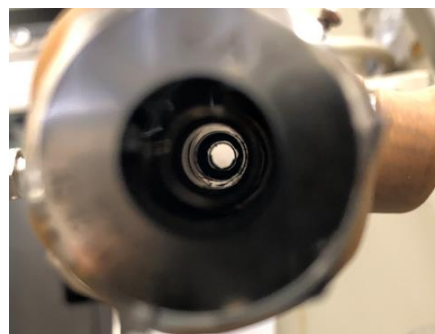
Cloud point measurement was achieved using a custom fabricated heating chamber with viewing windows tagged ‘the Trombone’ shown in Figure 23. 100 cc of surfactant solution is injected into the heating tube, sealed, and pressurized to 250 psi. Heating tape secured to the tube is then used to raise the solution's temperature while a thermometer probe placed within the chamber records temperature. The opacity of the heating solution is recorded using a camera mounted at one end and focused on the viewing window adjacent to the cell.

The temperature at which the solution becomes turbid is observed as the maximum opacity of the fluid, preventing visualization through both viewing windows. This temperature is recorded as ‘cloud point-heating’. The heater is turned off at this point, and the solution can equilibrate and cool at its own pace. As cooling occurs, the solubility of the surfactant is regained as the temperature falls below the cloud point. The temperature at which the camera recovers clear visuals through both viewing windows is recorded as ‘cloud point-cooling’.

It has been observed that heating and cooling cloud point temperatures vary regardless of the surfactant solution tested. Therefore, the selection criteria during the cloud point tests are based on the cooling temperature. It is closer in value to results obtained by visual determination using vials heated in water-baths, which is the traditional method of cloud point measurement.



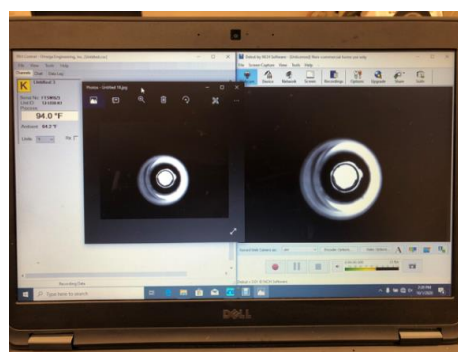
**Overview**



**Viewing Window**



**Overview**



**Laptop View**

**Figure 23: Setup for high-pressure cloud point measurement.**

### **Contact Angle and Interfacial Tension**

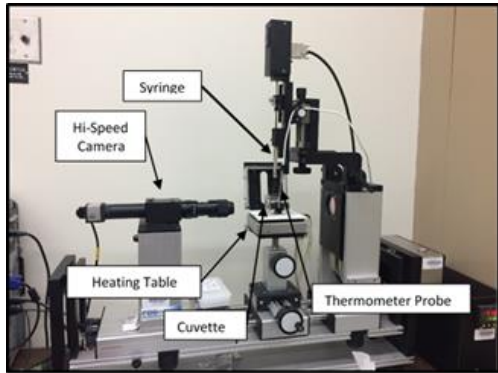
This study's contact angle data were measured by utilizing the captive bubble method on the Optical Contact Angle goniometer (OCA15 Pro) for establishing baseline wettability at room temperature and temperatures up to 170°F. The aged rock is placed on a stage in the aqueous phase contained within a glass cuvette, and a drop is dispensed using a j-shaped needle. Software was then used to estimate the oil-rock contact angle,  $\theta_m$ . To determine if the surface is water-wet or oil-wet, the water-rock contact angle is required. This is obtained by a simple conversion using the following equation:

$$180 - \theta_m = \theta_{water}$$

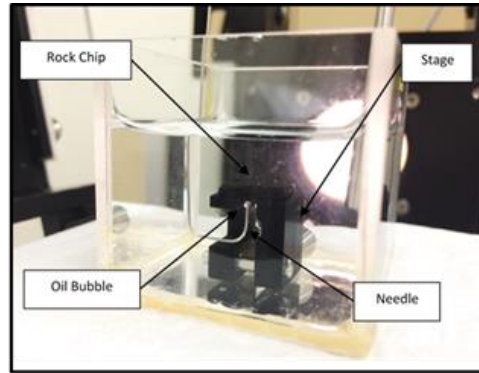
**Equation 8**

where  $\theta_m$  is the measured contact angle from the software and  $\theta_{water}$  is the contact angle with respect to the aqueous phase, in degrees.

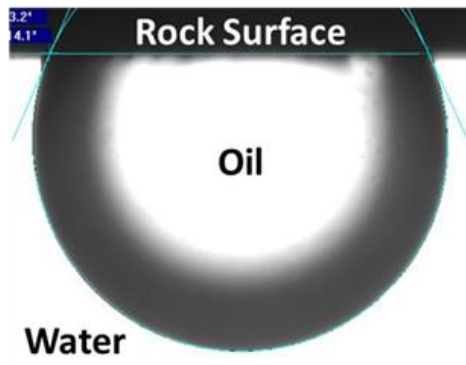
For each experimental condition, the contact angle was averaged with 6 measurements to ensure repeatability and consistency. It was observed that all surfactant formulations were able to alter wettability from the oil-wet state created after aging to either intermediate or water-wet depending on concentration and the thermal stabilizer used.



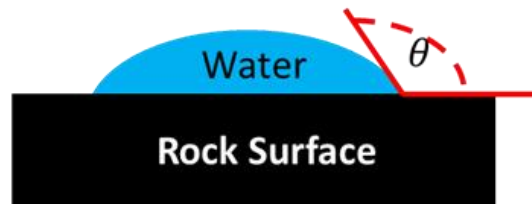
Dataphysics OCA 15 Pro



Set-up for contact angle



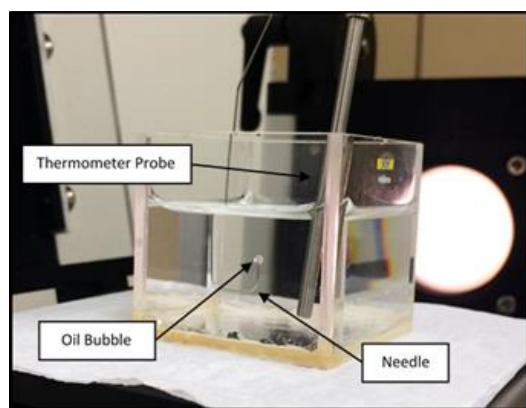
Measured angle



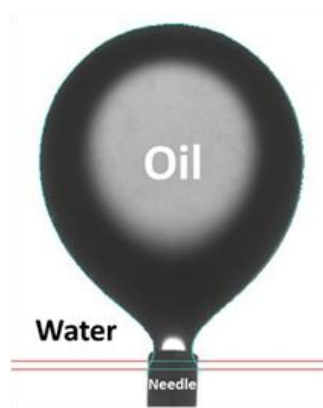
Convention angle

**Figure 24: Setup for contact angle measurement on the Dataphysics OCA 15 Pro.**

IFT measurements were also conducted on the Dataphysics OCA15 Pro apparatus. The pendant-drop method was used to measure IFT by suspending an oil droplet in the aqueous phase and conducting axisymmetric shape analysis of the droplet with software that calculates the IFT by fitting the drop profile with the Young-Laplace equation using a contour-fitting algorithm.



Set-up for interfacial tension



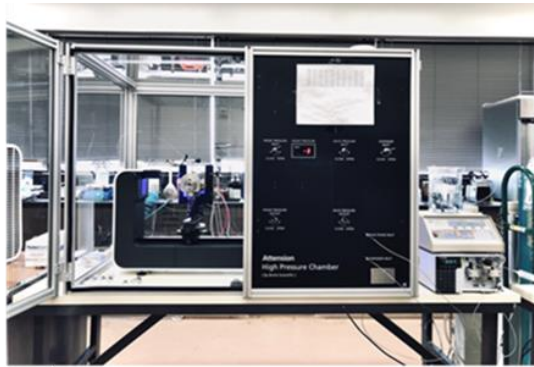
Captured bubble for IFT

**Figure 25: Setup for interfacial tension measurement on the Dataphysics OCA 15 Pro.**

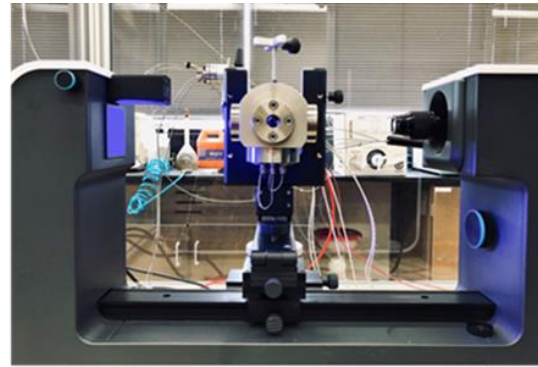
### **High-Pressure High-Temperature Contact Angle and IFT**

To determine if the surfactant solutions formulated are capable of wettability alteration at reservoir temperature, the Biolin Theta Flex mounted with a high-pressure chamber was used. Similar to the Dataphysics device, the rock chip was positioned on a stage that is enclosed in a high-pressure steel chamber. The aqueous phase used is introduced into the cell and then sealed. A needle was utilized to dispense an oil drop at the bottom-facing surface of the rock. Images of the drop were then recorded, and the contact angles were extracted from these images by the digital analysis software provided

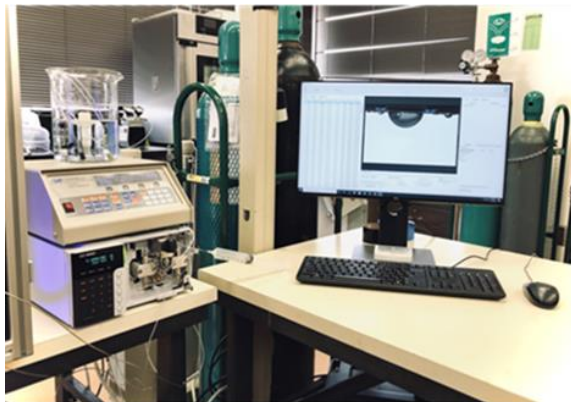
with the device. The drop is observed from room temperature to reservoir temperature of 325°F as pressure is increased from 500 psi to 3000 psi.



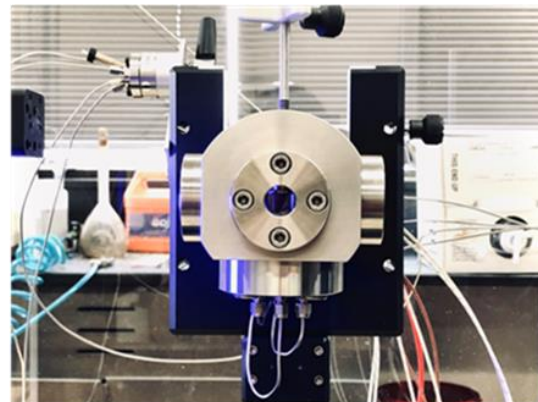
**Overview of HPHT CA-IFT**



**Cell and Camera System**



**Pump and Software Controller**



**HPHT Cell**

**Figure 26: Setup for the high-pressure high-temperature study on the Biolin Theta Flex.**

### **Spontaneous Imbibition**

Spontaneous imbibition is the process through which the non-wetting fluid is displaced by the adsorption of the wetting fluid as a result of capillary forces. For oil-wet rock, introduction of surfactants may alter wettability towards water-wet thereby increasing capillary forces and improving production via counter-current flow. Therefore,



the spontaneous imbibition experiment serves as the final stage in the qualitative test for wettability and validates the result of the preliminary wettability alteration tests. This is because the capillary forces which give rise to spontaneous imbibition is a result of the contact angle and interfacial tension in the oil-brine-rock system.

Clean cores intended for this experiment were first aged at reservoir temperature for a period of 24 weeks. The saturated cores were then placed in custom fabricated high-pressure Amott cells. The Amott cells were filled with the surfactant solutions and one sample with brine to serve as the base case; and placed in ovens to simulate reservoir temperature. During the period of the experiment, the aqueous phase was slowly imbibed into the core while oil was expelled. The produced oil was measured with the aid of a graduated cylinder, and the experiment was terminated when oil production from the cores was observed to plateau. The results of this study were then used to calculate the oil recovery factor and determine what surfactant successfully improved recovery from the high-temperature Eagle Ford reservoir.

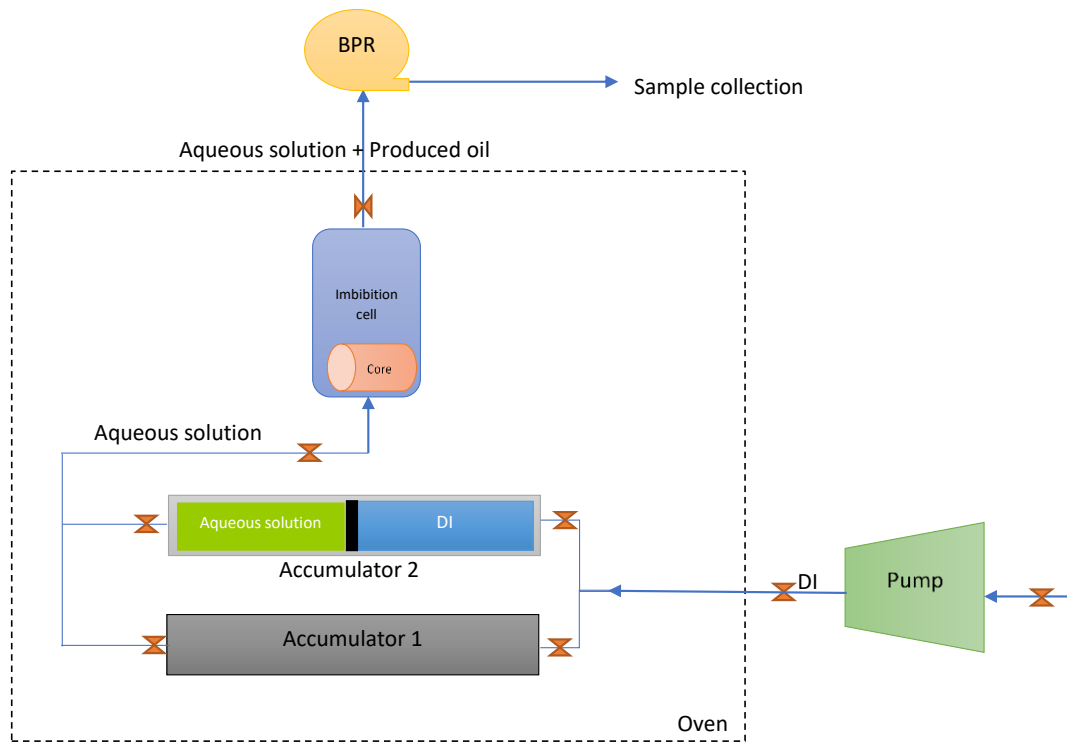


**Figure 27: Setup for spontaneous imbibition experiment.**

CT imaging was also used during this study to visualize the extent of penetration of the surfactant systems deployed in the spontaneous imbibition experiments. The non-destructive imaging technique uses x-rays to produce tomographic images of specific areas of the cores with a Toshiba Aquilion TSX-101A CT scanner. The shale cores were scanned prior to the start of the imbibition experiment and at the end. Image analysis is then performed using open-source imaging software such as ImageJ or Slicer. The difference in density between aqueous and oil phases leads to a difference in CT numbers with brighter colors (higher CT numbers) representing higher densities while darker colors (lower CT numbers) representing lower densities.

## CHAPTER IV

### CLOUD POINT

In the selection of surfactants and other chemical for EOR, stability under reservoir conditions is of great importance. Therefore, for nonionic surfactants known to exhibit phase separation at temperatures known as the surfactant cloud point, the high-pressure cloud point study was used to identify high-performance surfactant solutions for use in the harsh environment of the Eagle Ford reservoir.

The results presented in this section are of tests on single nonionic surfactants as well as nonionic-ionic surfactant blends created to extend cloud point beyond reservoir temperature. The effects of the surfactant molecular structure, surfactant charge, salinity, and other additives were evaluated to understand the mechanism of turbidity in nonionic surfactants and help select the suitable formulation for wettability alteration tests.

#### **Low-Pressure Test**

Various nonionic surfactants with varying structures, nonylphenol ethoxylates, tridecyl alcohol ethoxylate, alcohol ethoxylates and secondary alcohol ethoxylates; in addition to varying ionic surfactants, olefin sulfonates (IOS), tri/dimethyl ammonium chloride; were obtained from various chemical companies.

The nonionic surfactants were made into solutions of 0.4 wt% using synthesized makeup water which contained 0.18% TDS. To identify surfactants with the lowest cloud points, 100ml vials of solutions were placed in a water bath and heated at atmospheric pressure to boiling point with the aid of a plate heater. The first appearance of turbidity was then noted as the cloud point for the sample solution. Figure 28 shows the results for

some of the nonionic samples tested. Samples N1, N2, N3, and N7, were observed to have cloud points below boiling point while the other samples remained thermally stable, exhibiting no phase separation below 212°F.

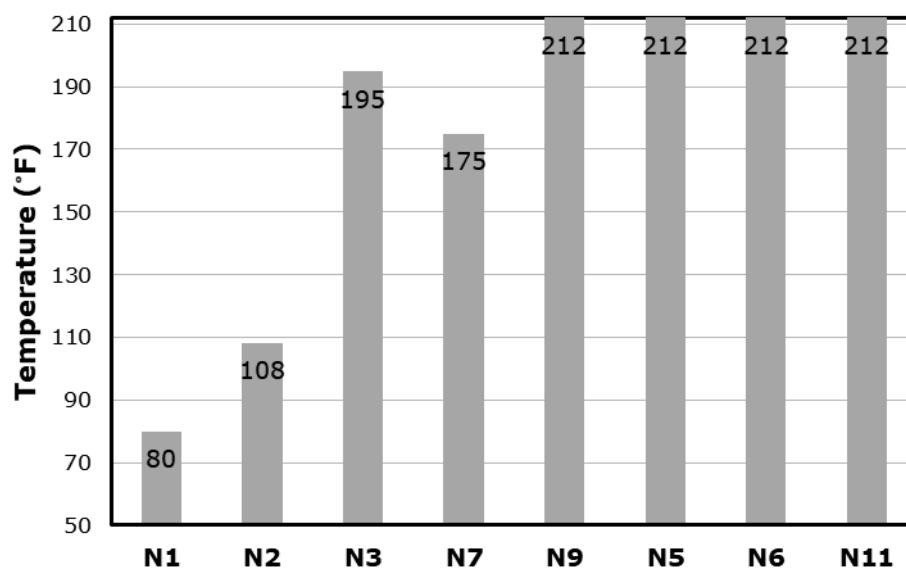


**Figure 28: Cloud points of various samples of nonionic surfactant. The increment in CPT occurs with an increase in EO groups. (N1, N2, N3 < 30 EOs ≥N5, N6, N9, N11) Note: concentration of surfactant was 0.4 wt%.**



**Figure 29: Image of surfactant samples during cloud point tests at low-pressure conditions before heating (left) and above the cloud point (right).**

Literature on nonionic surfactants has shown that the addition of small quantities of ionic surfactants into single-phase aqueous nonionic surfactant raises cloud point (Valulikar and Manohar 1985, Gu 1989, Sharma and Bahadur 2002). This study used this approach to improve the performance of the nonionic samples tested, creating a unique blend that would serve as the wettability and IFT altering blend for the high-temperature reservoir.

Upon Identifying single surfactants with cloud points above 212°F, surfactant N2 was selected as a proxy to serve as the nonionic surfactant in a series of solutions that included 0.02 wt% ionic surfactant. These sample solutions were then heated using the same setup made for the single nonionic samples. It was observed that both anionic, cationic, and zwitterionic surfactants were able to elevate the cloud point temperature of N2. Cationic samples C1 and C3 outperformed the other ionic and zwitterionic samples,

raising cloud point by approximately 60%, while anionic sample A1 was able to achieve an increase of approximately 50%.

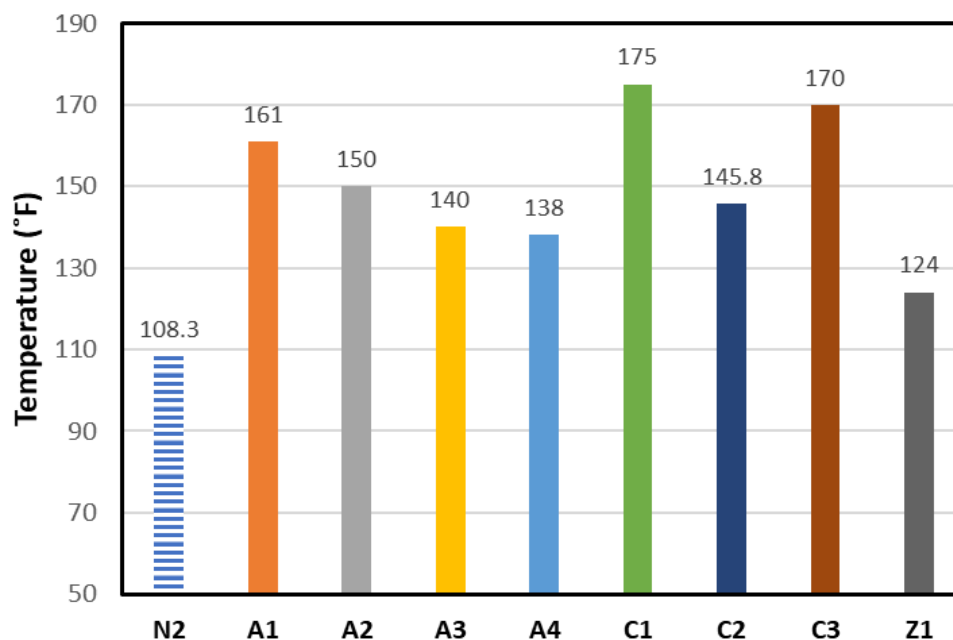


**Figure 30: Cloud point of single surfactant N2 (left) and blends containing anionic, cationic, and zwitterionic surfactants. Note: Main surfactant N2 is at a concentration of 0.2 wt%, and ionic surfactants at a concentration of 0.02 wt%.**

Based on the results from the proxy, surfactants C1 and A1 were then used in combination with the proxy to evaluate the effect of interference of ionic molecules. It was observed that the mixture of anionic and cationic surfactant tended to an intermediate performance as concentration was increased.

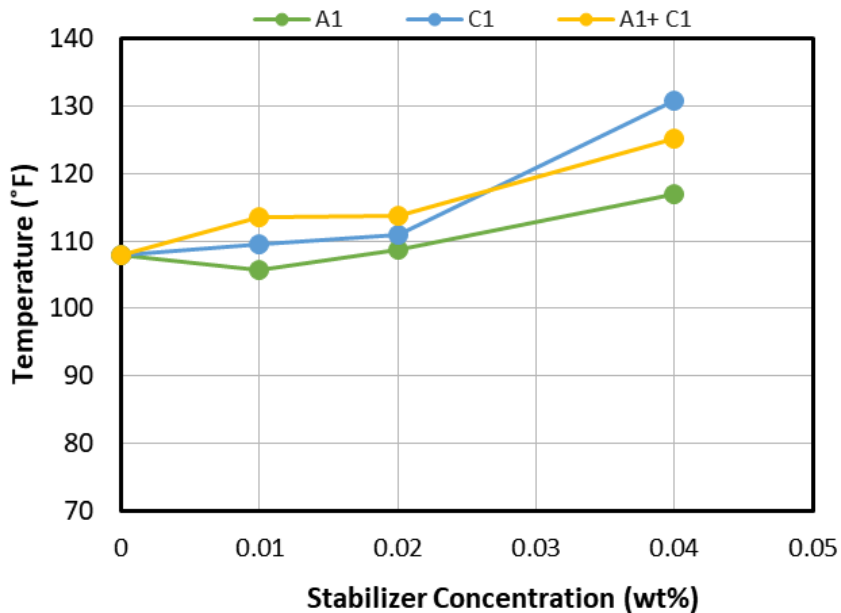


**Figure 31: Cloud point of surfactant blends showing increase in CPT with increasing co-surfactant concentration. For ternary mixture, change in CPT is between those observed with single ionic co- surfactant. Main surfactant, N2 at concentration of 0.2 wt%. Aqueous phase used produced water.**

### High-Pressure Test

To evaluate surfactant thermal stability at reservoir temperature, a custom pressurized heating instrument that allowed viewing of turbidity was used. Nonionic samples which were determined to have cloud points higher than 212°F were tested in the pressurized vessel to allow heating of fluid to 400°F. The influence of molecular structure, brine salinity, surfactant concentration was investigated to determine the ideal surfactant combination to be deployed for the reservoir under consideration.

### **Effect of Ethylene Oxide Number**

The solubility of nonionic surfactants depends on the formation of hydrogen bonds between the surfactant head group and the water molecule (Massarweh and Abushaikha 2020, Al-Sabagh 2011). Studies have shown that increasing the EO number leads to increasing cloud point due to an increased ability to hydrate and increased repulsion between micelles as the hydrophilic group increases (Curbelo 2013, Al-Sabagh 2011, Gu and Sjoblom 1991).

When combined with ionic surfactants, the cloud point of nonionic surfactants increases due to the creation of micelles that carry electrostatic charges. The increase in cloud point results from increased repulsion between the mixed micelles (Valulikar and Manohar 1985, Sadaghiana and Khan 1990, Li et al. 2009).

As shown in Figure 32, three groups of surfactants were tested, X (Tridecanol), Y (Nonylphenol), and Z (Secondary Alcohol Ethoxylate). The increase in the EO group was observed to lead to a decrease in cloud point.



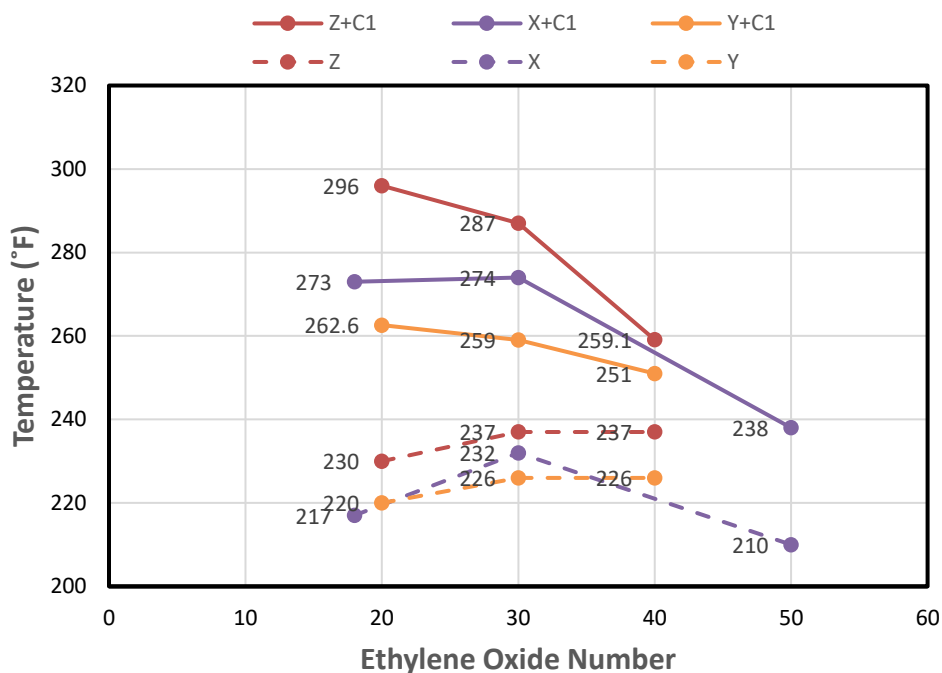


**Figure 32: Effect of EO number on cloud point. Single surfactants (X, Y, Z) display lower CPT compared to mixtures containing ionic co-surfactant. Note: Nonionic surfactant used is at 0.2 wt% and stabilizing ionic surfactant C1 is at 0.02 wt%.**

### Effect of Ionic Surfactant

The use of surfactant blends has been shown to improve performance. Given the investigation results into the influence of EO number, surfactants with smaller EO groups were chosen for this phase of the investigation.

First, 0.2wt% of the nonionic surfactants was tested in combination with C1, the best performing ionic stabilizer. The concentration of C1 was varied between 0.02 wt%, 0.05 wt%, and 0.1 wt%. It was observed that increasing the ionic surfactant concentration led to increasing cloud point temperatures, with all three surfactants tested displaying cloud point above reservoir temperature where 0.1 wt% of cationic surfactant was

introduced in solution. Surfactant N4 with a cloud point at 244°F showed the greatest improvement in thermal stability, having a cloud point temperature of 327°F when 0.1 wt% of C1 was introduced in the solution.

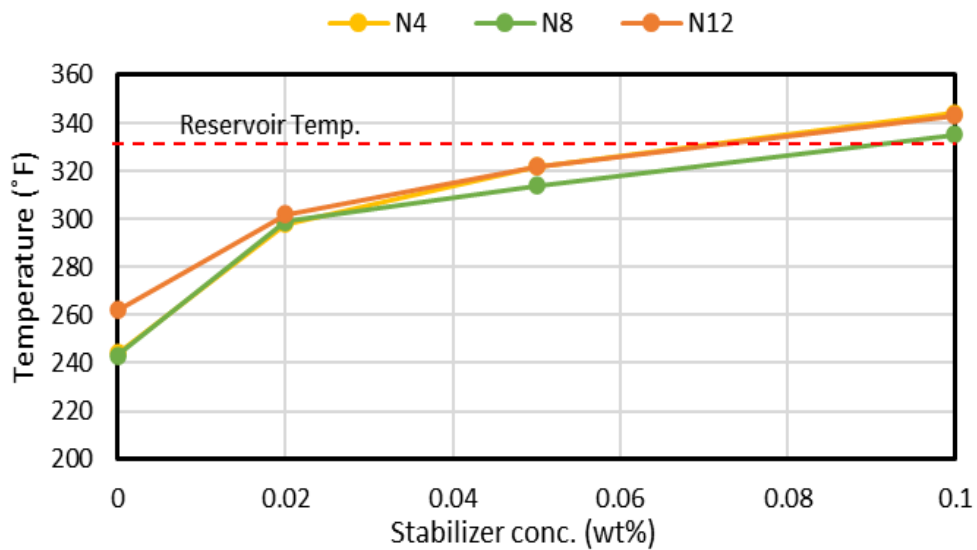


**Figure 33: Cloud point temperature of nonionic surfactants N4, N8, and N12 at a concentration of 0.2 wt% and ionic stabilizer C1 at 0.1wt%. Increasing the concentration of ionic co-surfactant leads to varying increments on the CPT for the different classes of nonionic surfactant with similar number of EOs.**

The investigation into ionic surfactants then proceeded with the use of N4 to create other ionic blends of varying total concentrations.

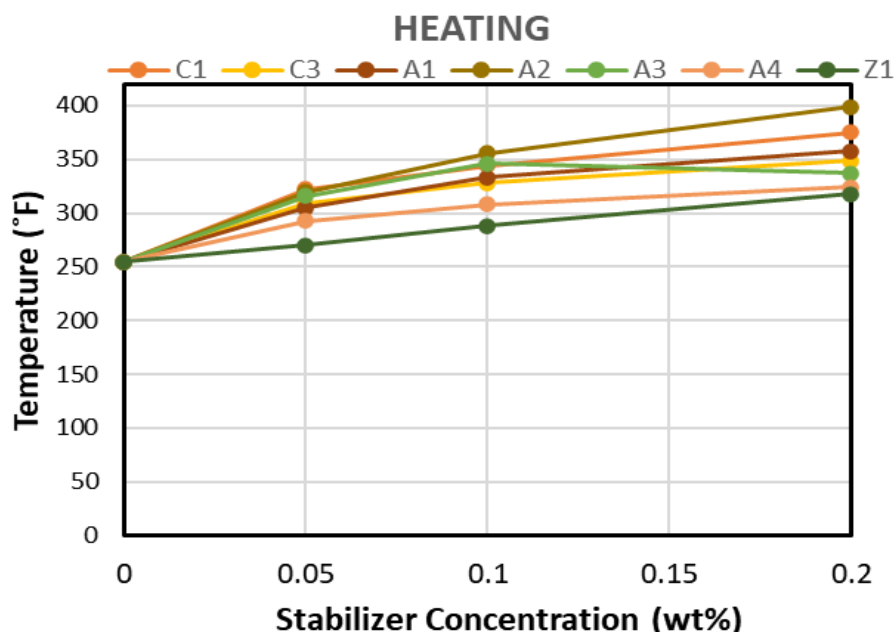


Figure 34: Cloud point temperature recorded during heating of solutions containing ionic stabilizers at varying concentrations. Increasing hydrophobicity and concentration of the ionic stabilizers leads to improved CPT. Note: Nonionic surfactant used N4 at a concentration of 0.2 wt%.

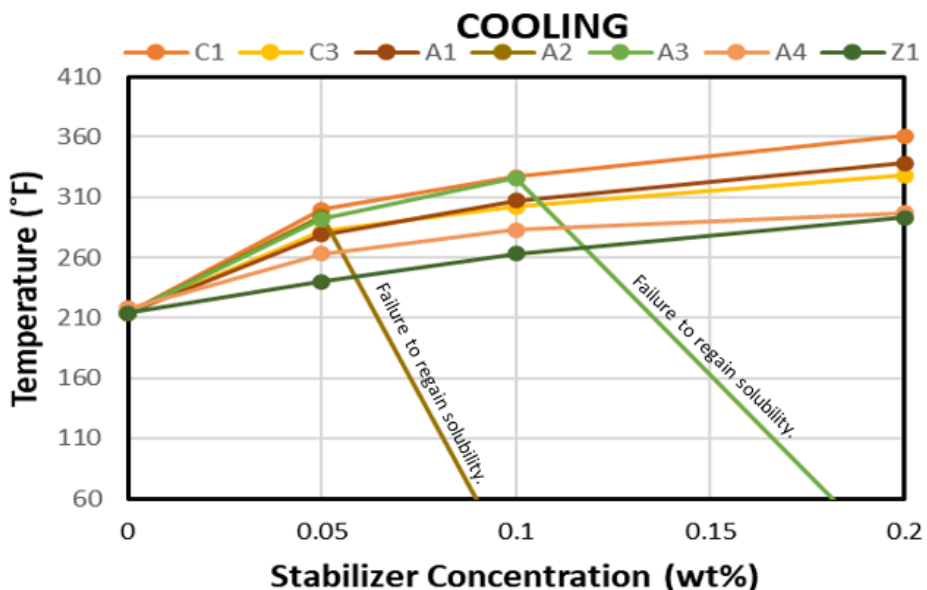
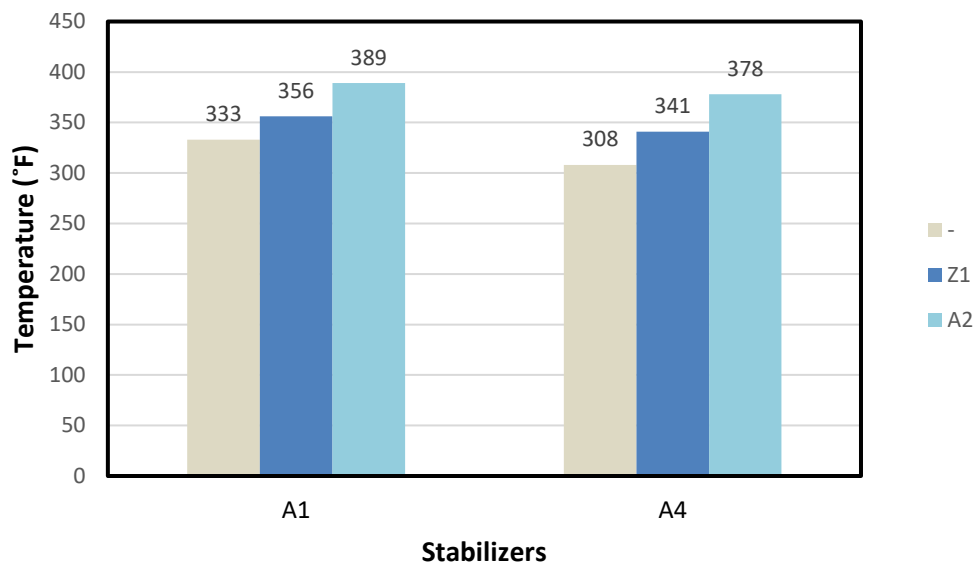


Figure 35: Cloud point temperature recorded during cooling of solutions containing ionic stabilizers at varying concentrations. Anionic surfactants are observed to

**remain turbid during cooling. Note: Nonionic surfactant used N4 at a concentration of 0.2 wt%.**

The effect of the different ionic surfactants is shown in Figure 34 and Figure 35. These plots show that both anionic and cationic surfactants have a tremendous effect on cloud points. The increase in cloud point temperature was observed to improve with the increase in the hydrophobic nonpolar tails of the ionic surfactant. Surfactant A2, which possessed the longest hydrocarbon tail, C20 to C24, was observed to raise cloud point from 255°F to 399°F. Interestingly, surfactant C3, whose molecular structure includes a double hydrocarbon chain of C-10, was observed to generate an improvement less than that of C1 (C-18) or A1 (C-15 to C-18), indicating the influence of the molecular structure. During high-pressure wettability tests, the surfactant blends containing single ionic stabilizers were observed to cloud below reservoir temperature. This necessitated the investigation of ternary surfactant blends made of two ionic surfactants to serve as a thermal stabilizer. Both ionic stabilizers were used at concentrations of 0.1 wt%, to result in a total ionic concentration of 0.2 wt%, which matches the main surfactant. As shown in Figure 36, surfactants A1 and A5 further increased the cloud point of N4 when Z1 and A2 were added. Similar to results seen for the single thermal stabilizers, A2 with a longer hydrophobic chain led to the greatest improvement in CP.



**Figure 36: Improvement in cloud point temperature of ternary surfactant blends compared to binary blends (grey). Increment in CPT is higher with the introduction of co-surfactant A2 compared to Z1. Note: Nonionic surfactant used N4 at a concentration of 0.2 wt%, ionic-cosurfactants, A1, A2, A4 and Z1 at concentration of 0.1 wt%.**

In general, increased interaction is observed when a hydrophobic nonionic surfactant is in solution with an ionic cosurfactant. The mixed surfactant system displays improved thermal stability which increases with the length of the hydrophobic tail on the ionic surfactant. Two theories offer up explanations of the remarkable increase in cloud point observed in the mixed surfactant system—first, intermicellar repulsion generated by the mixed micelles. Van der Waals interactions existing between the apolar hydrophobic tails allows for creation of surfactant micelle whose hydrophilicity is supported by the head groups of both nonionic and ionic surfactant; while possessing electrostatic charges from the ionic surfactant. And second is the effect of the more soluble ionic surfactant with a long alkyl chain. A study by Al-Sabagha (2011) explains why the length of the

alkyl chain affects CP. The increasing alkyl chain length is believed to increase the distortion motion of the surfactant molecule in solution, which in turn allows the EO chain decoil, and its exposure increases the number of sites for hydrogen bonding. The increased hydration, therefore, leads to higher CP temperatures.

### **Effect of Salinity**

The use of surfactants in low salinity brine has been shown to improve the thermal stability of nonionic surfactants, as cloud points decrease with increasing salinity (Curbelo 2013, Al-Sabagh 2011, Li 2009, Sharma 2002, Gu et al. 1989). In this study, brine formulations matching the ionic content of the formation fluid, 2.4% TDS, as well as brine simulating formation fluid at 8%, 16%, and 24% TDS were made. These values were selected to represent the wide range of salinity recorded in shale plays. The different brine samples were used as the aqueous phase for surfactant solutions containing N4 as a single surfactant and in combination with C1 and A3.

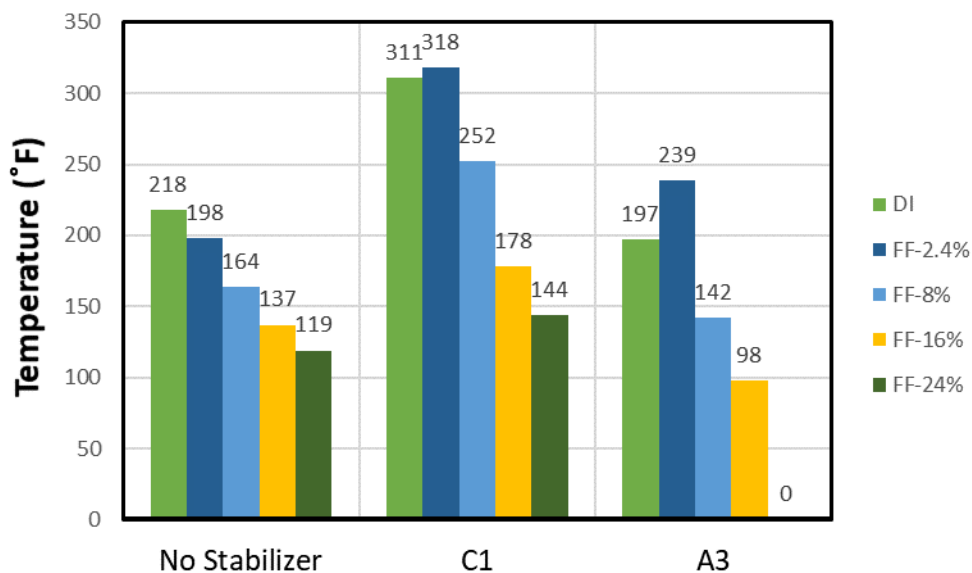


**Figure 37: Effect of salinity on cloud point temperature. For nonionic surfactant N,4 with no ionic co-surfactant to serve as thermal stabilizer, and surfactant systems with C1 and A3 as co-surfactant, increasing brine salinity leads to decrease in CPT. With exception of FF:2.4% in the mixed surfactant system which performs better than the DI case. Note: Main surfactant used N4 (0.2 wt%).**

As observed in Figure 37, increasing the salinity of the aqueous phase led to a corresponding decrease in the cloud point of both nonionic surfactant and nonionic-ionic blends. It was noted, however that at a TDS of 2.4%, cloud point was seen to slightly increase for the surfactant blends when compared to the base case in deionized water. It is believed that the presence of the structure making ions,  $\text{Cl}^-$ ,  $\text{Br}^-$  and multivalent cations in the brine improved the cloud point temperature when compared to DI as the aqueous phase. This is because these ions hinder the self-association of water molecules and lead to an increase in hydrogen bond formation between the water molecules and the nonionic surfactant ether group (Huibers et al. 1997, Sharma 2002, Li 2009). However, with the increase in the total salt concentration, the effect of  $\text{Na}^+$ ,  $\text{K}^+$ , and multivalent anions ( $\text{SO}_4^{2-}$

and  $\text{CO}_3^{2-}$ ); structure making ions increase, therefore leading to the salting-out phenomenon reported in the literature which reduces aqueous solubility of the nonionic surfactant and consequently the cloud point temperature.

### **Effect of Alcohols**

The presence of alcohols in the aqueous phase has been shown to improve the hydrogen bond formation between the head group of the nonionic surfactant molecule and the solution, resulting in improved solubilization (Nasr-El Din 1996). Li (2009) observed that short-chain alcohols, methanol, ethanol, and propanol; modified the solvent water, leading to the formation of a less polar medium. This in combination with the adsorption of these alcohols at the micelle–water interface creates a restriction in the micellization of surfactant molecules, which leads to an increase in cloud point. Here, methanol was used during the first set of experiments at 10%, 20%, and 30% of the aqueous phase. It was observed during the heating process that the solutions did not display a definitive cloud point, as the onset of turbidity was gradual and difficult to distinguish, as seen in Figure 38. Isopropanol deployed at 5%, 10%, and 30% was also observed to result in mild turbidity, which allowed some visualization at temperatures of 400°F. Therefore, the presence of alcohols can be seen to improve CPT, increasing with increasing concentration although varying for the different surfactant combinations, as seen in Figure 39 and Figure 40.



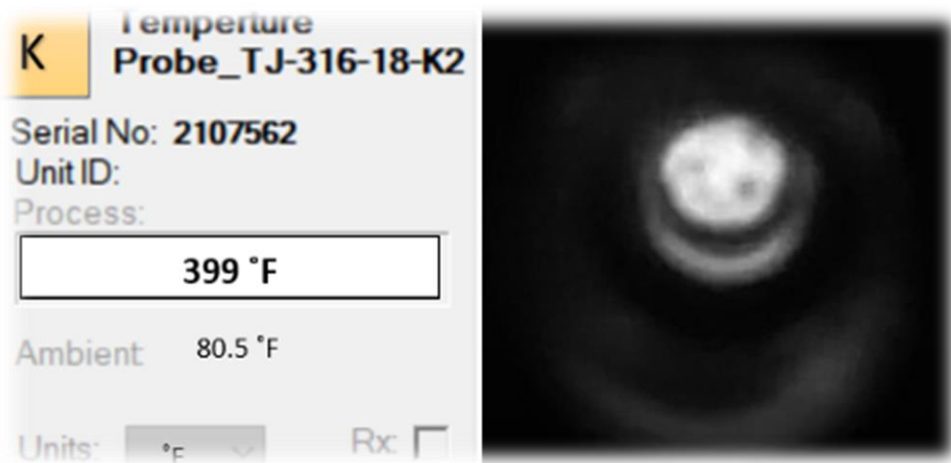


**Figure 38: Laptop view during cloud point experiment on the Trombone for solution with methanol. The photos show at 399°F on the RHS the solution shows slight change in turbidity compared to the clear solution on the LHS, i.e., turbidity is not distinct during heating.**

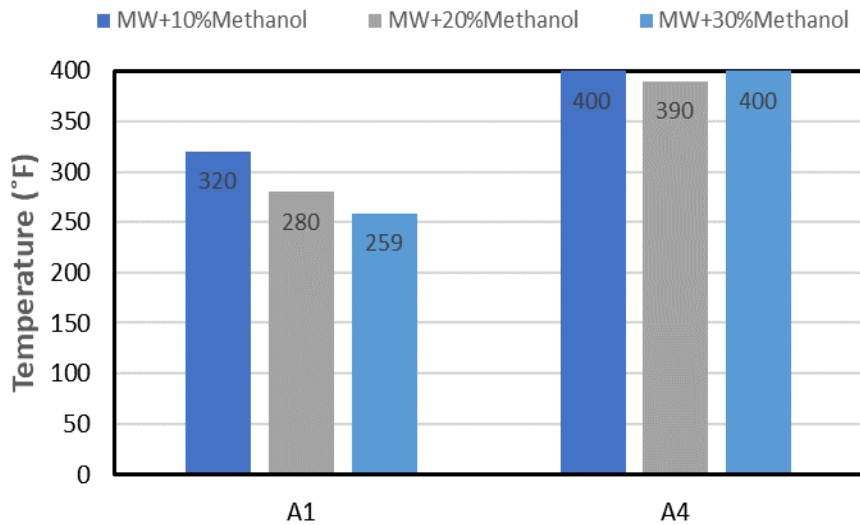


**Figure 39: Change in cloud point temperature (heating) due to addition of methanol. Data is grouped based on co-surfactant and shows better improvement with the more hydrophobic stabilizer A4. Note Main surfactant used N4 (0.2 wt%), ionic surfactant (0.2 wt%).**

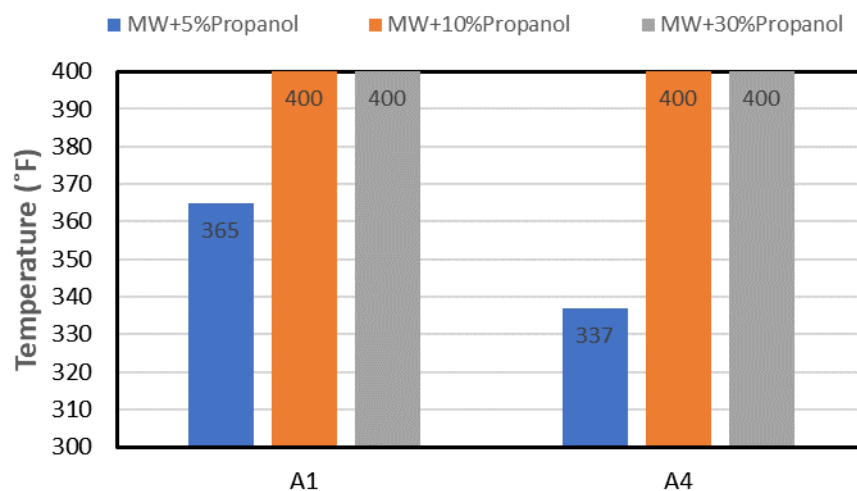


**Figure 40: Change in cloud point temperature (heating) due to addition of isopropanol. Data is grouped based on co-surfactant and it shows increase in CPT with increasing concentration of isopropanol. Note Main surfactant used N4 (0.2 wt%), ionic surfactant (0.2 wt%).**

## CHAPTER V

### CONTACT ANGLE AND INTERFACIAL TENSION

For surfactants deployed in EOR, the properties of concern include the ability to:

- i. provide low contact angle (i.e., wettability alteration),
- ii. moderate to low oil/water IFT and,
- iii. stability at reservoir temperature and salinity.

Using the cloud point test thermal stability of the various surfactant blends has been evaluated. The following steps in the screening and selection process are the wettability alteration and interfacial tension tests to determine if the surfactant shows synergistic properties with the rock/oil system.

In this section, results from contact angle and IFT tests performed at low-pressure conditions and at reservoir conditions are presented. Using aged rock samples cored from varying depth of the Eagle Ford, successful wettability alteration is determined by comparing the CA of the aged-rock chip in PW and that in the surfactant formulation, likewise for IFT.

#### **Low-Pressure Tests**

##### **Contact Angle**

Using cores cut from four depths of the Eagle Ford baseline reservoir wettability was established. Rock-chips cut from the preserved cores initially were observed to be strongly water-wet. After aging in the reservoir oil sample at high temperature for 7 weeks, the rock-chip were reverted to the original reservoir wettability by adsorption of the polar compounds in the oil; seen previously in Figure 19 and Figure 20.



**Figure 41: Oil droplets deposited on rock-chips from varying depths of the Eagle Ford a. before aging and b. at the 7-week mark of the aging process.**

Nonionic surfactants have been selected as the primary focus of this study due to their lower CMCs as compared to ionic surfactants, their high degree of surface-tension reduction, and their relatively constant properties in the presence of salt, which result in better performance and lower concentration requirements (Muherei and Junin 2008). Given this focus, CA measurements were first attempted on the aged rock chips using single nonionic surfactants at concentrations of 0.2 wt%. Multiple contact angles were measured on the same rock chip, and to minimize error, the reported CA values are an average of 6 of the most repeated measurements. The results shown in Figure 42 demonstrate that nonionic surfactants do indeed alter the oil-wet reservoir rock to very water-wet; for instance, the initial CA of a chip from S2 was  $125^\circ$ , while the final CA with nonionic surfactant N9 was as low as  $17^\circ$ .

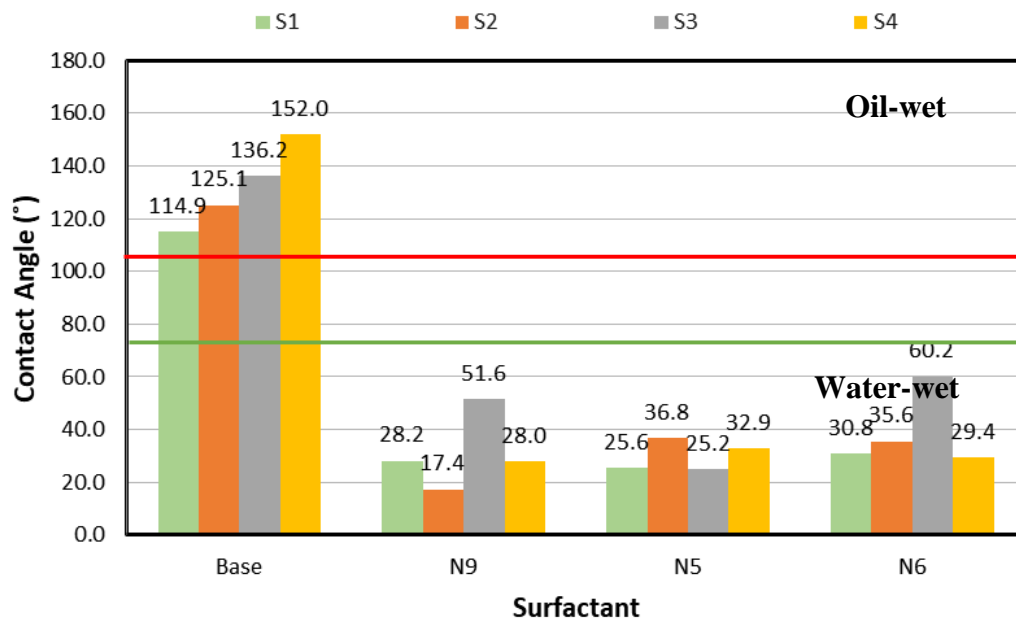


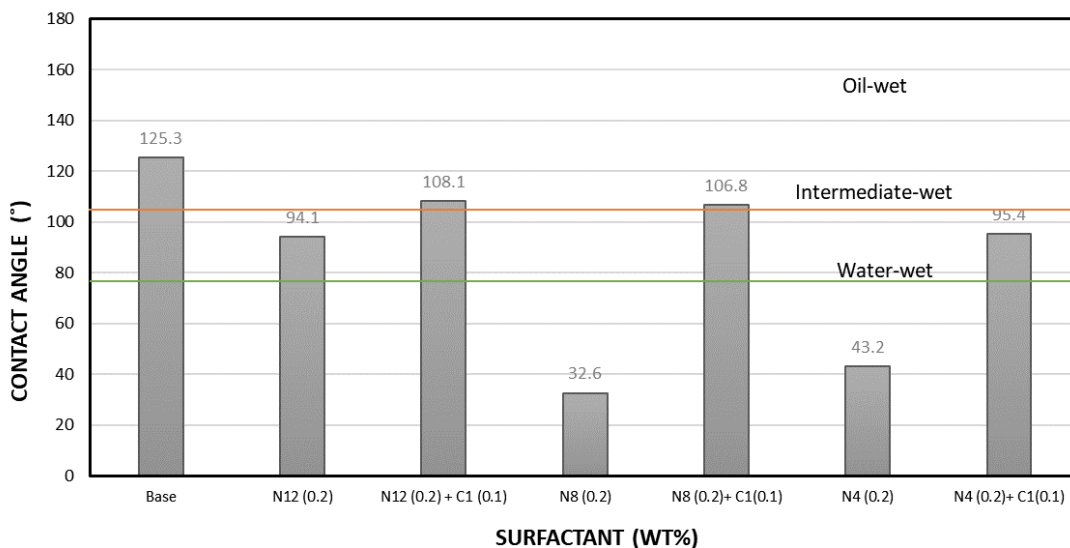
**Figure 42: Contact angle measurements on aged rock-chips (base case) using single surfactants to prove wettability alteration potential of nonionic surfactants. Note: concentration of surfactant used was 0.2 wt%.**

To simplify the CA experiments, chips from depths of 14049.20 to 14049.90 ft (S2) and 14206.65 to 14207.50 ft (S3) were selected as the representative reservoir rock samples for the remainder of the tests.

### Effect of the main surfactant on contact angle

Nonionic surfactants with lower EO groups have been shown to display improved wettability alteration, especially at higher temperatures than those with larger EOs due to increased adsorption (Das et al. 2020). From the results of the cloud point experiments on nonionic surfactants with varying EO groups, we observed that the smaller the number of EOs, the better the CP when the surfactant is used in combination with an ionic

cosurfactant as a thermal stabilizer. Surfactants N4, N8, and N12 in combination with C1 were therefore selected as the first of many CA measurements using binary surfactants to investigate the effect of the different nonionic structures on wettability alteration. Recall, the cloud point data for these blends are presented in Figure 33. It was observed that the blend of cationic surfactant, C1, increased the contact angles from water-wet ( $43.2^\circ$ ) to intermediate-wet ( $95^\circ$ ) for the N4, tridecanol of 18 EOs, while making the combination with N8, nonylphenol with 20 EOs slightly oil-wet ( $107^\circ$ ). N12, secondary alcohol ethoxylate with 20 EOs, made the aged chips intermediate-wet ( $94^\circ$ ) when used as a single surfactant and in combination became oil-wet ( $108^\circ$ ). These results show that although the nonionic surfactants can alter wettability, their performance is affected when deployed in combination with ionic surfactants which are intended to serve as thermal stabilizers. The change in performance may be antagonistic or synergistic.



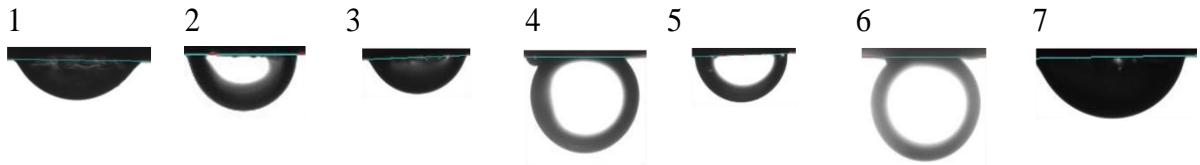


**Figure 43: Effect of cosurfactant as thermal stabilizer C1 on the contact angle of S2 chips measured at 170°F. Note: Base represents the contact angle after the aging 125.3° (oil-wet). Numbers 1 to 7 represent the sequence in the bar chart. CA decrease significantly in the presence of nonionic surfactant and increases when cationic-co-surfactant C1 is included.**

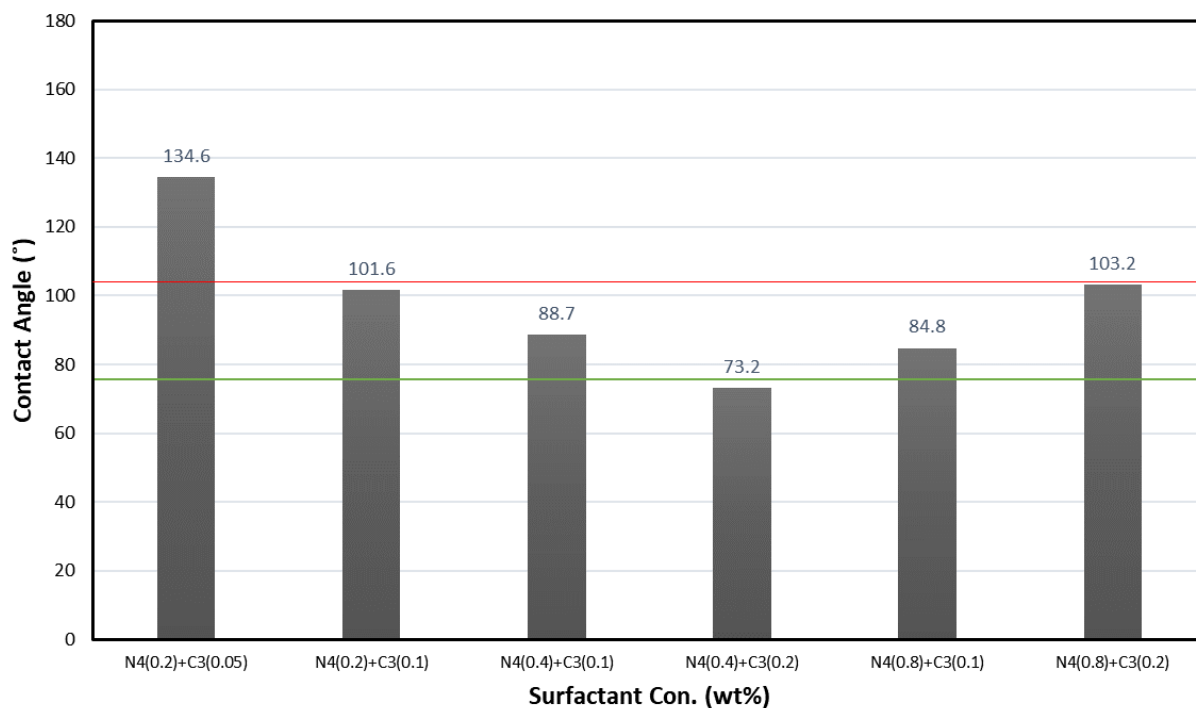
Due to the poor performance during these tests, LPT evaluations were discontinued on the N12 surfactant as it showed antagonistic behavior between the secondary alcohol ethoxylate and the brine/rock/oil system. The focus was then placed on the tridecanol, N4, which showed the best results in combination.

### **Effect of Charge of Ionic Stabilizer**

The effect of surfactant solutions on the wettability of a reservoir rock depends on the interactive forces at play in the brine/oil/rock system. Where oil-rock interactions are high, the CA observed is high, and the surface is preferentially oil-wet. Suppose the surfactant is successful in forming bonds with the oil (ion pairing), thus removing it from the rock surface while establishing interactions (electrostatic or hydrogen bonds) with the rock. In that case, the surface becomes preferentially water-wet, and the CA would be smaller.

Contact angle measurements performed on the Eagle Ford rocks lead to the observation of a difference in wettability alteration depending on the charge carried by the ionic thermal stabilizer. Cationic surfactants were observed to create mostly intermediate-

wet angles, indicating low synergy between the surfactant formulation and the rock/oil system. In Figure 44, where surfactant C3 was used, an initial test using 0.05 wt% of cationic surfactant was observed to increase the CA from 125° to 135°, indicating an increase in oil-wet behavior. Further increase in C3 concentration was observed to create more water-wet angles. Likewise, increasing the concentration of the main surfactant N4 led to smaller CA. Except in the case of 0.8 wt% N4, where increasing concentration of C3 from 0.1 to 0.2 wt% did not further decrease the CA. In contrast, where surfactant A3 was used, shown in Figure 45, water-wet angles were observed at low concentrations, and increasing the concentration of the surfactant led to further decreases in the CA. Like the case of C3, increasing the concentration of N4 led to decreases in CA.





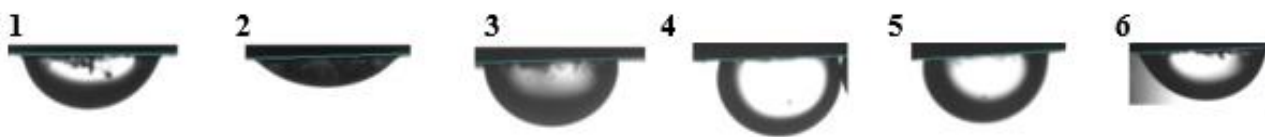


**Figure 44: Effect of cosurfactant as thermal stabilizer C3 on the contact angle of S2 chips measured at 170°F. Note: Base represents the contact angle after the aging 125.3° (oil-wet). Numbers 1 to 6 represent the sequence in the bar chart.**

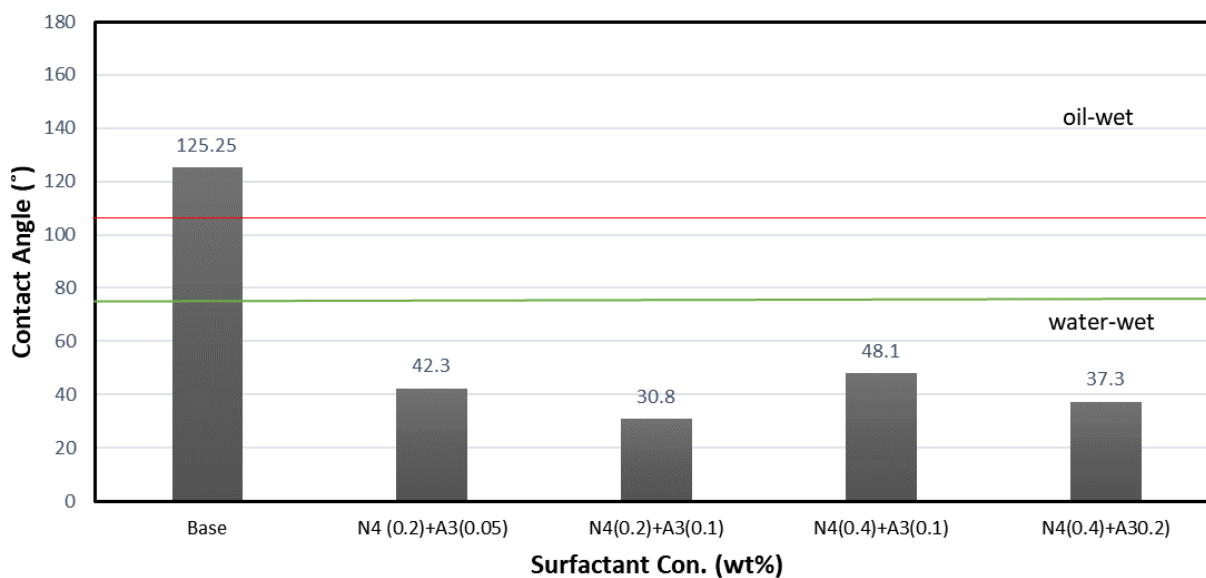


**Figure 45: Effect of cosurfactant as thermal stabilizer A3 on contact angles measured on S2 chips at 170°F. Note: Base represents the contact angle after the aging 125.3° (oil-wet). Numbers 1 to 5 represent the sequence in the bar chart. Surfactant blends with anionic co-surfactant A3 produced water-wet CAs.**

The poor performance of surfactant combinations using cationic surfactants is also visible in Figure 40, where C1 was used as a thermal stabilizer. This shows that the interactions within the system are such that the presence of cation surfactant retards

adsorption of the nonionic. This observation indicates that the calcite-rich surface creates electrostatic repulsive forces, which hinders adsorption of the positively charged mixed micelles of the surfactant; hence adsorption is only possible via hydrophobic bonding to the adsorbed hydrocarbon molecules. Because the hydrophobic interactions are weak, the surfactant is only weakly adsorbed, and it prefers to remain in the aqueous phase, thereby improving cloud point to a higher degree than an anionic molecule with a similar alkyl chain. Meanwhile, the nonionic/anionic surfactant with negatively charged mixed micelles are adsorbed via electrostatic interaction unto the available mineral sites, altering wettability and leaving less surfactant in the bulk solution allowing for lower cloud points.

### **Effect of Temperature**

Evaluating the effect of temperature on surfactant performance, CA measurements were conducted at 70°F and 170°F. Surfactant N4, as single surfactant, was observed to alter wettability to strongly water-wet; 30.6° and 27.3° at 70°F for chips from S2 and S3 respectively, and 43° and 34.3° at 170°. The addition of cosurfactant led to changes in the CA, especially at 70°F where the surfactants were observed to create mostly intermediate wet surfaces with increasing stabilizer concentration.

At 170°F cationic thermal stabilizers on S2 chips were observed to display a distinct change in behavior, becoming more-oil-wet as concentration increases from 0.05 wt% to 0.1 wt%, followed by a sharp change to strongly-water wet once more. Comparing with chips from S3, it is observed that the increase in temperature leads to strongly water-wet surfaces for all classes of ionic stabilizers. The difference in performance between S2

and S3 chips suggest slight variations in lithology between the two depth. In contrast, the data from S2 chips suggests cationic surfactants are antagonistic to the wettability alteration process.

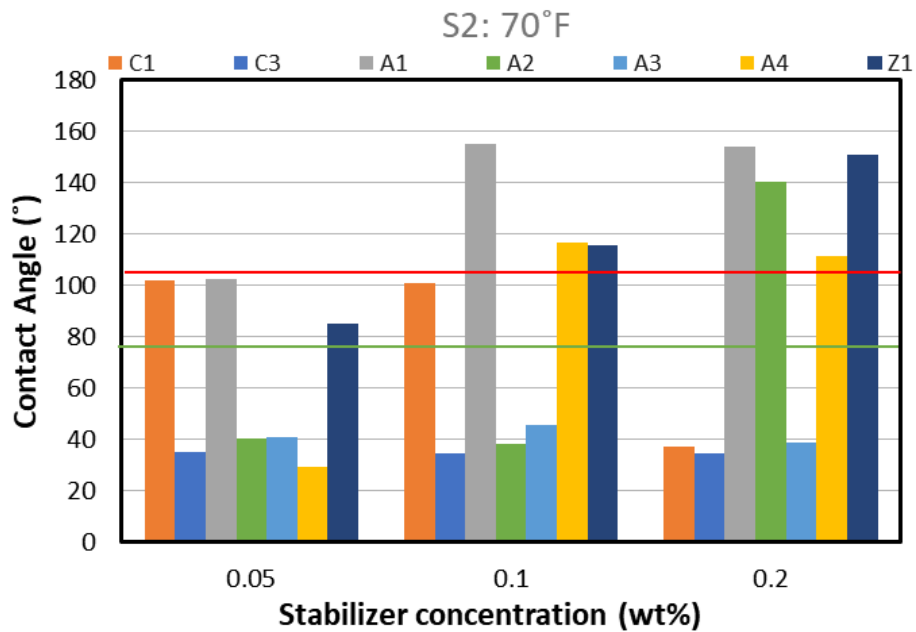


**Figure 46: Wettability alteration by surfactant N4 (0.2wt%) as single surfactant and in combination with thermal stabilizers on rock chips from S2. No clear trend in CA was observed for the mixed surfactants at room conditions. Note: temperature is 70°F.**

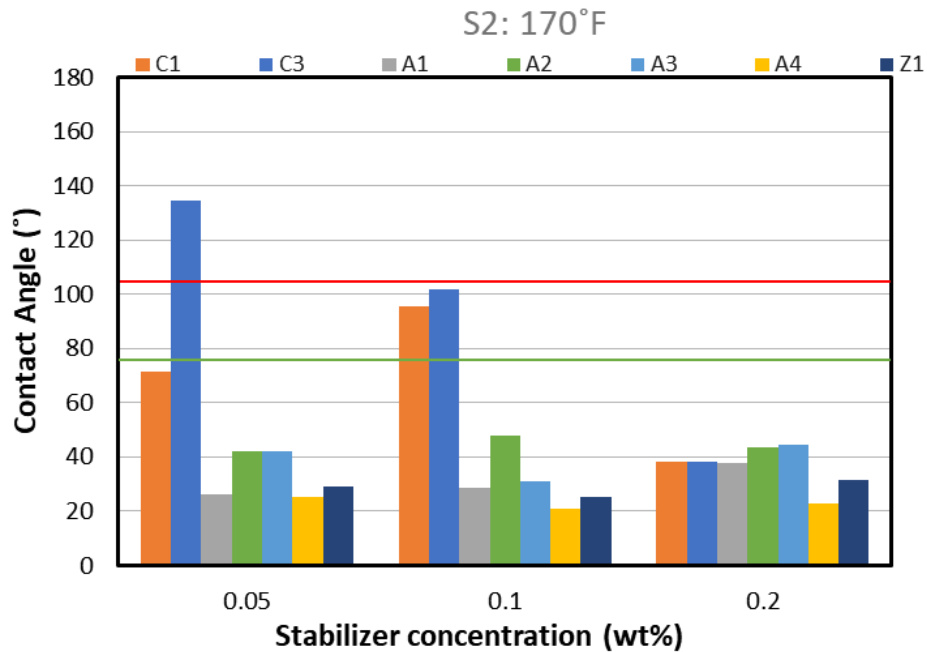


**Figure 47: Wettability alteration by surfactant N4 (0.2wt%) as single surfactant and in combination with thermal stabilizers on rock chips from S2. Cationic co-surfactants perform poorly when compared to anionic and zwitterionic at low concentrations at elevated temperature. Note temperature is 170°F.**

### Effect of Alcohol

Having confirmed that the nonionic surfactant and the nonionic surfactant blends successfully altered the wettability of the aged rock samples to water-wet, the influence of alcohol was investigated. Isopropanol at concentrations of 5 wt% and 10 wt% was introduced to the MW and used to create solutions of N4+A1 (1:1) and N4+A4(1:1), total surfactant concentration of 0.4 wt%. CA on chips from S2 and S3 both remained strongly water-wet in these solutions. As shown in Figure 48 **Error! Reference source not found.**, the binary surfactant N4+A4 created more water-wet surfaces when compared to N4+A1

at both propanol concentrations, which is similar to solutions without cosolvent. Also, the increase in the concentration of isopropanol led to a slight decrease in CA.

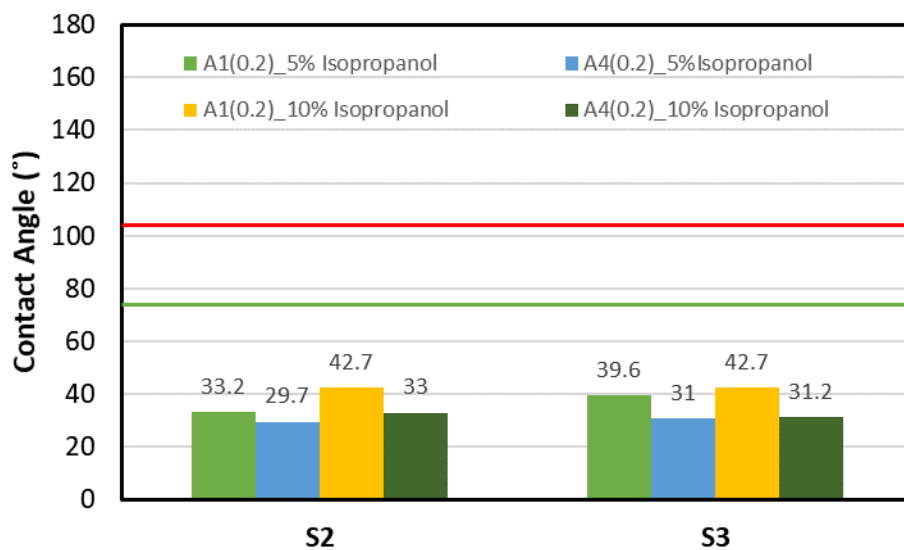


**Figure 48: Wettability alteration of binary surfactant blend N4 (0.2 wt%) and ionic cosurfactant (0.2 wt%) in aqueous solution containing isopropanol as cosolvent. Increasing concentration of co-solvent increase CA which is more prominent in co-surfactant system with A1.**

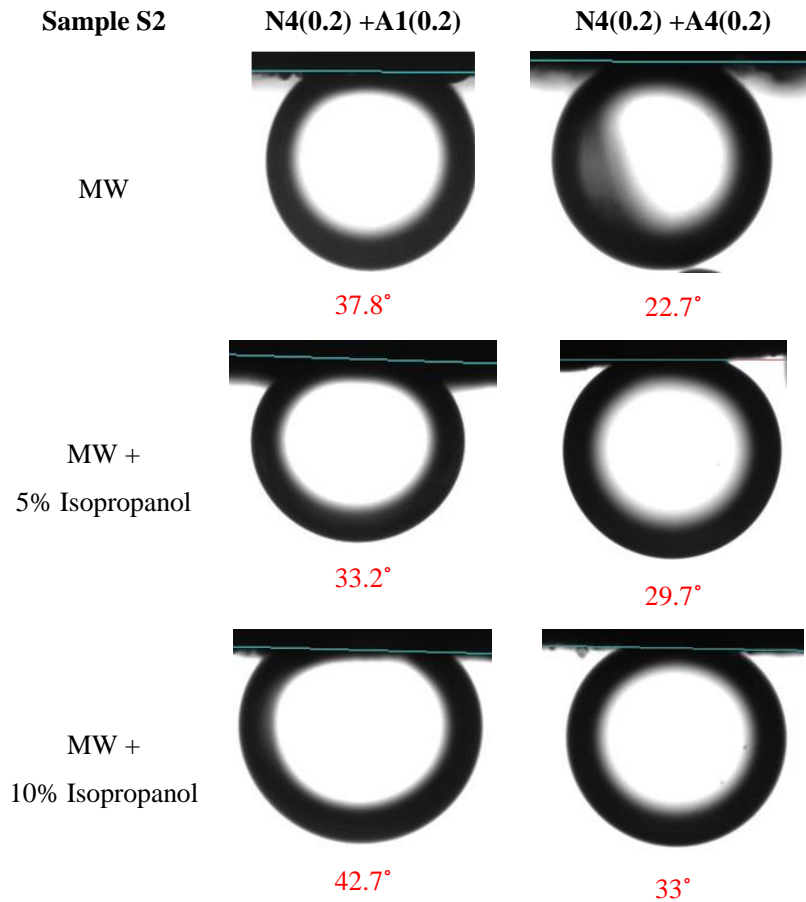


**Figure 49: Images showing wettability alteration of binary surfactant blend N4 (0.2 wt%) and ionic cosurfactant (0.2 wt%) in aqueous solution containing isopropanol as cosolvent.**

### Interfacial Tension

The presence of surfactant in fracturing fluid can lead to increased oil recovery in shale reservoirs as it causes a shift in capillary forces responsible for holding the oil and brine phases within the tight reservoir pores. Conventional theories favor the reduction in IFT because it results in lower capillary pressure, as seen in the Young-Laplace equation, Equation 5. In addition, when oil-wet rock wettability is altered to water-wet by the accumulation of surfactant molecules at the brine-rock interface, capillary forces can turn

from negative to positive for spontaneous imbibition, increasing the ease of mobility of the oil within the reservoir pores.

Interfacial tension of the Eagle Ford oil and makeup water was measured as 52.6 mN/m at 72°F and 46.2 mN/m at 170°F. All surfactant solutions made using the makeup water led to a decrease in IFT. As seen in Figure 50, surfactant N4 led to a dramatic decrease in IFT. An increase in surfactant concentration and temperature also result in a further decrease in IFT. The decline with temperature is due to the decrease in solubility of the surfactant, which forces the surfactant molecules to the oil/brine interface as opposed to remaining in the bulk solution. In comparison, the decline with increasing concentration is believed to be the result of increased surfactant molecules as micelles rather than monomers at the oil/brine interface.

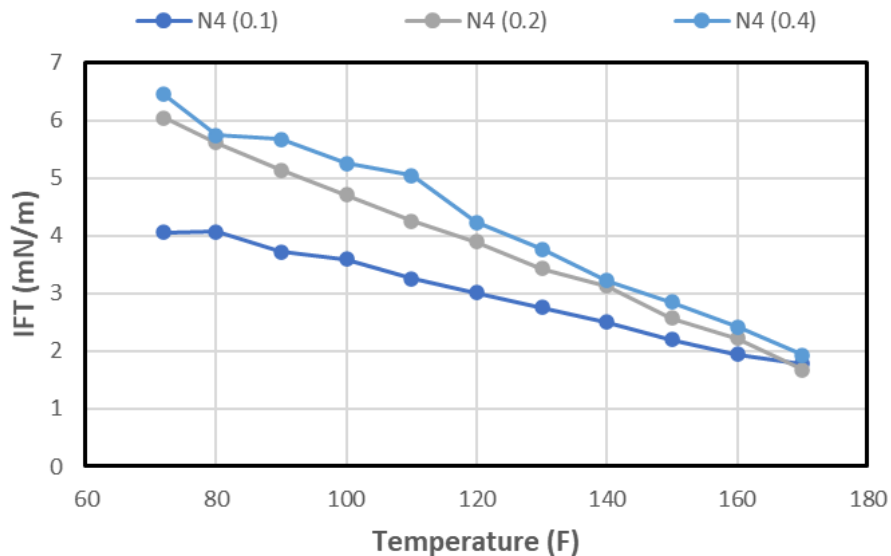


**Figure 50: IFT of main surfactant N4 at concentrations of 0.1, 0.2 and 0.4 wt% at atmospheric pressure and with increasing temperature. Higher IFT is observed at room temperature with higher surfactant concentration, however, IFT declines with increasing temperature to result in similar IFT at 170°F.**

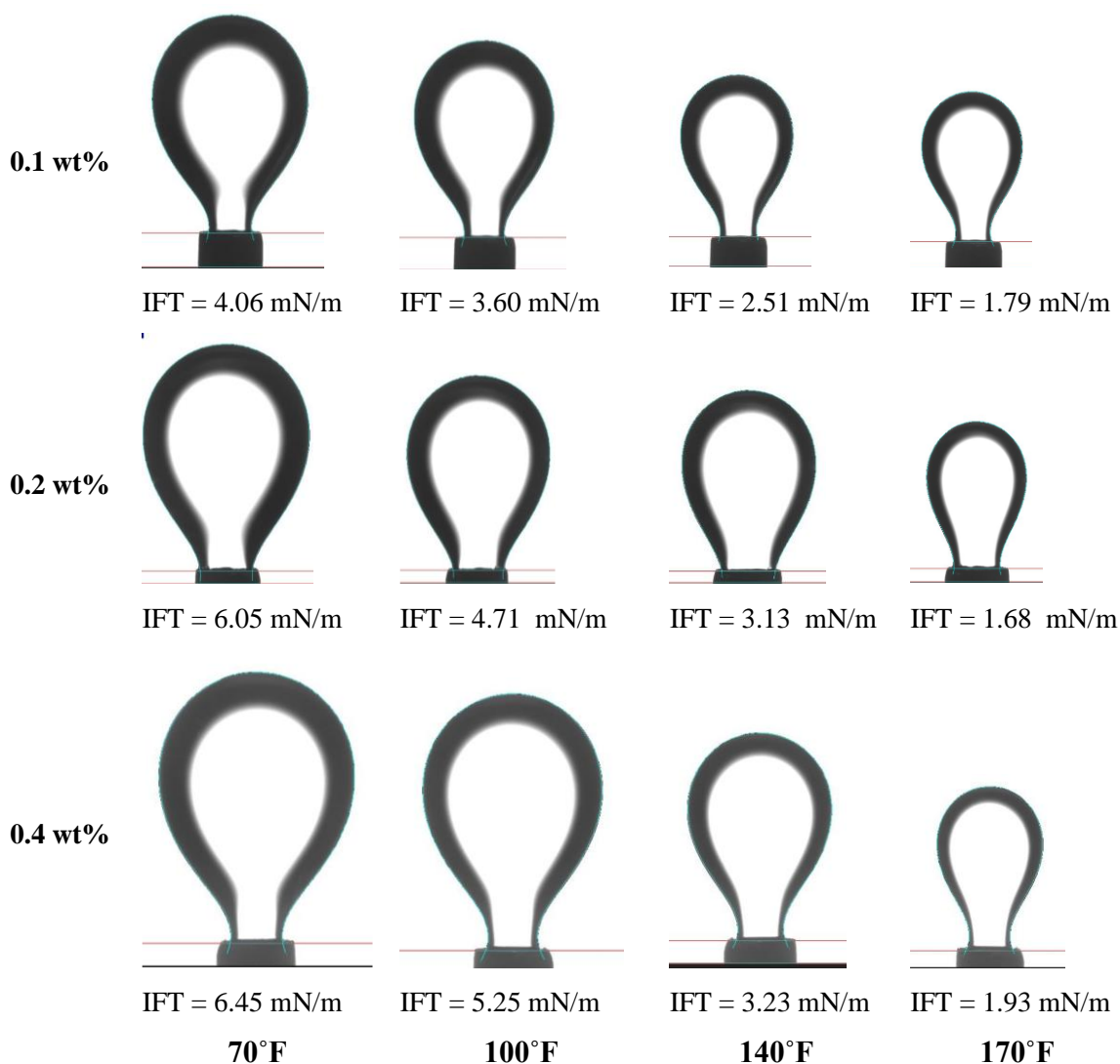


**Figure 51: Images of oil drop in surfactant solution N4 at 0.1 wt%, 0.2 wt%, and 0.4 wt%.**

The addition of thermal stabilizers to surfactant solution N4, at a concentration of 0.2 wt%, was observed to further decrease IFT. At 70°F, cationic surfactants C1 and C2 led to the largest reductions in IFT. At ratio surfactant 1:1, N4:C1 reduced IFT to 0.58 mN/m, while N4:C2 reduced IFT to 0.75 mN/m. In general, a trend of decreasing IFT with increasing stabilizer concentration was established for most of the ionic surfactants as seen



in Figure 52. At 170°F, the response of IFT to increasing stabilizer concentration is observed to vary across the various samples. As seen in Figure 53, C2 and A1 displayed increasing IFT with increasing concentration, while surfactant A2 was the only sample to maintain the trend of decreasing IFT with increasing concentration.

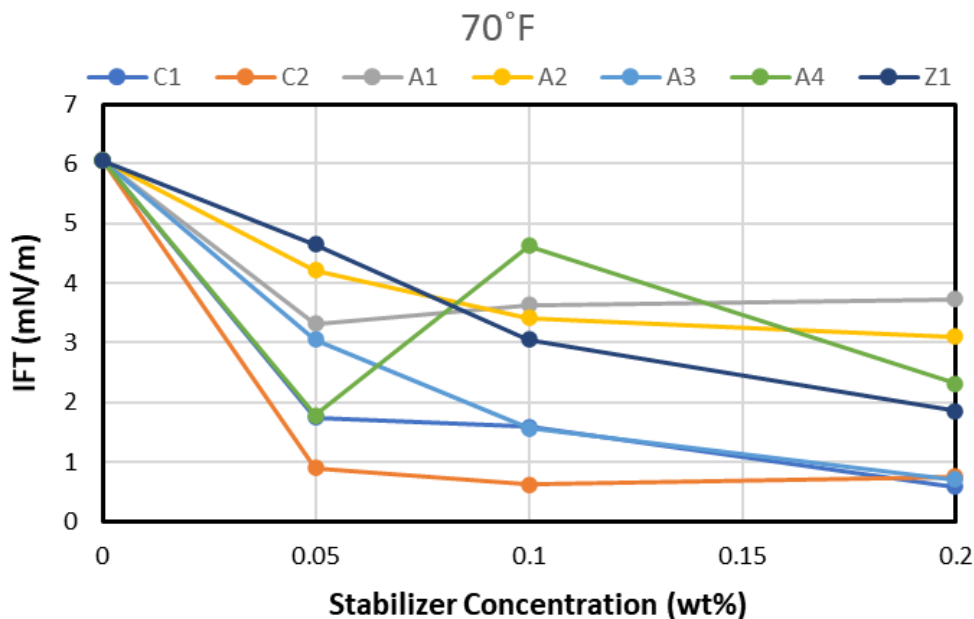


**Figure 52: Interfacial tension of surfactant blends containing N4 (0.2wt%) as a single surfactant and in combination with thermal stabilizers at 70°F at atmospheric pressure. Presence of ionic co-surfactant leads to decrease in IFT, with increasing concentration generally leading to further reduction.**

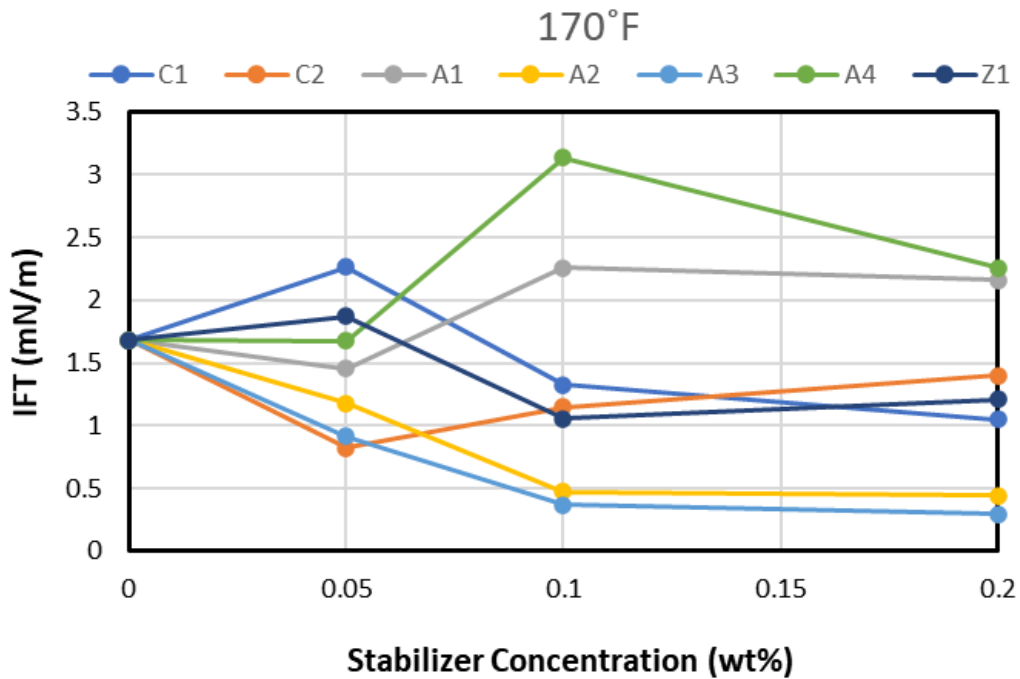


**Figure 53: Interfacial tension of surfactant blends containing N4 (0.2wt%) as a single surfactant and in combination with thermal stabilizers at 170°F at atmospheric pressure.**

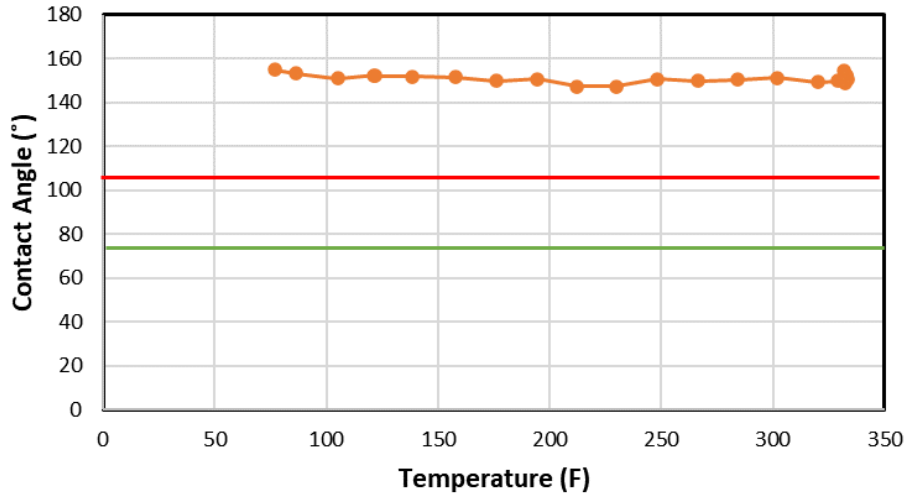
### High-Pressure Tests

The high-pressure tests were conducted by raising the temperature and pressure of the system from room condition to reservoir temperature to observe the influence of the surfactant on the brine/oil/rock and brine/oil systems at temperature and pressure conditions similar to those in the actual reservoir.

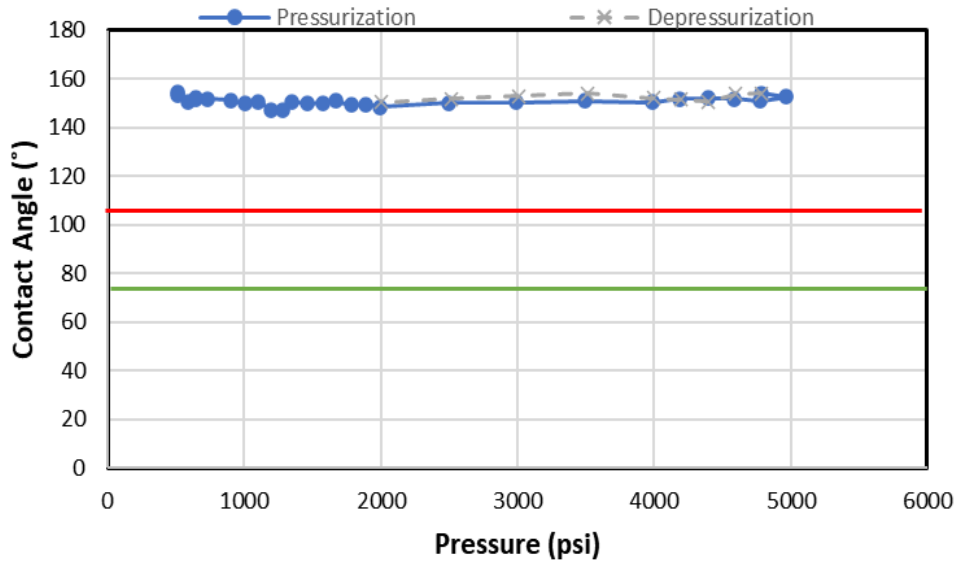
### Contact Angle

Base case wettability was first established by measuring the CA of the brine/oil/rock system in the absence of surfactant. It was observed that the increase in

temperature did not affect wettability as the surface remained strongly oil-wet with an average contact angle of 151°, as seen in Figure 54a. At reservoir temperature, pressure was decreased while the temperature was held constant, and it was determined that the change in pressure did not affect the wettability of the reservoir (Figure 54b).



(A)



(B)

**Figure 54: Contact angle data from HPT on aged rock sample. (a) Increasing temperature, (b) increasing and decreasing pressure, do not alter wettability in the absence of surfactant. Note: Aqueous phase was produced water with no surfactant.**

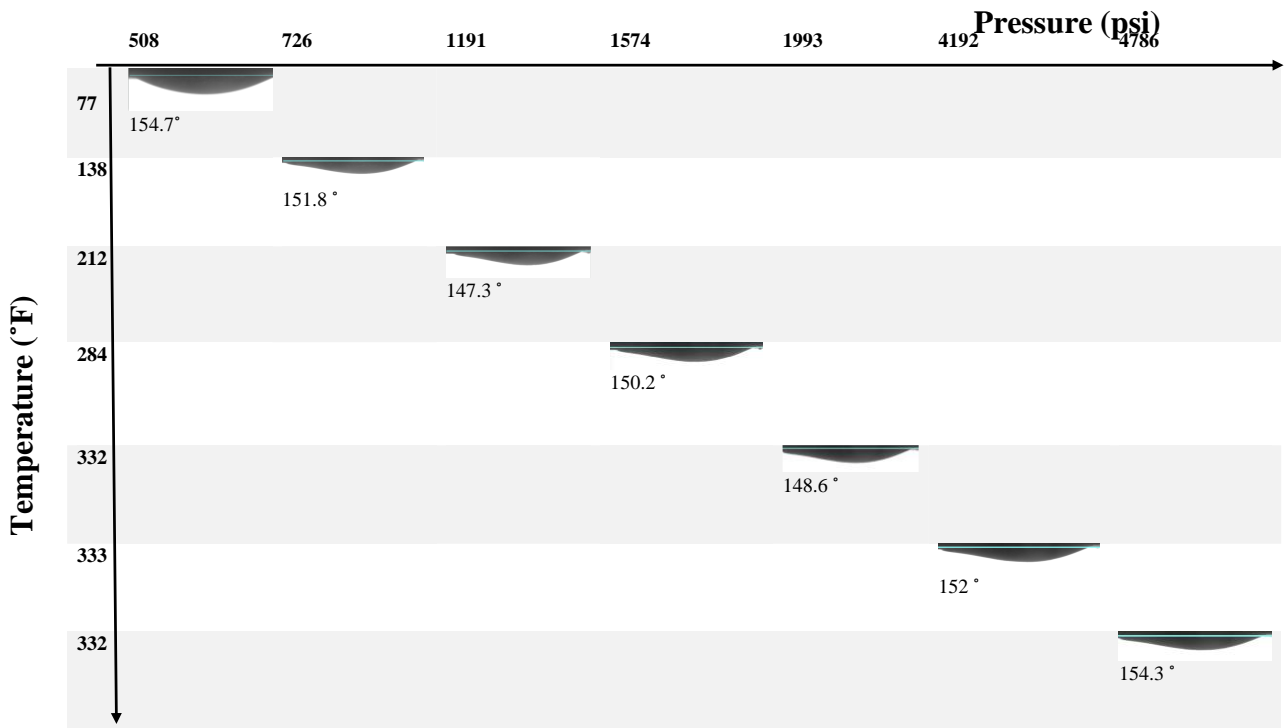


**Figure 55: Images of the oil drop on aged rock chip in the presence of produced water with no surfactant. Note: wettability remained constant on the strongly oil-wet surface.**

### Effect of Concentration of Nonionic Surfactant

As mentioned earlier, the one reason nonionic surfactants cannot be deployed in high-temperature reservoirs is their tendency to phase separate at temperatures above the surfactant cloud point. For this reason, ionic surfactants which are more thermally stable are blended into the nonionic solution. Nonionic surfactant N4 had successfully altered the wettability of the oil-wet Eagle Ford rock as a single surfactant and when used in combination with various ionic surfactants. The influence of the nonionic surfactant on

reservoir wettability was observed in a series of high-pressure tests in which concentration was increased from 0.2 wt% to 0.4 wt% and finally 0.8 wt%. The results shown here in Figure 56, increasing concentration of the nonionic species led to a more water-wet surface. Initial contact angles were 32°, 70°, and 22° for the surfactant blends of N4 and C3 in ratios 2:1, 4:1, and 8:1, respectively. Although all 3 solutions initially created water-wet surfaces, there was a shift in CA from water-wet through intermediate and finally to oil-wet as the temperature approached 325°F. Therefore, it can be concluded that the nonionic surfactant is the driver of the wettability alteration process.

The increase in nonionic concentration, however, had detrimental effects on cloud point temperature. N4:C3, 2:1 was observed to lose solubility and become turbid at 348°F, while 4:1 displayed turbidity at 280°F and 8:1 at 287°F.

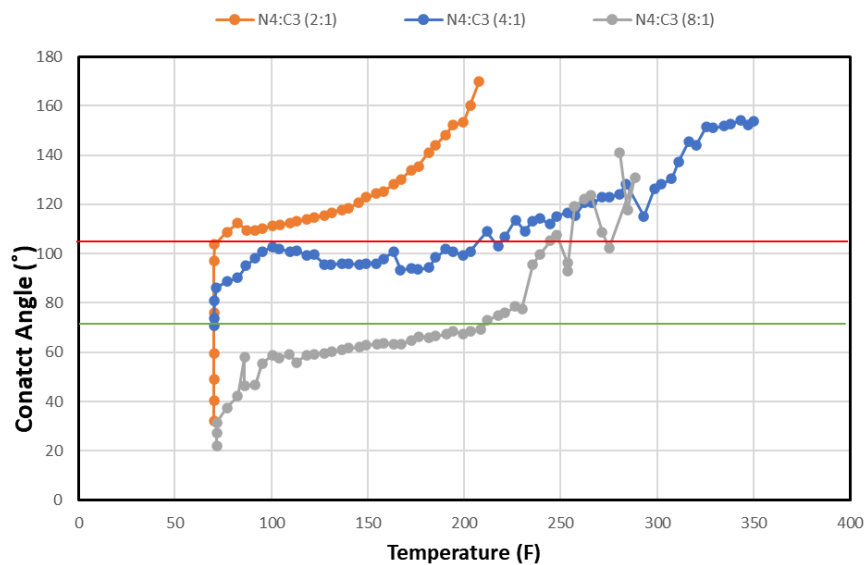


**Figure 56: Influence on wettability alteration of changing main surfactant (N4) concentration from 0.2 wt% to 0.4 wt% to 0.8 wt%. Increasing ratio of nonionic concentration creates stronger water-wet CAs. Note: Thermal stabilizer used is cationic sample C3 at 0.1 wt%.**

## **Effect of Charge of Ionic Stabilizer**

From contact angle measurements conducted at atmospheric conditions, it was observed that wettability alteration with binary surfactant blends containing anionic stabilizers led to better results when compared to binary blends with cationic stabilizers at similar concentrations. As seen here, Figure 57, Figure 60, and Figure 62 reveal that the different ionic stabilizers behave differently when exposed to high pressure and temperature conditions, which results in a change in contact angle.

The combination of cationic stabilizer C1 at 0.1 wt% to nonionic surfactant N4 at 0.2 wt% initially rendered the surface water-wet. However, with increasing pressure and temperature, CA moved towards oil-wet, indicating poor synergy between both surfactants at elevated temperatures. Investigation of the rock sample at the end of the experiment revealed that the surfactant's antagonistic behavior also resulted in degradation of the rock surface. This behavior was repeated with cationic stabilizer C3 as seen in Figure 59 revealing that the combination of nonionic and cationic surfactant is not suitable for the reservoir in question as it may lead to the production of fines which can clog pore throats and impede production.

Anionic stabilizer A3 was observed to alter wettability to intermediate at concentrations of 0.1 wt% at the start of the experiment and create an increasingly water-wet surface as temperature increased. The shift in CA towards strongly water-wet is a result of a decrease in solubility with increasing temperature, which is a function of the nonionic surfactant. Strongly water-wet surfaces with CA less than 20° were also produced

with stabilizers A1 and A4, while A2 altered wettability from intermediate to water-wet with increasing temperature.

The use of zwitterionic surfactant Z1 at a concentration of 0.1 wt% was observed to result in strongly water-wet surfaces similar to those observed at low-pressure conditions. However, CA changes slightly as temperature increases.

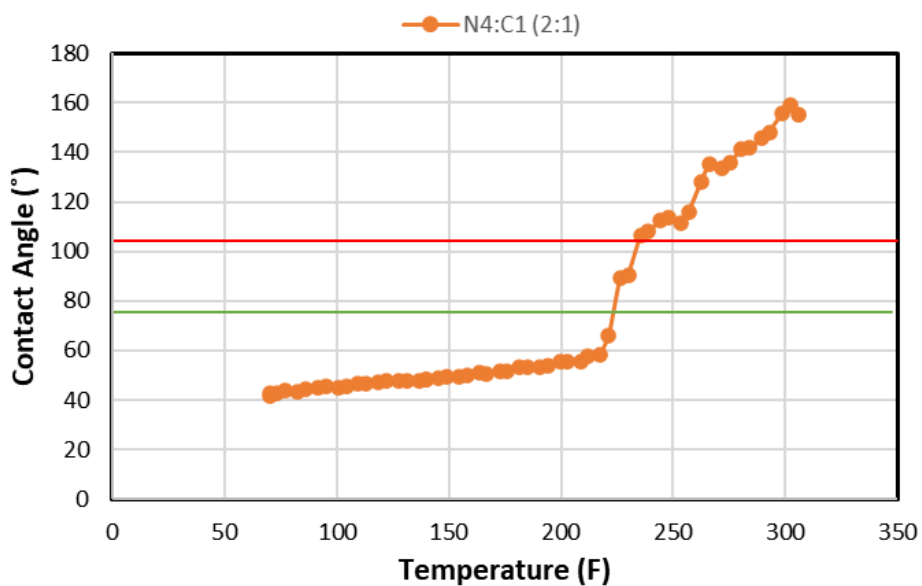


**Figure 57: Plot of contact angle against temperature for binary surfactant N4 (0.2 wt%) and cationic thermal stabilizer C1 (0.1 wt%). CA remains water-wet at temperature below 212°F.**

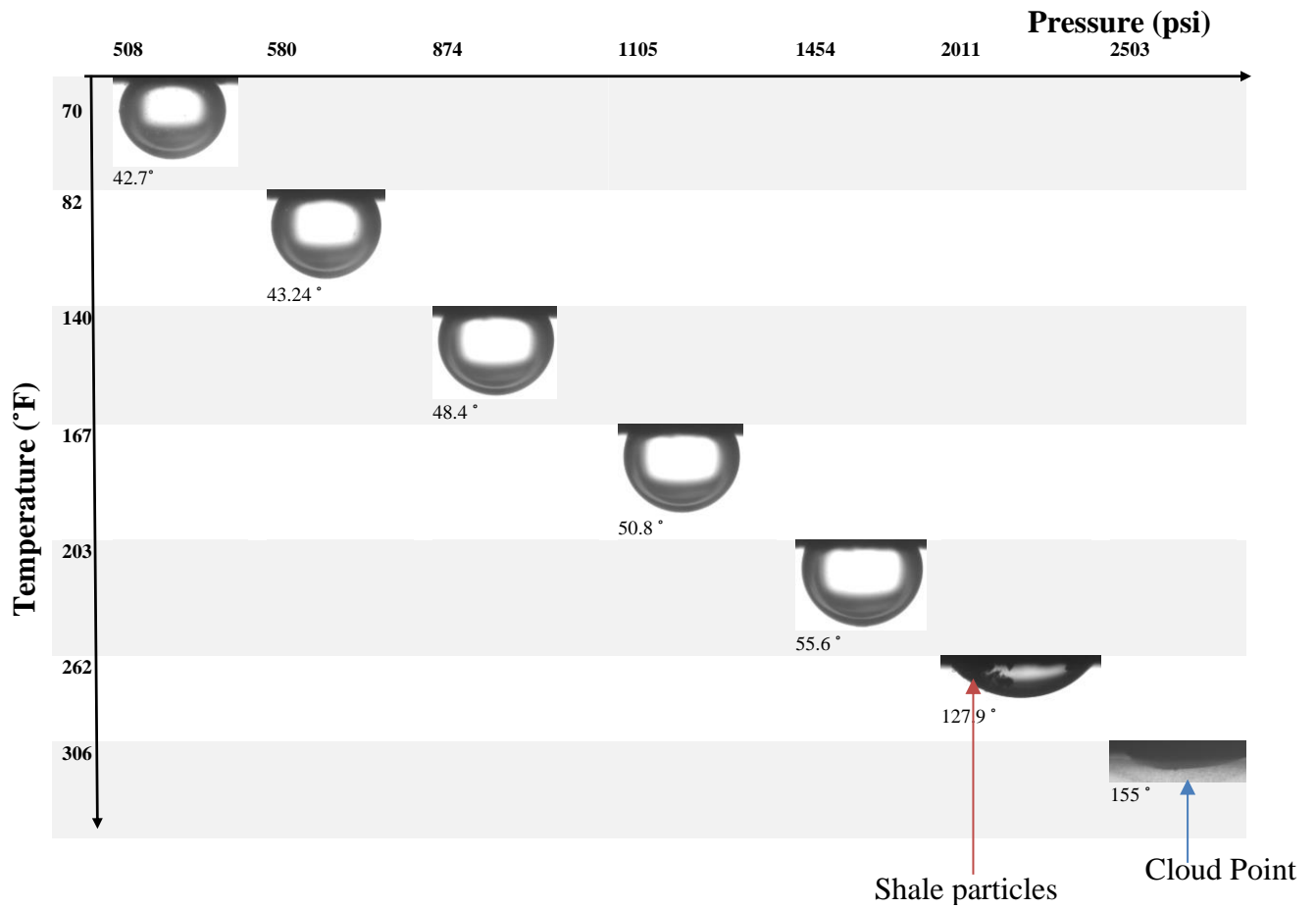


**Figure 58: Images showing wettability observed with binary surfactant N4 (0.2 wt%) and cationic thermal stabilizer C1 (0.1 wt%).**



**Figure 59: Images of the rock surface at the start of experiment(left) and at the end (right) in N4 (0.4 wt%) + C3 (0.2 wt%) showing degradation of the rock surface.**



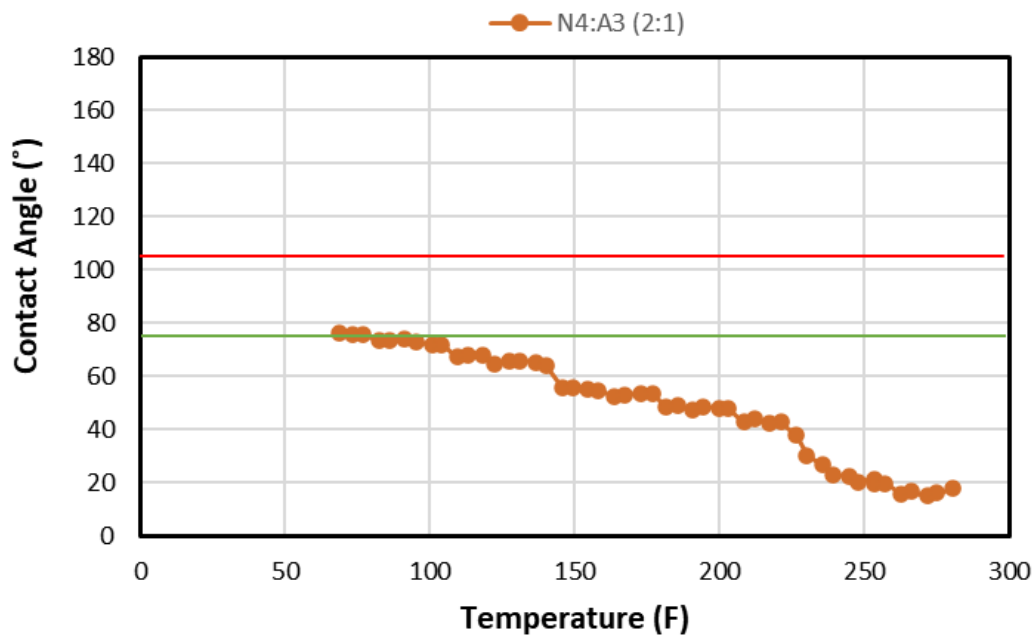


**Figure 60: Plot of contact angle against temperature for binary surfactant N4 (0.2 wt%) and anionic thermal stabilizer A3 (0.1 wt%). Main surfactant causes a decrease in solubility with increasing temperature which forces the surfactant to the interface and improves wettability.**

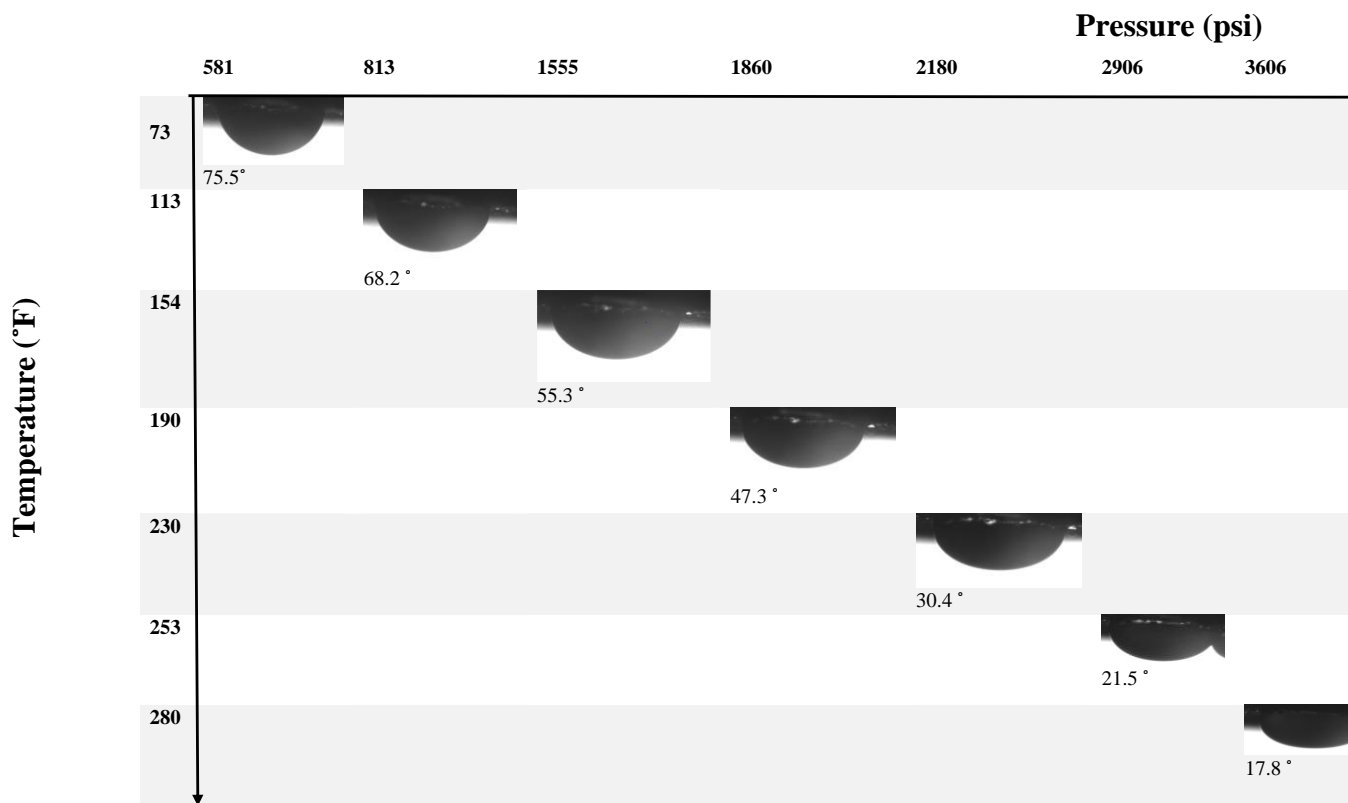


**Figure 61: Images showing wettability alteration observed with binary surfactant N4 (0.2 wt%) and anionic thermal stabilizer A3 (0.1 wt%).**

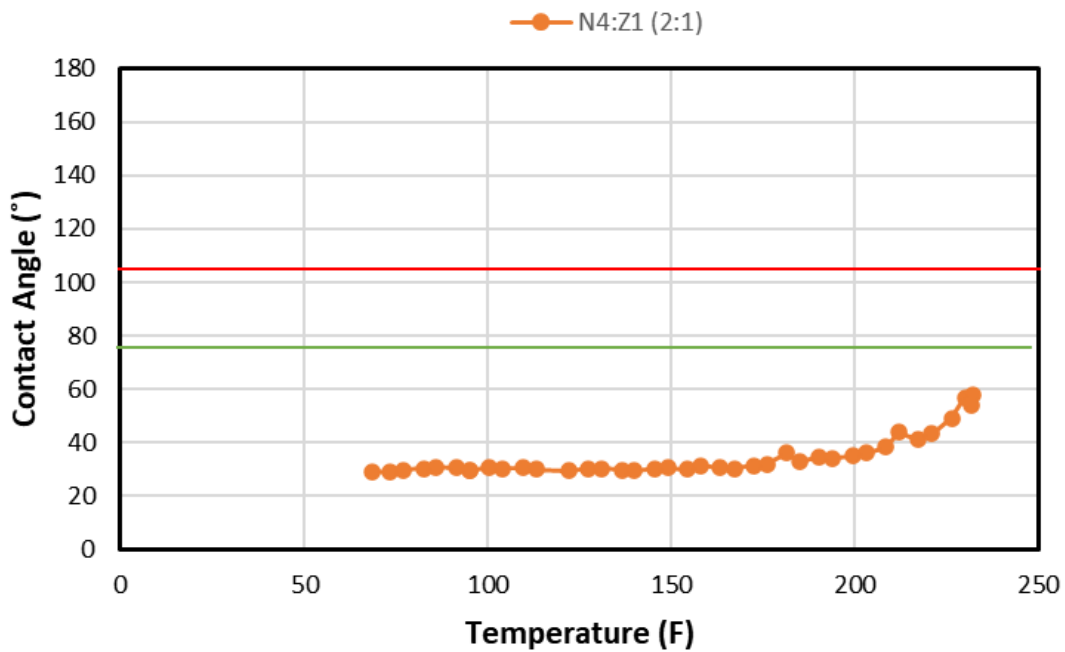


**Figure 62: Plot of contact angle against temperature for binary surfactant N4 (0.2 wt%) and zwitterionic thermal stabilizer Z1 (0.1 wt%).**

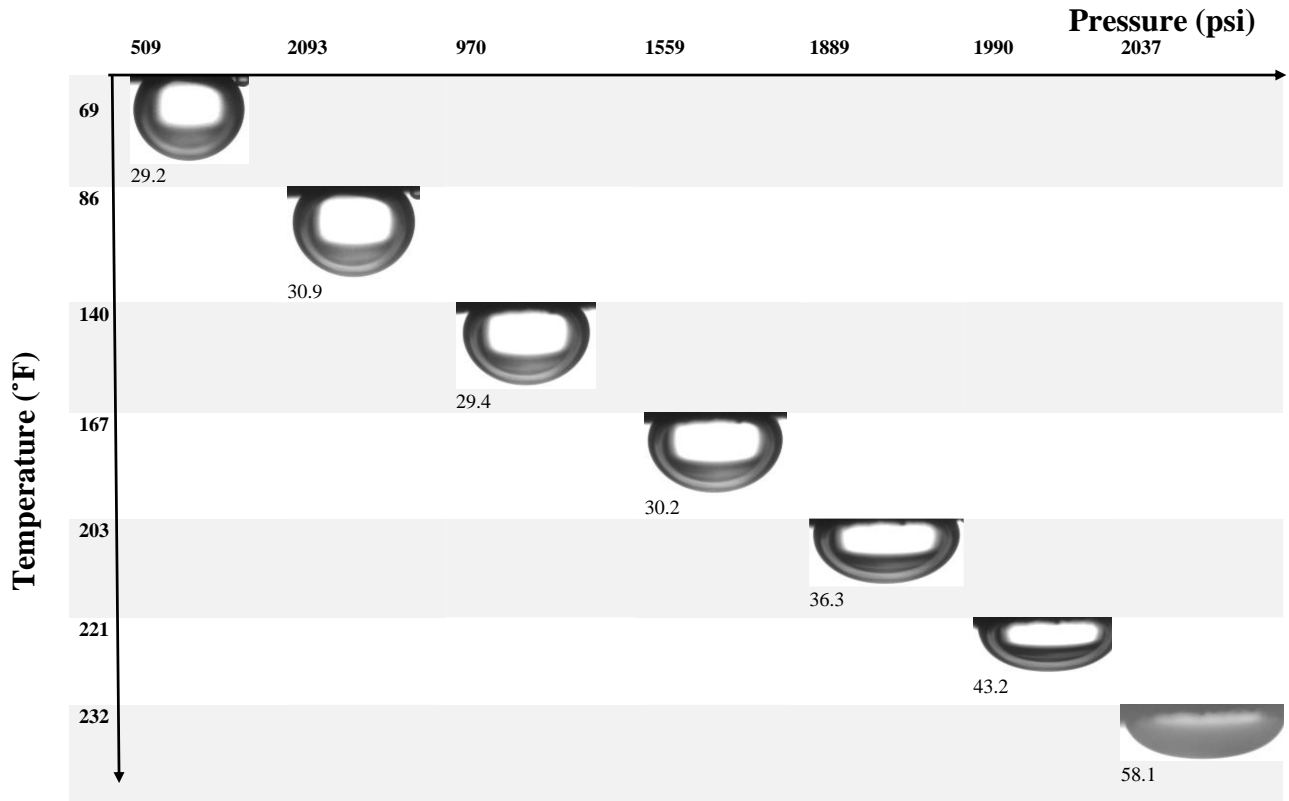


**Figure 63: Images showing wettability alteration observed with binary surfactant N4 (0.2 wt%) and amphoteric thermal stabilizer Z1 (0.1 wt%).**

### Effect of Stabilizer Concentration

Increasing the concentration of the thermal stabilizer was observed to both improve cloud point and increase water-wetness. The zwitterionic cosurfactant which was observed to be initially intermediate-wet at concentrations of 0.1 wt%, is shown in Figure 64 to become very water-wet when concentration is doubled such that it is at the same concentration of 0.2 wt% as the main surfactant. The change in CP was not enough to attain stability at reservoir temperature as the 2:1 ratio reached CP at 232°F and the 1:1

ratio at 262°F. The combination of N4 and A1 yielded very water-wet surfaces at all concentrations, with CPT increasing from 280°F at ratio 2:1 to 316°F at ratio 1:1. For the cosurfactant A2, which displayed the best cloud point temperature during the high-pressure cloud point experiments, wettability alteration proved difficult at a cosurfactant concentration of 0.2 wt%. The decrease in IFT during the heating portion of the experiments meant the system had to be pressurized to its maximum capacity of 340 bar (about 4900 psi), which was very close to the pressure limit. For this reason, the experiment was terminated without attaining CP, and the data was disrupted by the introduction of stray oil drops released due to low IFT. Table 4 indicates the changes in the CP observed during other HPHT experiments.

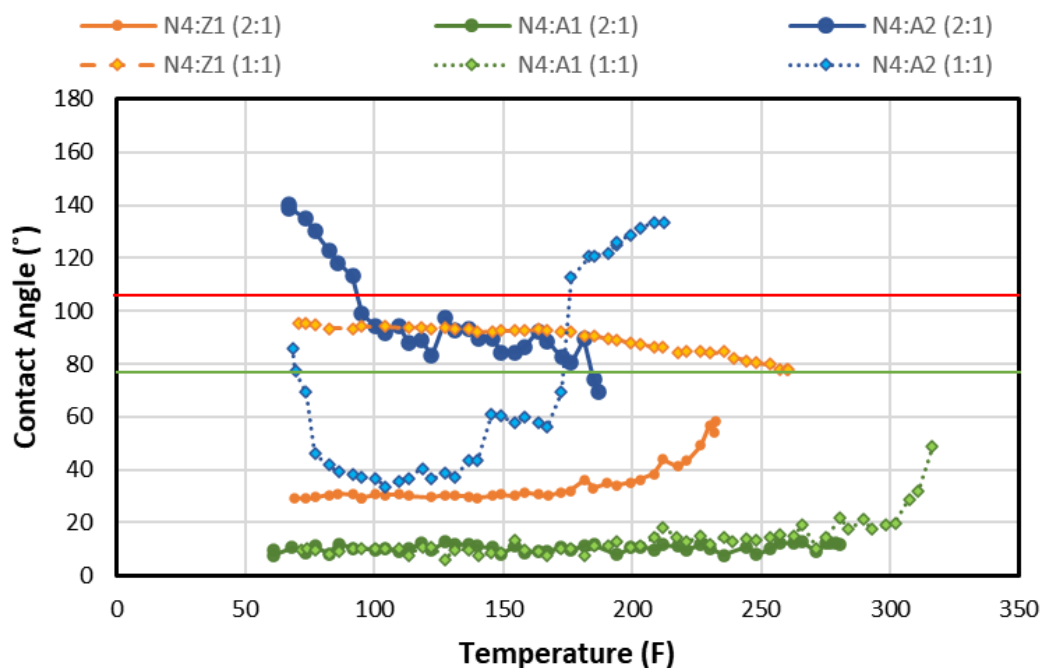


**Figure 64: Influence on wettability alteration of increasing concentration of thermal stabilizer. Increasing ratio of co-surfactant to create 1:1 Surfactant blends leads improved CPT and very water-wet CAs for mixture with A1. Shift to intermediate CAs for the combination with Z1. While the mixture with A2 displays a more erratic**

trend decreasing CAs followed by a sharp increase. Note: Main surfactant used is N4 at 0.2 wt%.

**Table 4: Effect of surfactant ratio on cloud point temperature for ternary surfactant blends**

Surfactant	Ratio	Total Concentration (wt%)	Cloud Point (°F)
N4:A1:A2	2:1:1	0.4	340
N4:A4:A2	2:1:1	0.4	320
N4:A1:A2	2:1:1	0.2	336
N4:A4:A2	2:1:1	0.2	320
N4:A1:A2	4:3:1	0.4	348
N4:A4:A2	4:3:1	0.4	316
N4:A1:Z1	2:1:1	0.2	316

### Effect of Temperature

The heating and cool portions of the HPHT experiment revealed CA does not follow the same path as seen in Figure 65 and Figure 67. The CA hysteresis was attributed to changes that occur on the rock surface. It was observed that the aged rock surface produced microdroplets of oil during the experiment. This oil production can be taken as a positive sign that imbibition was occurring, and the surfactant system was accomplishing its intended purpose. For this reason, the oil drop deposited was likely to have changed slightly in volume, thereby affecting the CA. The microdroplets produced also had the potential to cause the spreading of the droplet under investigation. Given these observations, the case of CA hysteresis was not investigated further. However, the ability of the drops under investigation to display water-wet CAs does serve as proof that the

surfactant performs its function under cloud point temperature and the phase separation noted at CP is reversible.

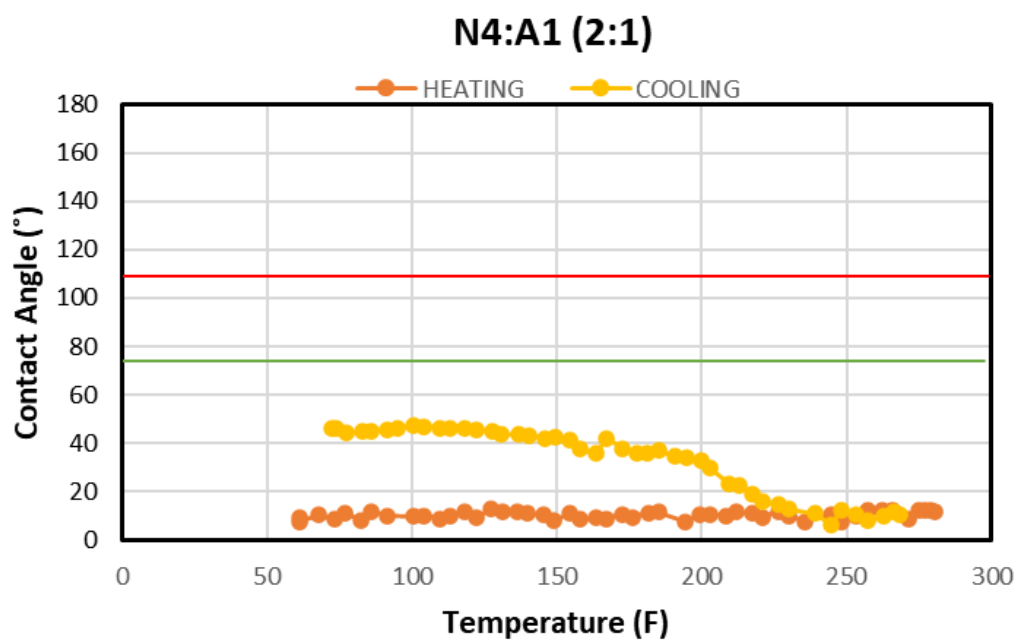
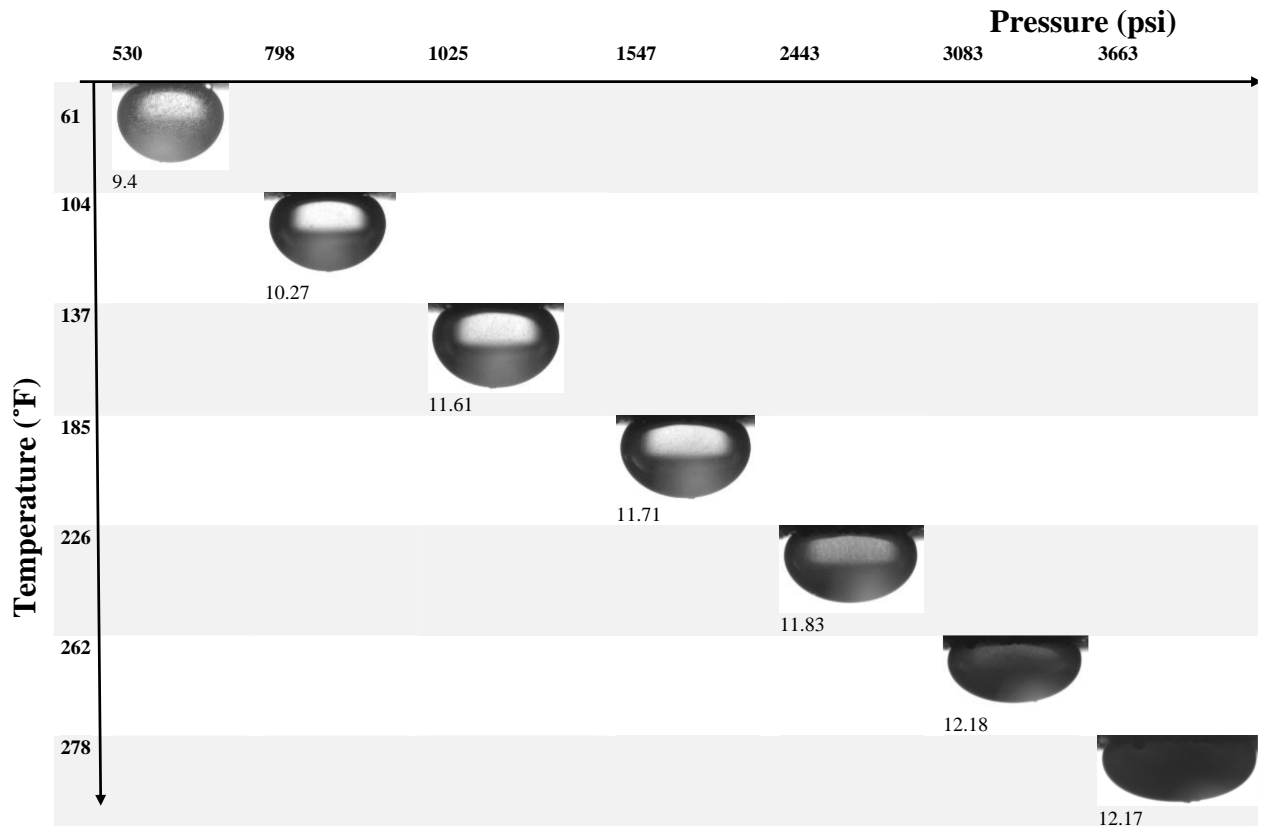
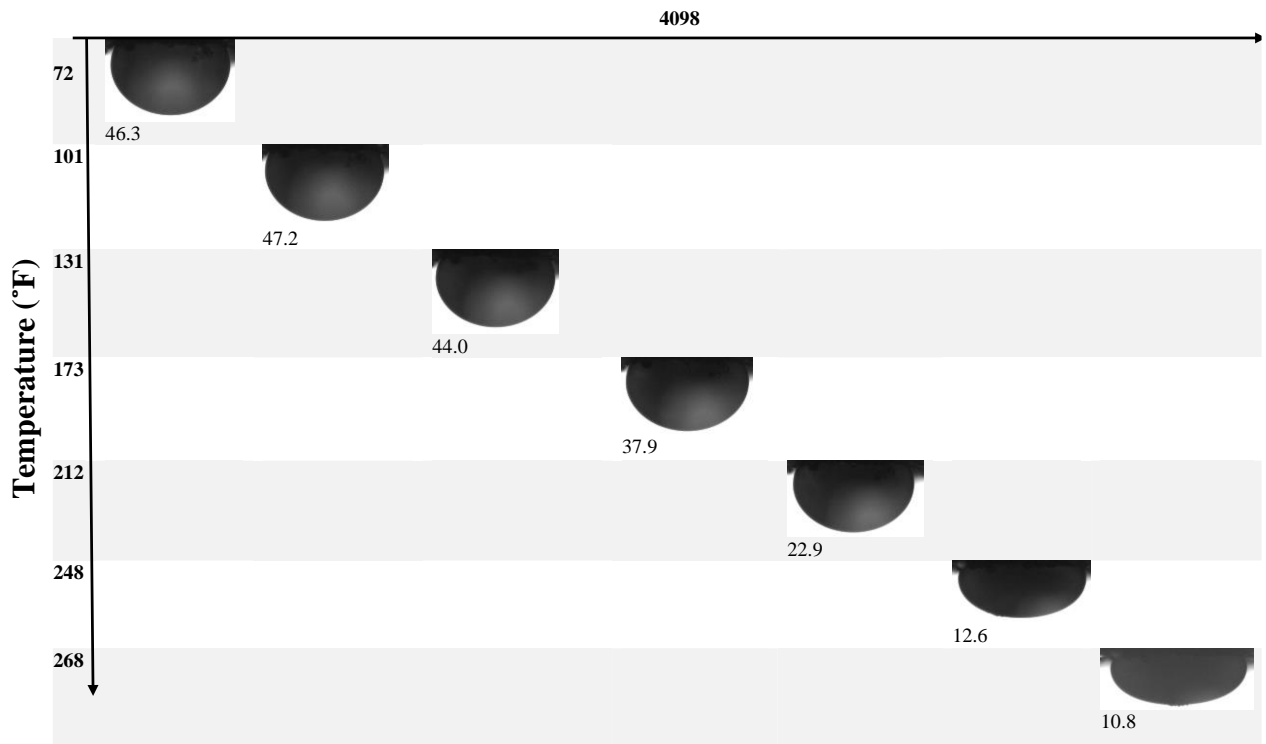


**Figure 65: Contact angle hysteresis observed for surfactant N4+A1 (1:1) as temperature is lowered at constant pressure.**



(A)

Pressure (psi)



(B)

**Figure 66: Images of oil drop on aged rock surface: a) Increasing temperature and pressuring during heating. b) Decreasing temperature and constant pressure during cooling for N4+A1 (2:1).**

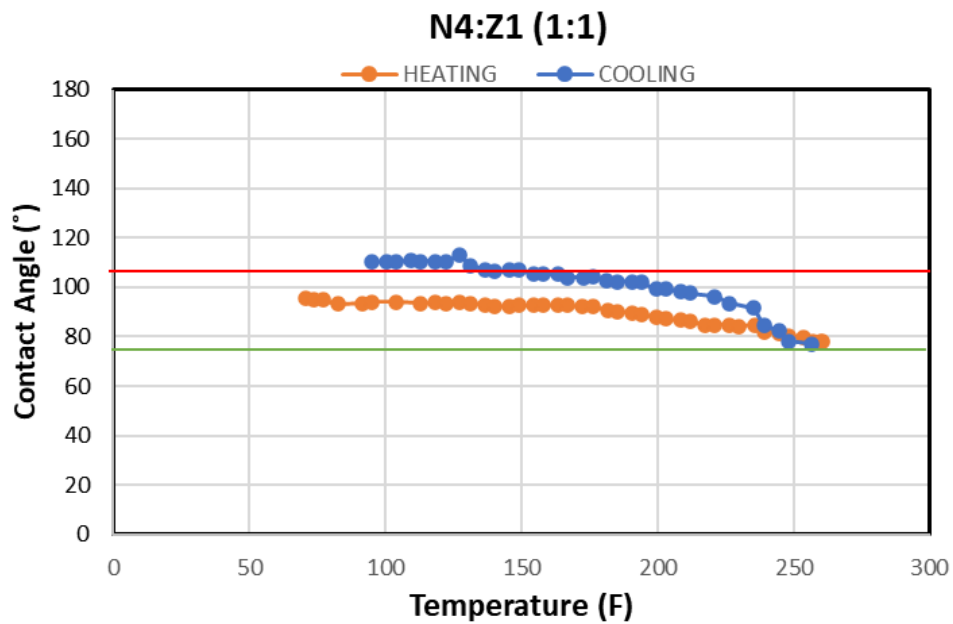
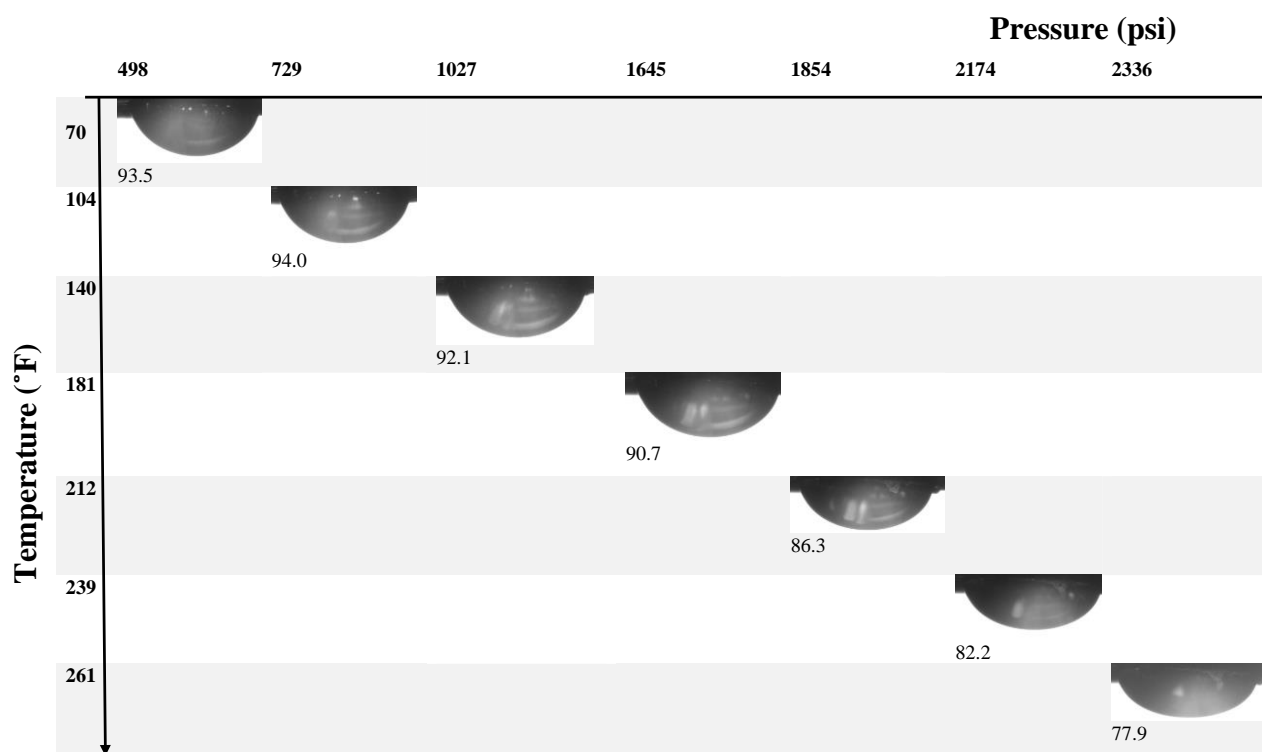
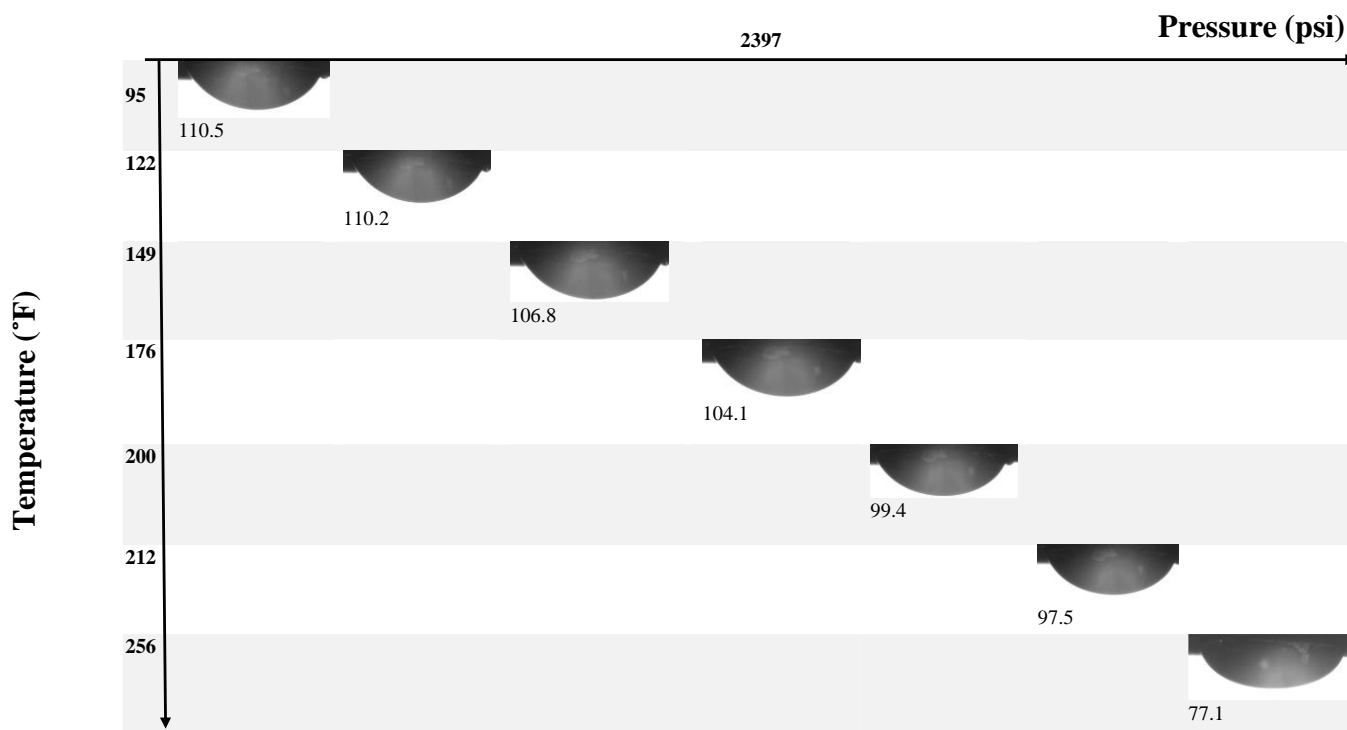




**Figure 67: Contact angle hysteresis observed for surfactant N4+Z1 (1:1) as temperature is lowered at constant pressure.**



(A)



(B)

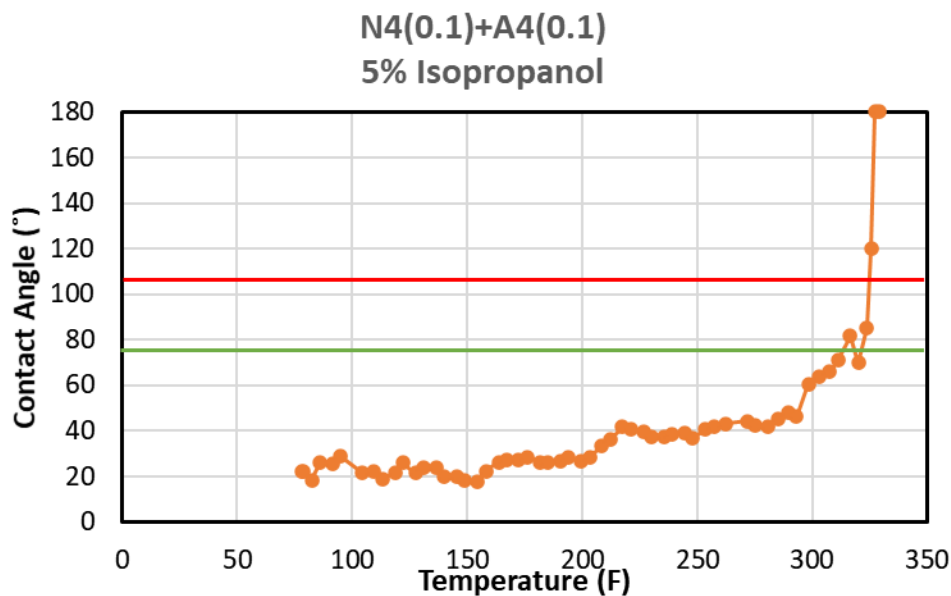
**Figure 68: Images of oil drop on aged rock surface: a) Increasing temperature and pressuring during heating. b) Decreasing temperature and constant pressure during cooling, for surfactant N4+Z1 (1:1).**

### Effect of Alcohols

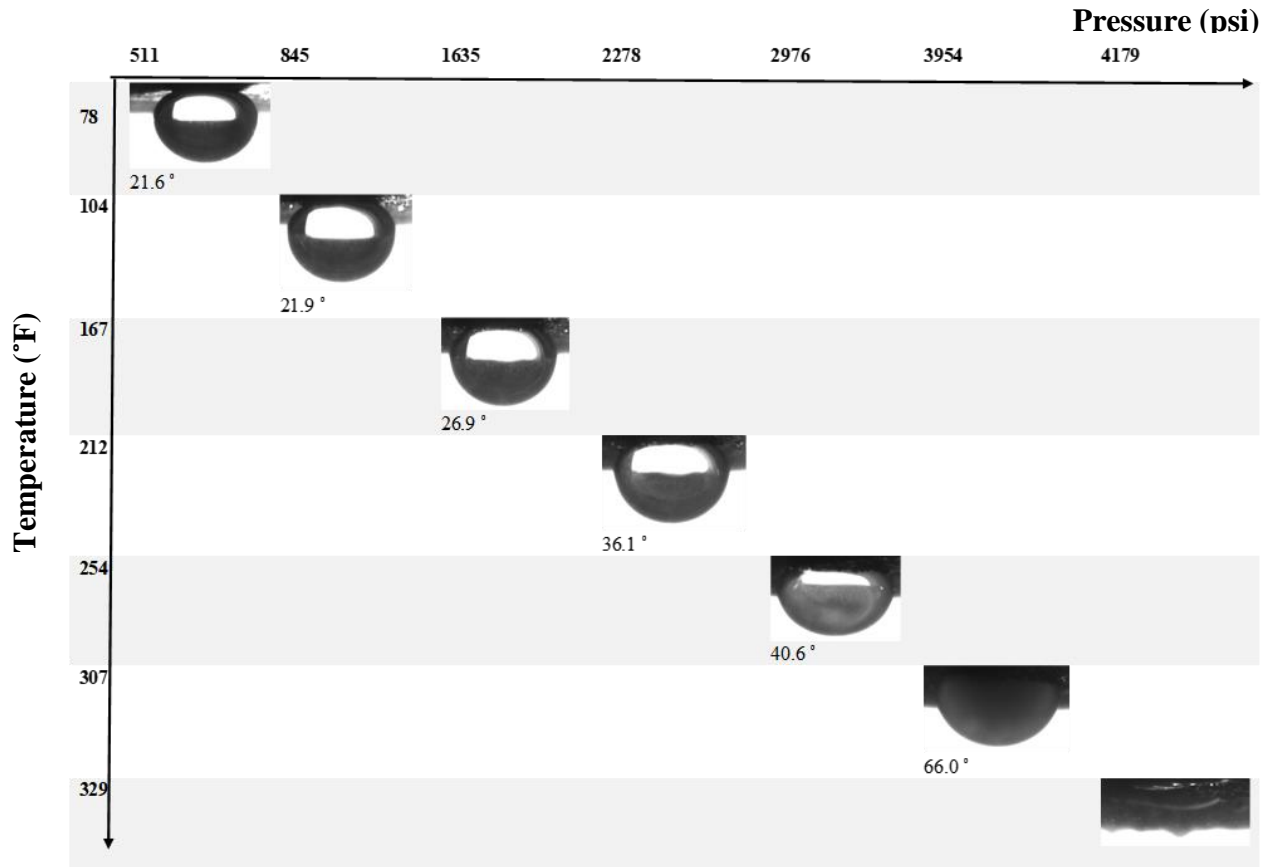
As seen in the high-pressure cloud point experiments, at elevated temperature and pressure, the presence of isopropanol has the capacity to raise CPT above reservoir temperature for binary surfactant blends N4+A1 and N4+A4 at a total surfactant concentration of 0.2 wt%. For surfactant N4(0.1)+A4(0.1), the improved CP was not matched with the surfactant's ability to maintain a water-wet surface, as seen in Figure 69, CA started at 22° (strongly water-wet) and reverted to oil-wet at about 170°. For N4(0.1)+A1(0.1), turbidity was observed beginning at 293°F, however, the solution remained relatively clear at reservoir temperature. CA, which began at 26° during the

experiment's heating portion, ended at 56° at reservoir temperature, indicating the successful alteration of the surface wettability at reservoir conditions. The cooling part of the experiment shown in Figure 72b also maintained the water-wet CA convention ranging between 61° to 75°.

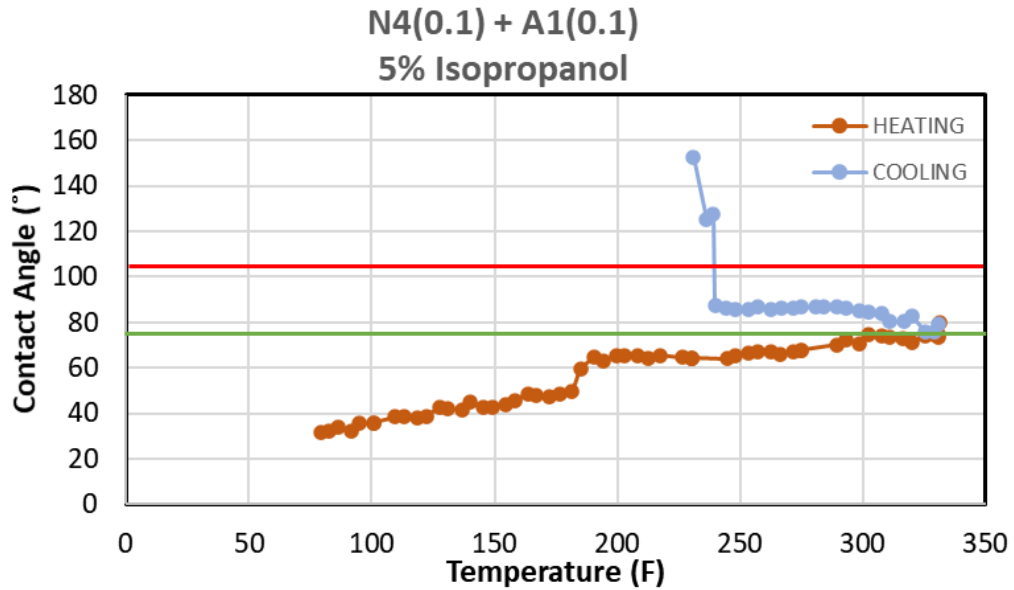
Increasing the total surfactant concentration to 0.4 wt%, surfactant N4+A1 remained stable at reservoir temperature with CPT at about 330°F and a maximum contact angle of 56° during the heating portion of the experiment. For surfactant N4+A4 at 0.4 wt%, although maintaining water-wet CA during the heating and cooling process, shown in Figure 75, the solution reached CP at a temperature of 295°F.



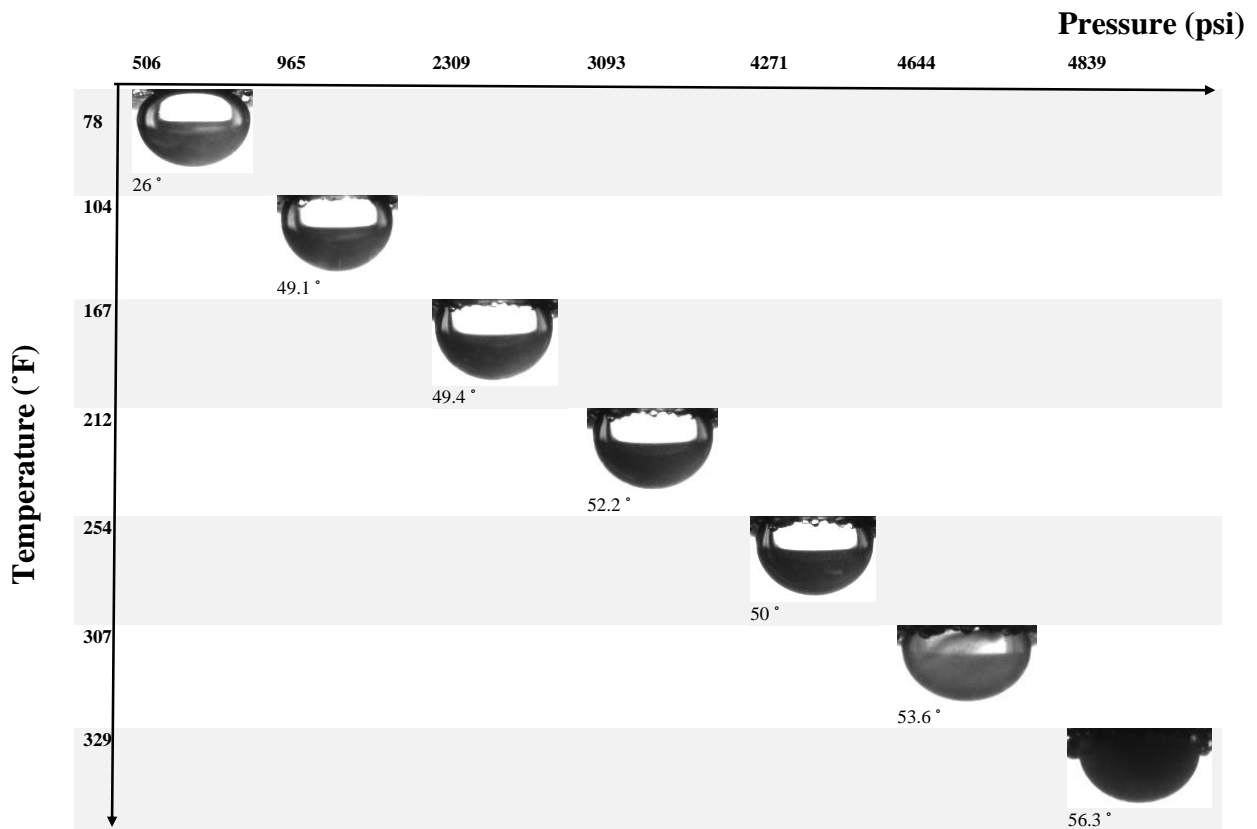
**Figure 69: Plot of contact angle against temperature showing wettability alteration for surfactant N4+A4 (1:1) total surfactant concentration of 0.2 wt% in solution with 5 wt% isopropanol.**

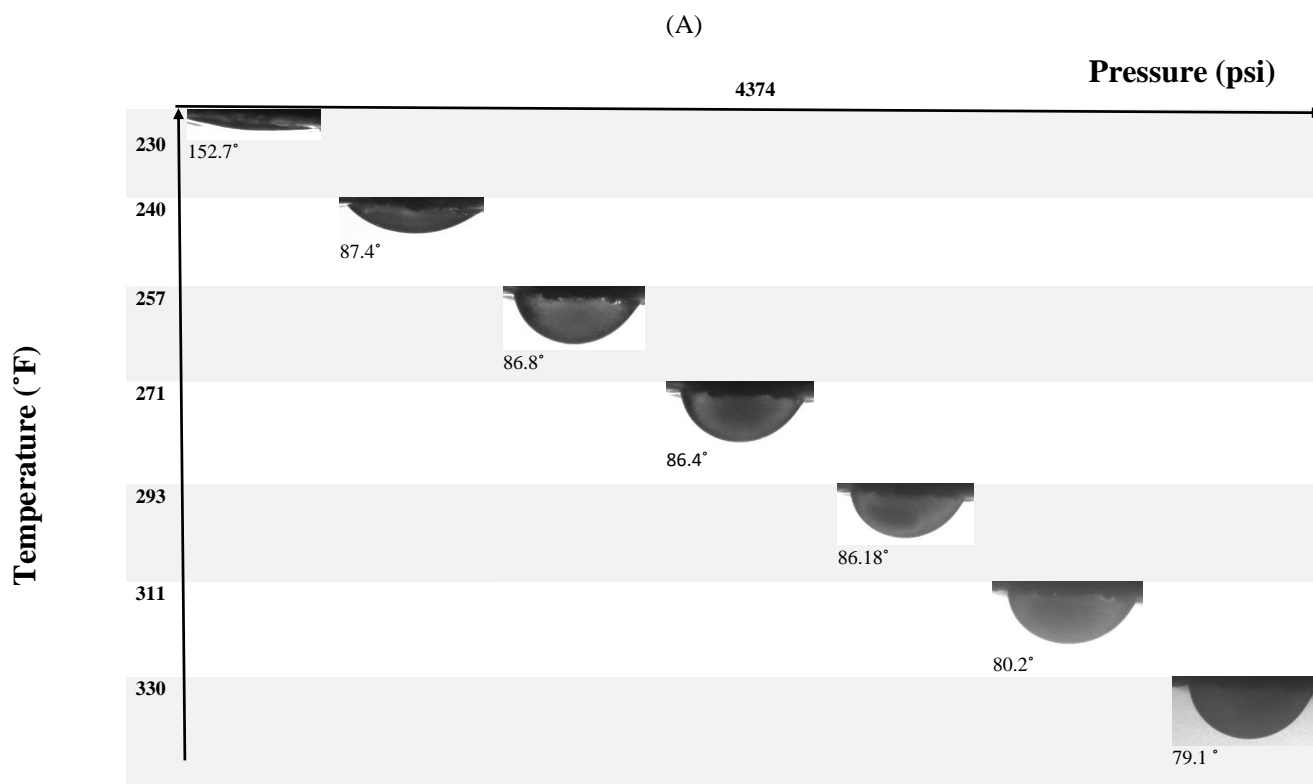


**Figure 70: Images of an oil drop on aged rock surface showing contact angle with increasing temperature and pressuring during heating for surfactant N4+A4 (1:1) total surfactant concentration of 0.2 wt% in solution with 5 wt% isopropanol.**



**Figure 71: Plot of contact angle against temperature showing wettability alteration for surfactant N4+A1 (1:1) total surfactant concentration of 0.2 wt% in solution with 5 wt% isopropanol.**





(B)

**Figure 72: Images of an oil drop on aged rock surface: a) Increasing temperature and pressuring during heating. b) Decreasing temperature and constant pressure during cooling; for surfactant N4+A1 (1:1) with total surfactant concentration of 0.2 wt% in solution with 5 wt% isopropanol.**

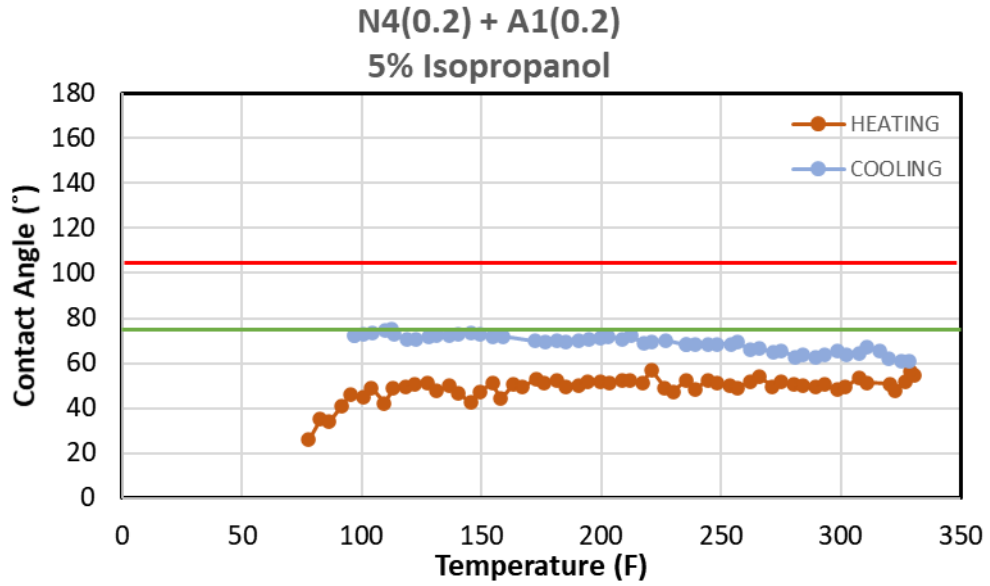
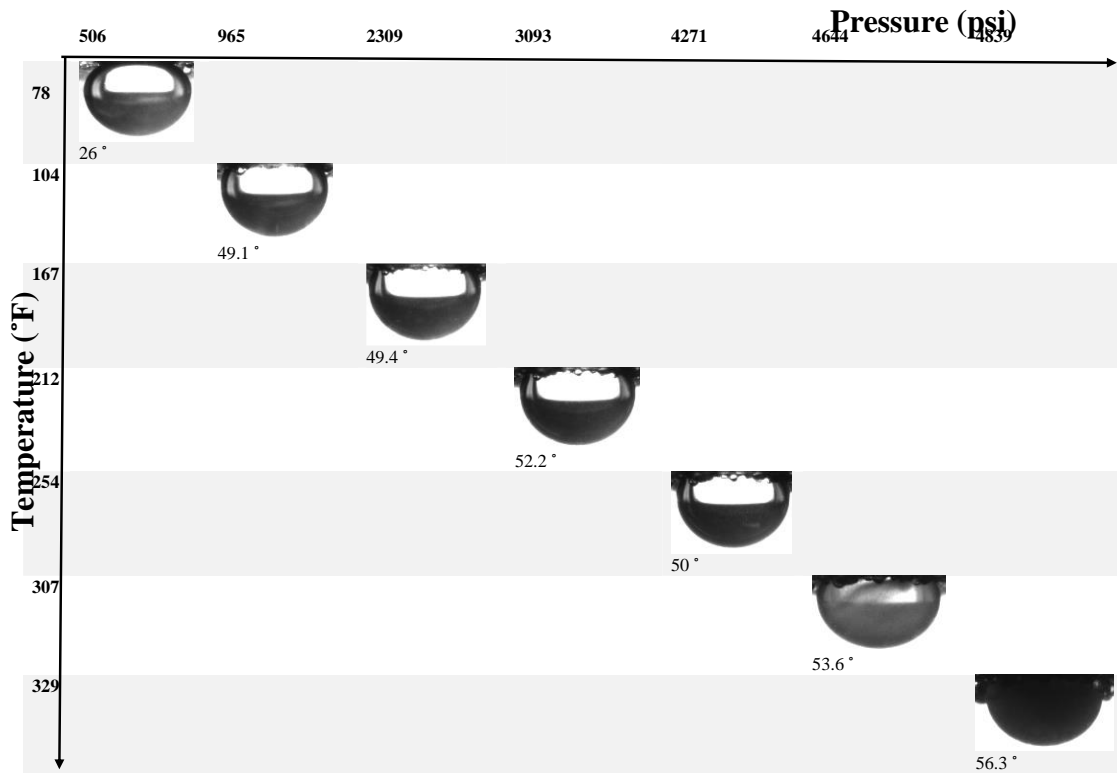
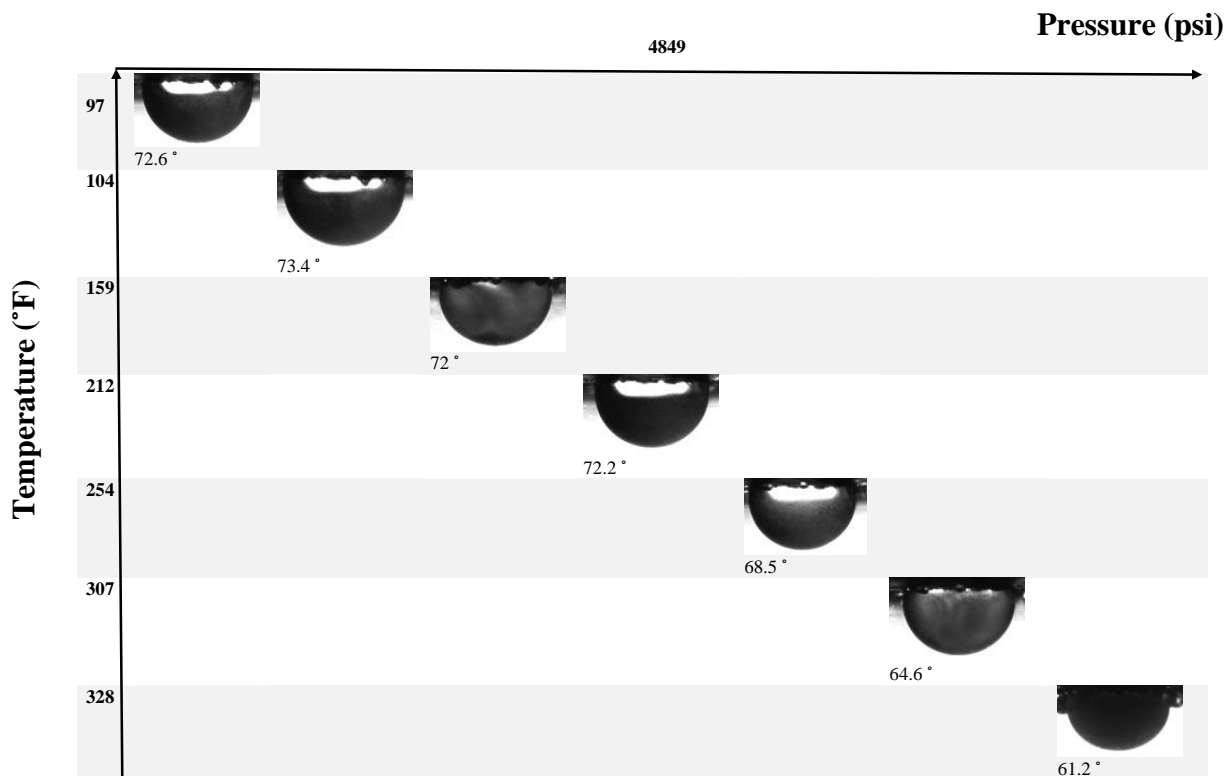


**Figure 73: Plot of contact angle against temperature showing wettability alteration for surfactant N4+A1 (1:1) with total surfactant concentration of 0.4 wt% in solution with 5 wt% isopropanol.**



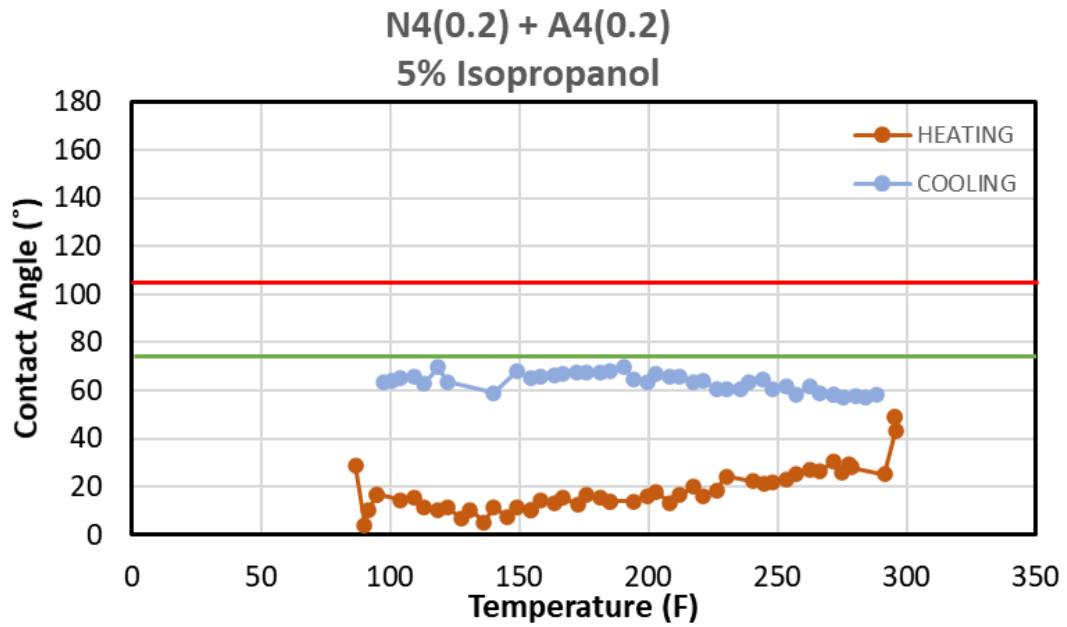
(A)



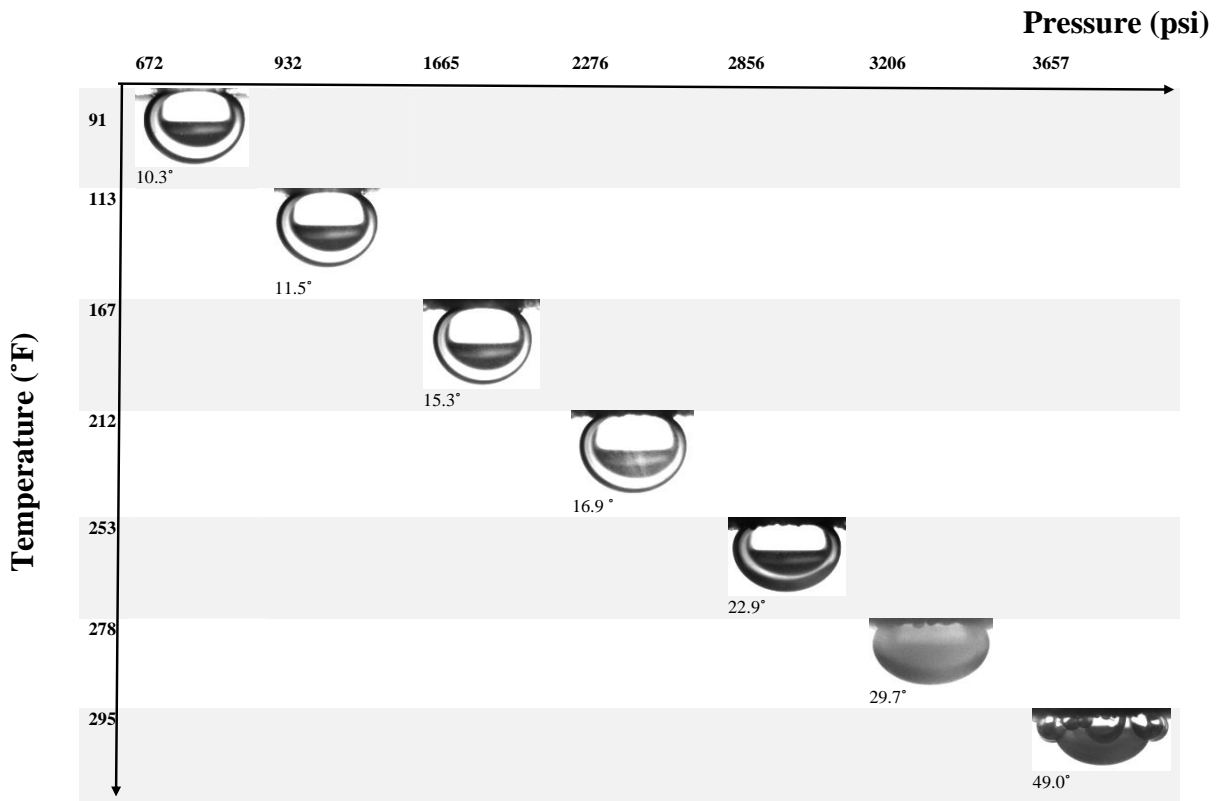
(B)

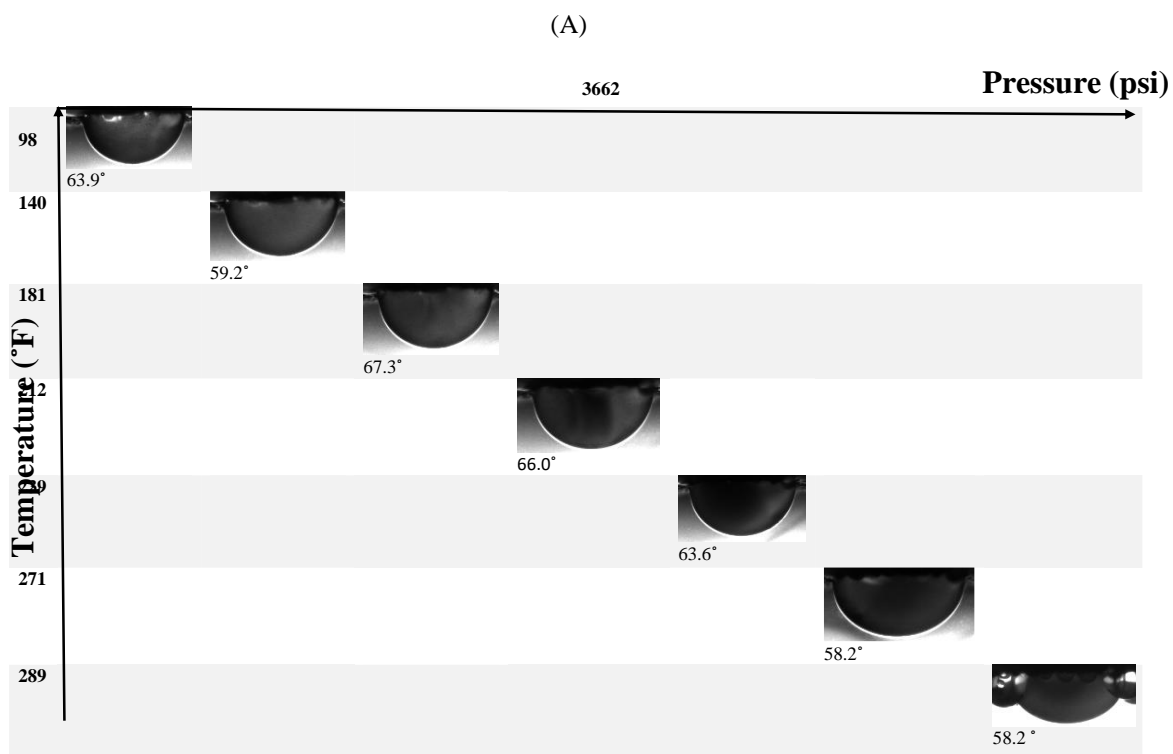
**Figure 74: Images of an oil drop on aged rock surface: a) Increasing temperature and pressure during heating. b) Decreasing temperature and constant pressure during cooling; for surfactant N4+A1 (1:1) with total surfactant concentration of 0.4 wt% in solution with 5 wt% isopropanol.**





**Figure 75: Plot of contact angle against temperature showing wettability alteration for surfactant N4+A4 (1:1) with total surfactant concentration of 0.4 wt% in solution with 5 wt% isopropanol.**





(B)

**Figure 76: Images of an oil drop on aged rock surface: a) Increasing temperature and pressure during heating. b) Decreasing temperature and constant pressure during cooling; alteration for surfactant N4+A4 (1:1) with total surfactant concentration of 0.4 wt% in solution with 5 wt% isopropanol.**

### Combination of Thermal Stabilizers

The increase in the hydrophobe chain length for the ionic stabilizers was observed to correspond to high CPT during the high-pressure cloud point tests. In contrast, wettability alteration tests for single thermal stabilizers indicated that an increase in the contact angle towards oil-wet might be associated with systems exhibiting higher cloud points. These findings, therefore, lead to the conclusion that the length of the hydrophobe on the ionic stabilizer is key in designing a surfactant blend for the reservoir system in

question. Surfactants with longer hydrophobes exhibit lower adsorption, resulting in poorer wettability alteration and better synergy between the nonionic surfactant and ionic stabilizer in the bulk phase, improving cloud point. Hence, a combination of stabilizers was tested to strike a balance between thermal stability and wettability alteration.

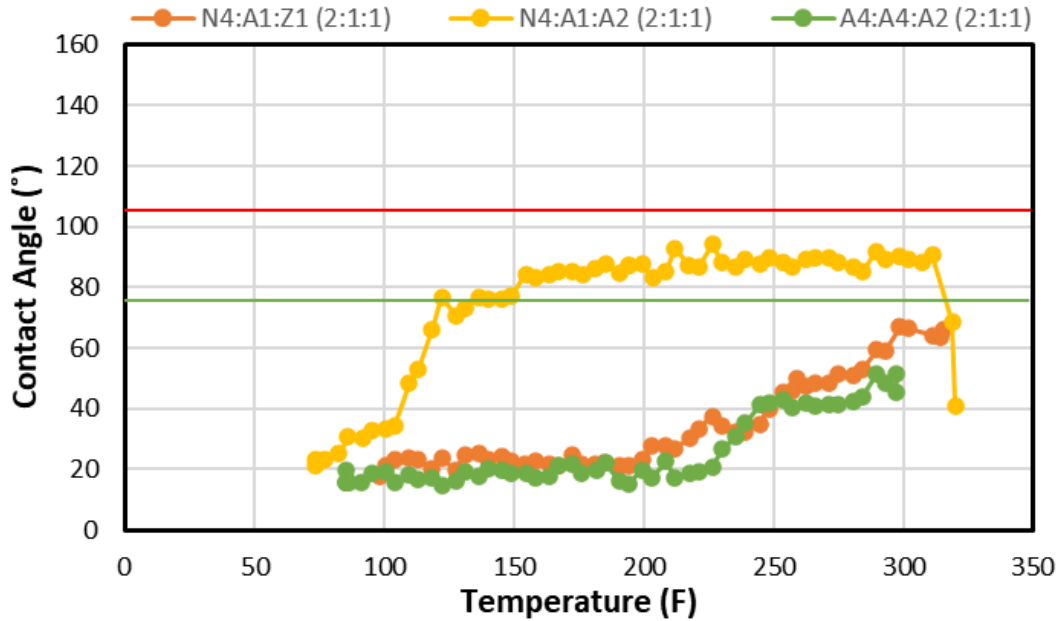
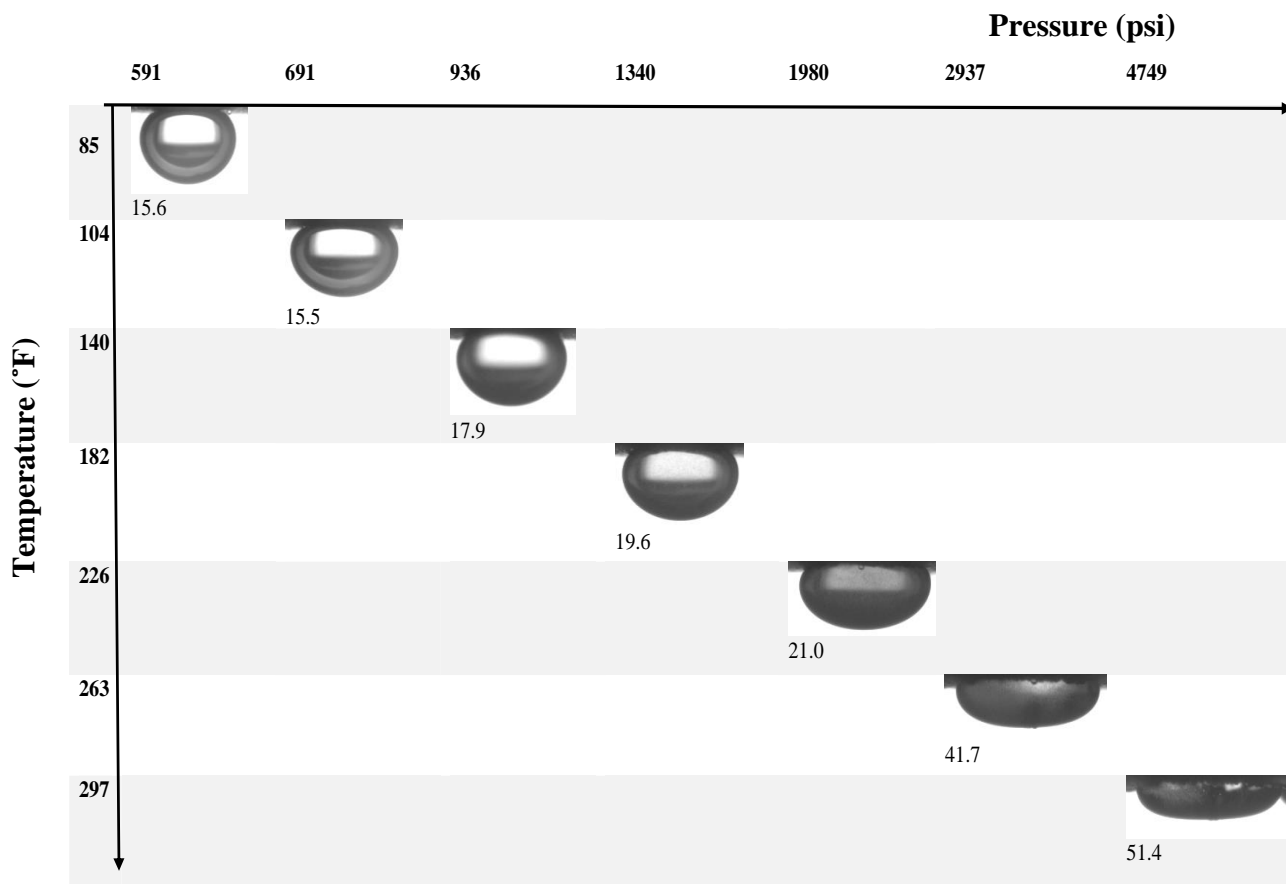


Figure 77: Wettability alteration with surfactant N4 and two ionic thermal stabilizers. Note: Total surfactant concentration 0.4 wt%.



**Figure 78: Images showing a change in contact angle of an oil drop on aged rock in ternary surfactant blend containing N4:A4:A3 (2:1:1). Note: Total surfactant concentration is 0.4 wt%.**

As seen in Figure 77, nonionic surfactant N4 at 0.2 wt% was used in three blends. For combination N4:A1:A2 and N4:A4:A2, anionic cosurfactant surfactant A2 was selected for its ability to improve CPT while A1 and A4 render the surface very water-wet. N4:A1:A2 in ratio 2:1:1 started strongly water-wet at room conditions, but CA increased towards intermediate with increasing temperature. This blend, however, remained stable at reservoir temperature of 325°F without exhibiting cloud point. For N4:A4:A2, the contact angle remained water-wet up to CPT of 320°F. The images shown in Figure 78 show the stable oil droplet on a water-wet surface with N4:A4:A2.

Zwitterionic cosurfactant, Z1, which rendered the rock surface strongly water-wet when used in a 2:1 ratio with N4, and intermediate at a ratio of 1:1; was then tested in place of the anionic A2. It was observed that though the surface remained water-wet, CP was below reservoir temperature at 316°F.

In verifying the hypothesis on the influence of each surfactant, the ratio of the ionic cosurfactants were altered. Figure 79 revealed that the CA remained strongly water-wet when A4, surfactant with the shorter hydrophobic tail, was the cosurfactant at higher concentration. The CPT also was observed to decrease from 320°F to 316°F with the decrease in concentration of A2, the surfactant with the longer hydrophobe. It can therefore be concluded that the hydrophobic tail lengths on the ionic cosurfactants play an important role in the wettability alteration and CP enhancement process.

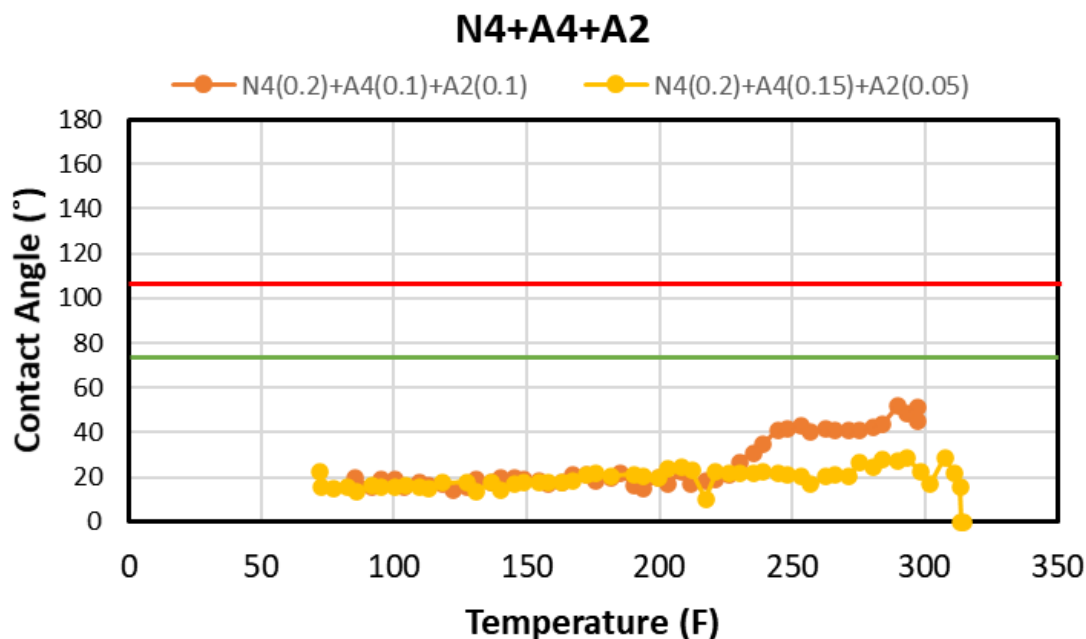


**Figure 79: Wettability alteration using ternary blend N4+A4+A2 varying anionic surfactant ratios from 1:1 to 3:1.**

## Interfacial Tension

As established during experiments at atmospheric conditions, IFT decreases with increasing temperature, seen in Figure 80. The oil-brine system displays a decrease in IFT as temperature increases due to the increase in free energy in the molecules in both phases, enhancing mobility, thereby reducing IFT. Hence, data gathered at high-temperature and high-pressure conditions were observed to follow the same trend.

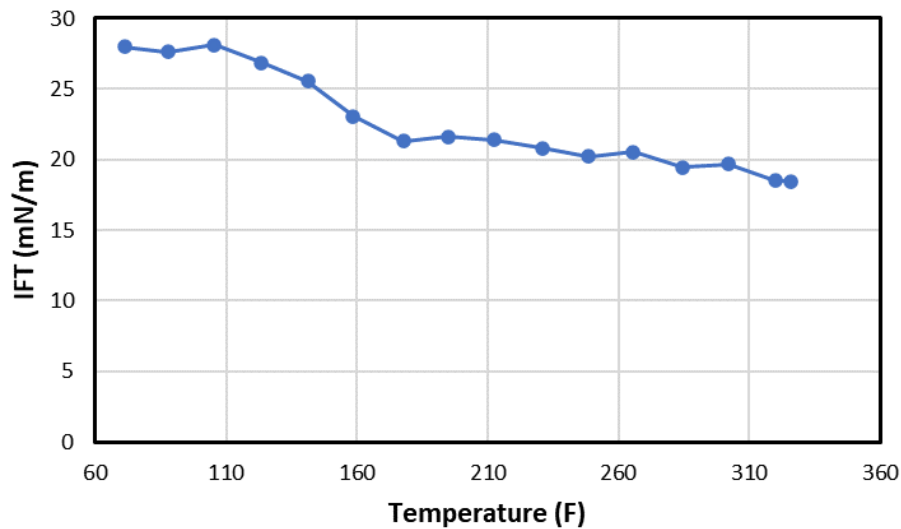


**Figure 80: IFT Eagle Ford oil in make-up water with no surfactant.**

For surfactant/oil/brine systems, interesting observations were made at conditions approaching reservoir temperature; IFT was observed to increase, followed shortly after by the onset of CP. The increase in IFT prior to CPT was observed for all surfactant blends tested, as shown in Figure 81 and Figure 82.

Comparing surfactant blends of N4:A1 and N4:A4, it was observed that the former was more effective in IFT reduction. Ternary surfactant blends of N4+A1+A2 were

observed to create ultra-low IFT at elevated temperature; N4(0.2)+A1(0.1)+A2(0.1) reduced IFT to 0.0066 mN/m at 287°F, while N4(0.2)+A1(0.15)+A2(0.05) reduced IFT to 0.0251 mN/m at 286°F. N4+A4+A2, in comparison, reduced IFT to mN/m at a total concentration of 0.4 wt% and at a total concentration of 0.2 wt%. In general, IFT was observed to increase with the total concentration at initial conditions of low temperature and then yield lower IFT at high temperatures close to CPT. To show this behavior, the images in Figure 85 and Figure 88 have been scaled to allow for comparison of the IFT readings in Figure 83 compared to Figure 84, and Figure 86 compared to Figure 87.

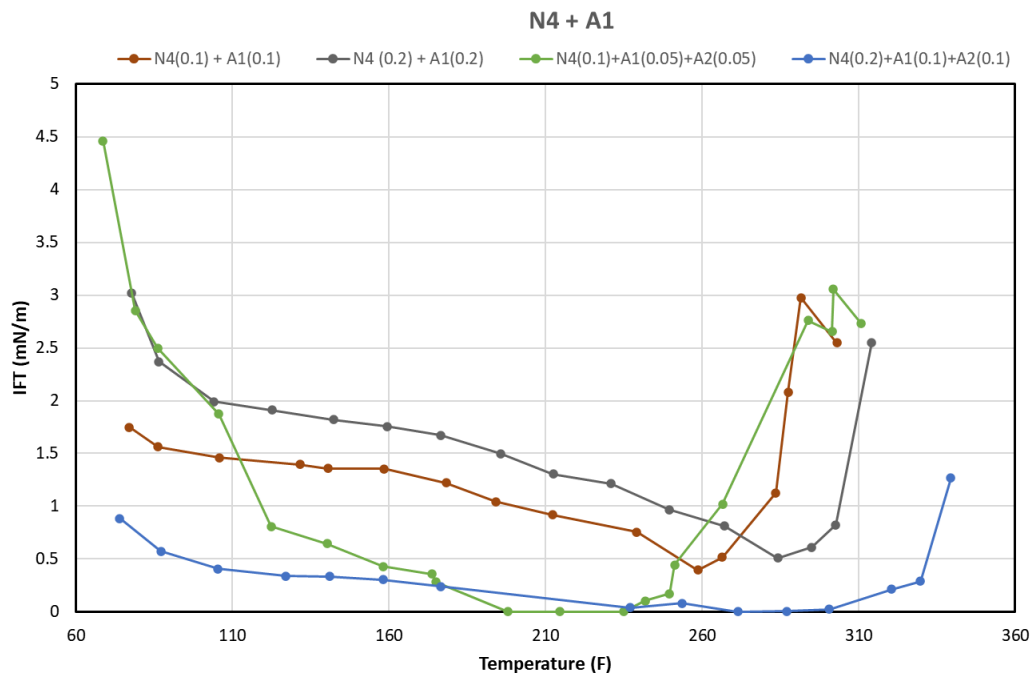


**Figure 81: Interfacial tension of N4+A1 surfactant blends under high-pressure high temperature conditions. Note: IFT observed to decrease and then increase with increasing temperature and pressure.**

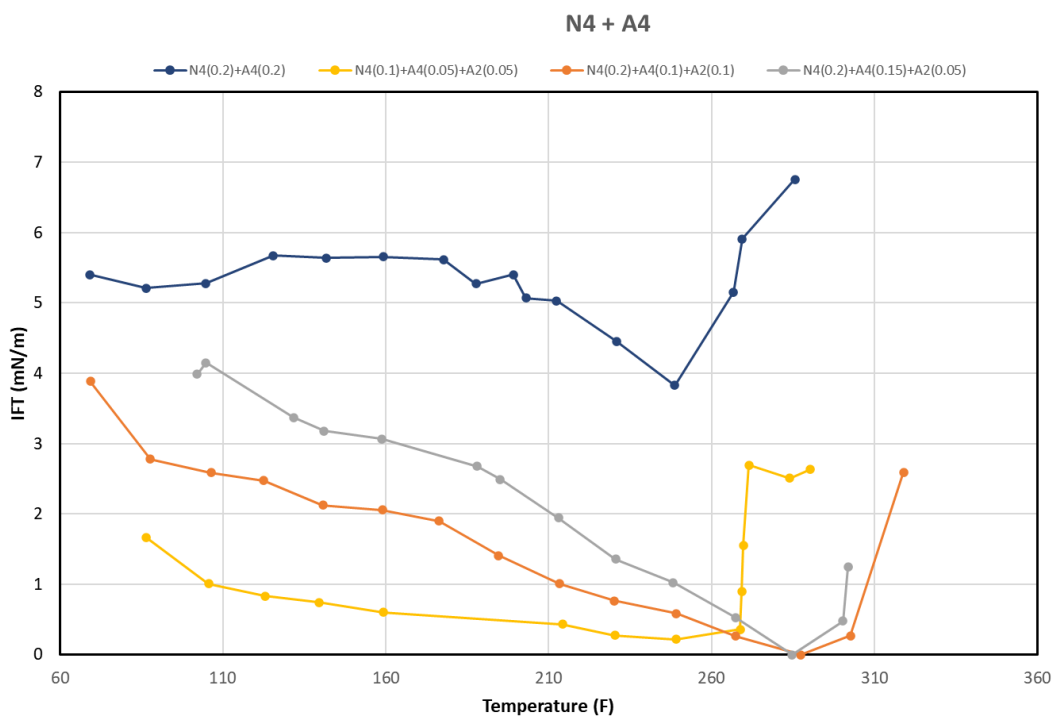


**Figure 82: Interfacial tension of N4+A4 surfactant blends under high-pressure high temperature conditions. Note: IFT observed to decrease and then increase with increasing temperature and pressure.**

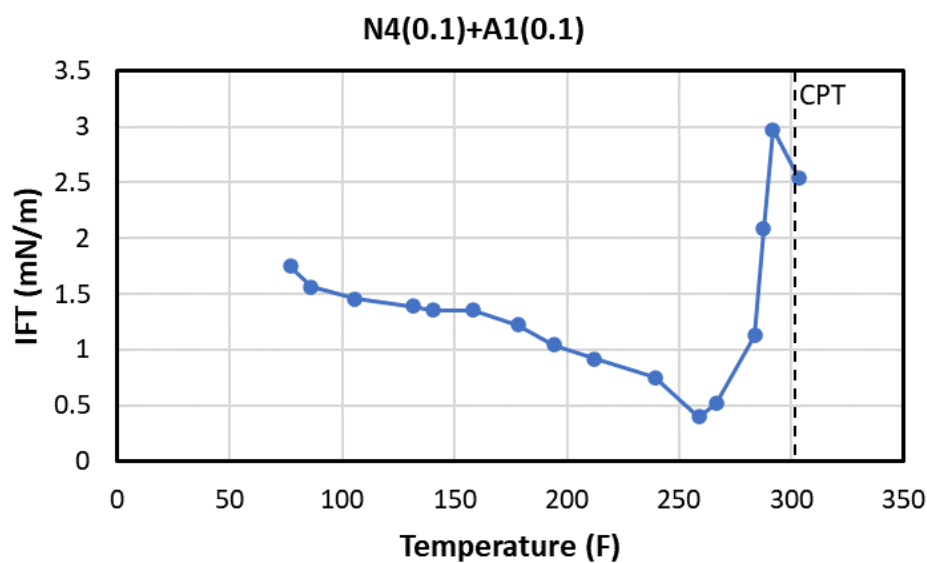


**Figure 83: Interfacial tension of ternary surfactant blend: N4(0.1)+A1(0.2).**



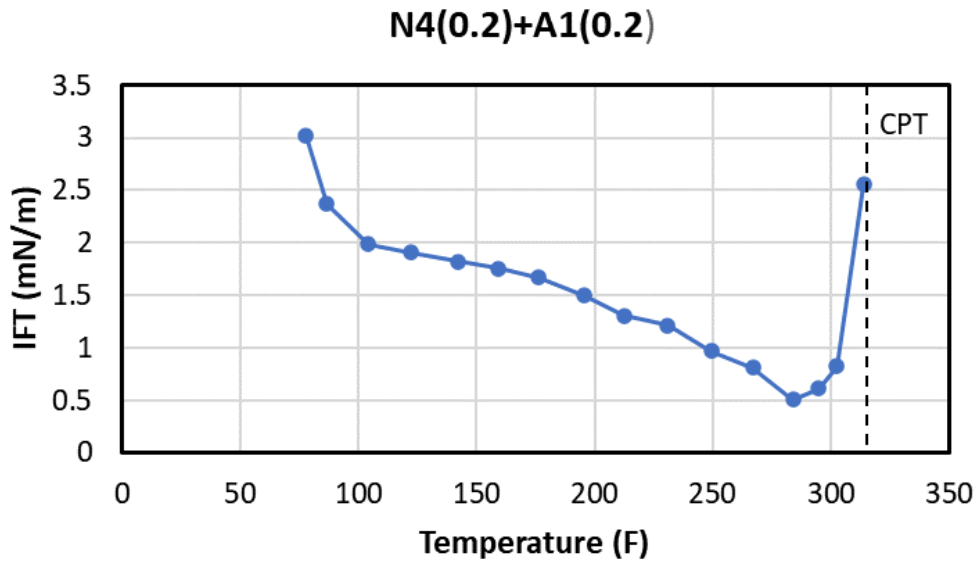


**Figure 84: Interfacial tension of ternary surfactant blend: N4(0.2)+A1(0.2)**



**Figure 85: Images of oil drops during IFT experiment using surfactant blends of N4 and A1 in ratio 1:1 showing a decrease in IFT followed by an increase.**

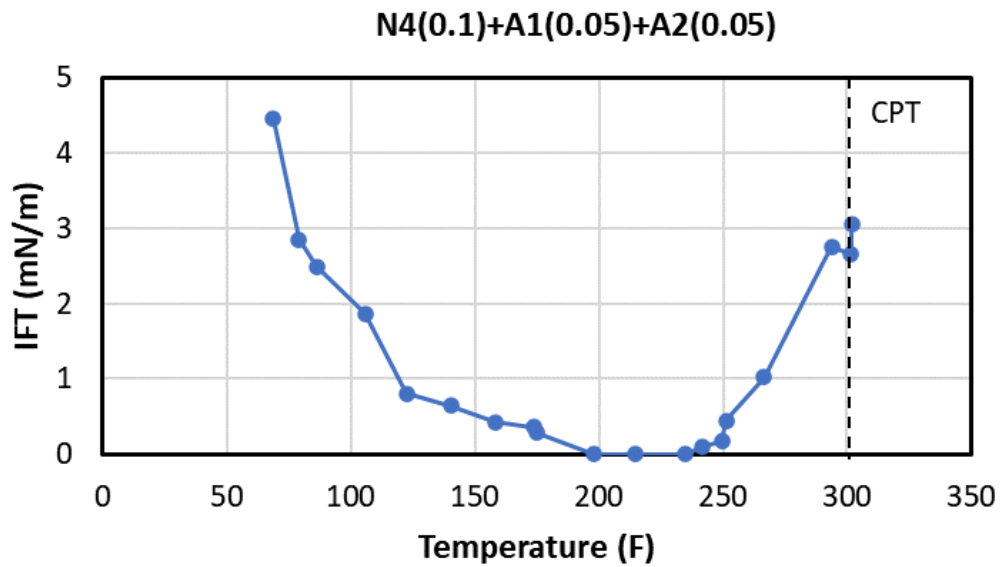


**Figure 86: Interfacial tension of ternary surfactant blend: N4(0.1) + A1(0.05) + A2(0.05).**

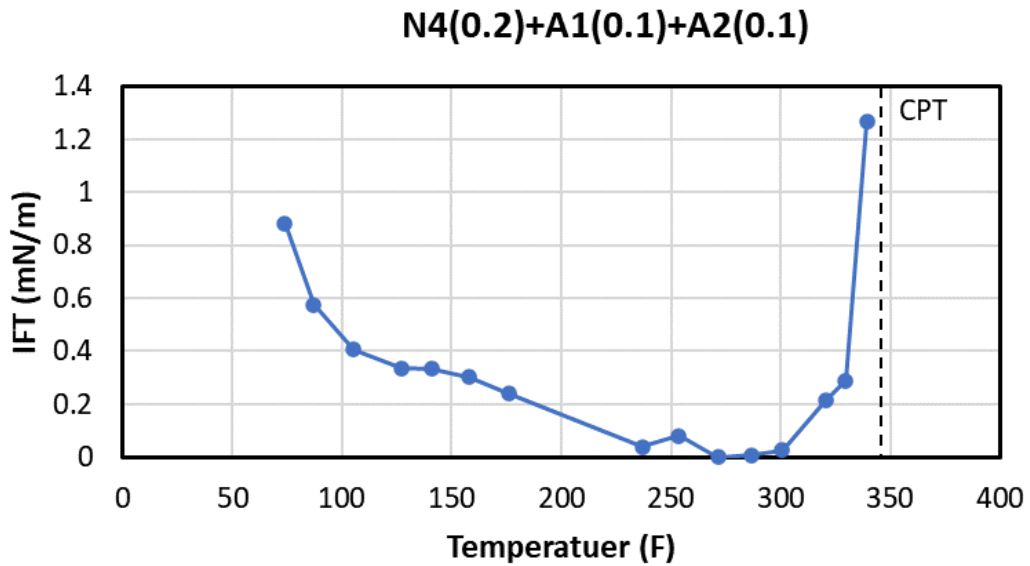


**Figure 87: Interfacial tension of ternary surfactant blend: N4(0.2)+A1(0.1)+A2(0.1).**



**Figure 88: Images of oil drops during IFT experiment using surfactant blends of N4 and A2 in ratio 1:1 showing a decrease in IFT followed by an increase.**

## CHAPTER VI

### SPONTANEOUS IMBIBITION

The final test for surfactant formulations which successfully altered wettability at reservoir conditions is the spontaneous imbibition trial. It is used to validate the findings of previous experiments and quantitatively determine the EOR potential in the ULR. The laboratory-scale tests used aged cores immersed in aqueous solutions made of the MW and the select surfactants. Reservoir temperature was simulated by heating a custom Amott cell which was pressurized to 500 psi. CT scans were taken of the cores before the start of imbibition and at the end to provide visuals on the extent of penetration of the imbibed fluid.

#### **Recovery Factor**

The rate of spontaneous imbibition is usually a function of rock and fluid properties, absolute and relative permeability, viscosity, interfacial tension, and wettability (Zhang et al., 1996); with capillary forces having to overcome the resistance created by viscous force. As the aqueous phase containing surfactant flows into the matrix, it alters wettability and reduces IFT; the oil becomes the non-wetting phase and is displaced easily by the invading surfactant system.

For these experiments, cumulative oil production after eight days of soaking in the surfactant system was measured in a graduated cylinder and converted to recovery factor by normalizing the oil volume data to the OOIP of each core plug. The OOIP was determined by converting the weight difference of the core after and before the aging process to volume with the help of density data. A total of 7 cores were used with an

average OOIP of 3.19 cc and porosity of 13%. Incremental recovery due to surfactant was evaluated by comparison to recovery from the base case, MW with no surfactant and CA of 150°. A total of six nonionic-anionic surfactant blends were tested, four of which were at a total surfactant concentration of 0.4 wt% and two at a total concentration of 0.2 wt%. Due to the complexity of the HPHT SASI setup, production was carried out twice, on the fifth and eighth day of imbibition, and it was observed that no additional oil was produced from the core after the fifth day. The production schedule was subsequently designated to the sixth day of soaking i.e., 144 h.

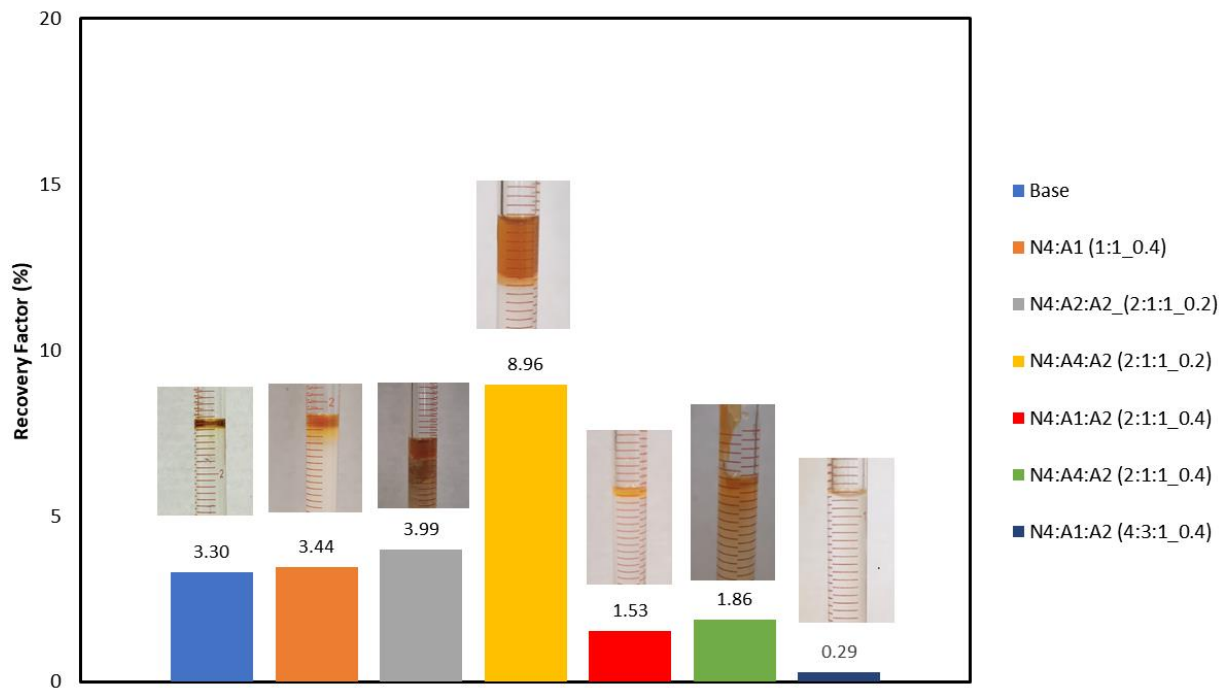


**Figure 89: Oil recovery factor for novel nonionic systems developed.**

As expected, the negative capillary forces in the core's hydrophobic pores resulted in a low recovery factor of 3.3% for the base case. The blend N4+A1 at a total surfactant concentration of 0.4 wt% recovered only 3.4% of OOIP. Upon production from the HPHT

imbibition cell, the effluent was observed to be turbid due to significant emulsion generation, as shown in Figure 90. The next surfactant system, N4+A1+A2, at ratio 2:1:1, total surfactant concentration of 0.2 wt% and CPT of 336°F also failed at significantly improving recovery with a RF of 4%. Emulsions were observed alongside waxy production shown in Figure 91. For the N4+A4+A2 blend at 0.2 wt%, recovery was significantly improved compared to the base case; 0.325 cc of oil was produced, equating to 8.93% recovery. At 0.4 wt%, N4+A1+A2 and N4+A4+A2, at ratio 2:1:1, led to the lowest oil recoveries at 1.54% and 1.86% respectively; lower than the base case with no surfactant. N4+A4+A2 also produced waxy emulsions at the higher concentration ( Figure 92), unlike N4+A1+A2, which produced waxy emulsions at the lower concentration. Surfactant system N4+A1+A2 with ratio 4:3:1 was observed to produce the least amount of oil during the HPHT spontaneous imbibition experiment, less than 0.05 cc oil was recovered along with tight emulsions.

Note: the wax produced during the imbibition is believed to be a very condensed phase created due to increased oil volume in the core when compared to the oil volume present in earlier experiments, contact angle and IFT. The increased volume of oil cannot be solubilized with the given surfactant system leading to behavior which deviates from classic phase behavior (Puerto and Reed 1982).

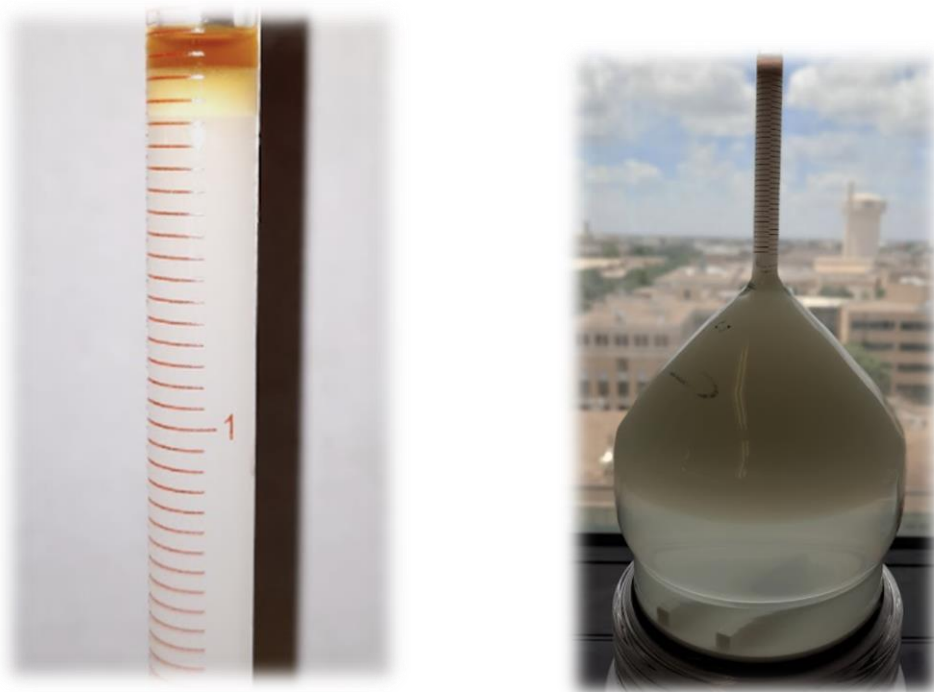


**Figure 90: Images showing recovery (left) and effluent from HPHT Imbibition cell (right) using surfactant N4+A1.**

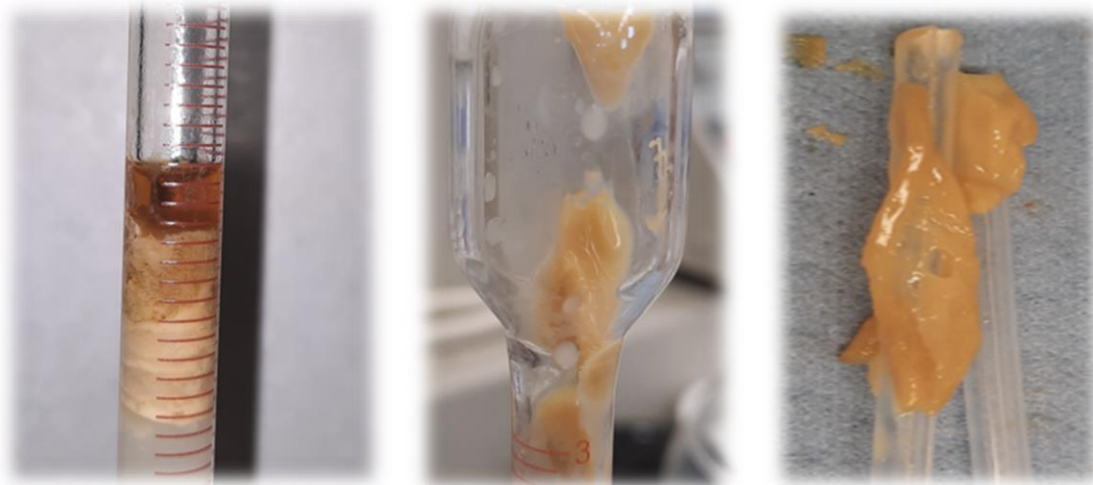


**Figure 91: Wax produced during HPHT SASI experiment with surfactant system N4(0.1)+A1(0.05)+A2(0.05).**

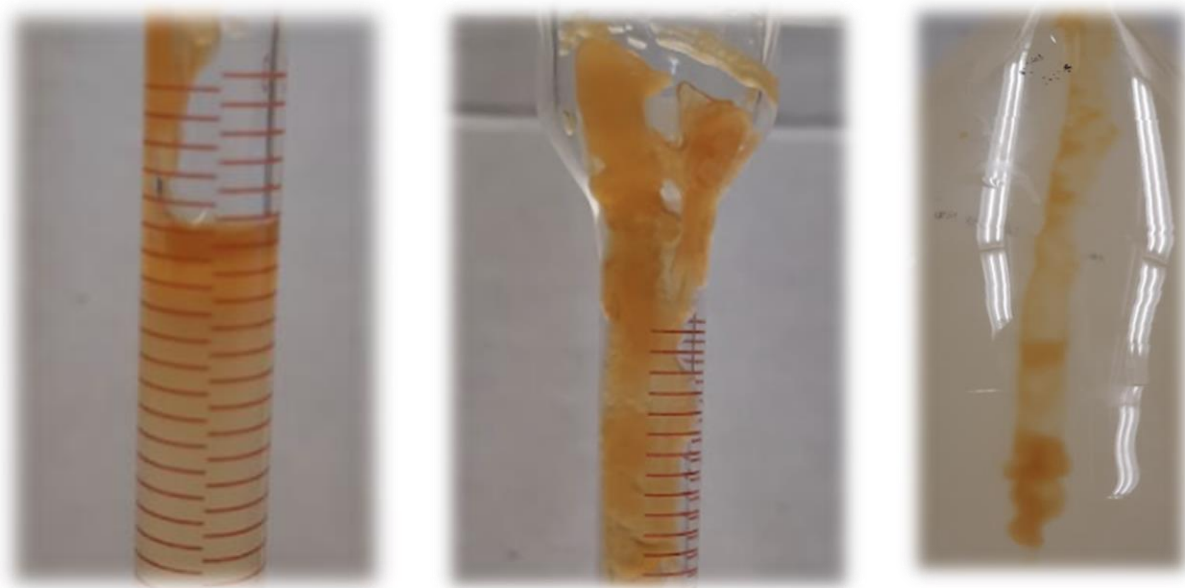


**Figure 92: Wax produced during HPHT SASI experiment with surfactant system N4(0.2)+A4(0.1)+A2(0.1).**

**Table 5: Summary of spontaneous imbibition experiments showing recovery factors and improvement in recovery compared to the base case.**

Surfactant	Ratio	Total Concentration (wt%)	CP (°F)	Recovery Factor (%)	Improved Oil Recovery (%)
Base	N/A	N/A	N/A	3.27	-
N4:A1	2:1	0.4	320	3.36	0.03
N4:A1:A2	2:1:1	0.2	330	3.99	0.22
N4:A4:A2	2:1:1	0.2	320	8.93	1.73
N4:A1:A2	2:1:1	0.4	340	1.55	-0.53
N4:A4:A2	2:1:1	0.4	320	1.86	-0.44
N4:A1 :A2	4:3:1	0.4	348	0.29	-0.91



Except for the best performing surfactant, N4+A4+A2 (2:1:1) at 0.2 wt%, whose contact angle was estimated manually to be slightly oil-wet, the surfactant systems designed all displayed low IFT along with water- to intermediate-wet contact angles. A combination that shifts capillary pressure from negative to positive, improving spontaneous imbibition and enhancing oil recovery. Calculation of capillary pressure neglecting the pore radius denoted as  $P_c*r$  (Table 6) showed the change from negative to positive with all, but surfactant blends N4+A2 (1:1) and N4+A4+A2 (2:1:1) at 0.2 wt%. Unfortunately, plots of recovery factor against CA, IFT, and  $P_c*r$  shown in Figure 93, Figure 94, and Figure 95 did not display distinct trends.

**Table 6: Estimated capillary pressure at 320°F.**

Surfactant	Total Concentration (wt%)	CA (°)	IFT (mN/m)	$P_c*r$
Base	N/A	149	18.481	-8.270
N4:A1	0.4	48	2.725	-3.489
N4:A1:A2	0.2	94	2.729	5.291
N4:A4:A2	0.2	109	2.697	-3.104
N4:A1:A2	0.4	88	0.213	0.426
N4:A4:A2	0.4	51	2.595	3.852
N4:A1:A2	0.4	51	0.304	0.451

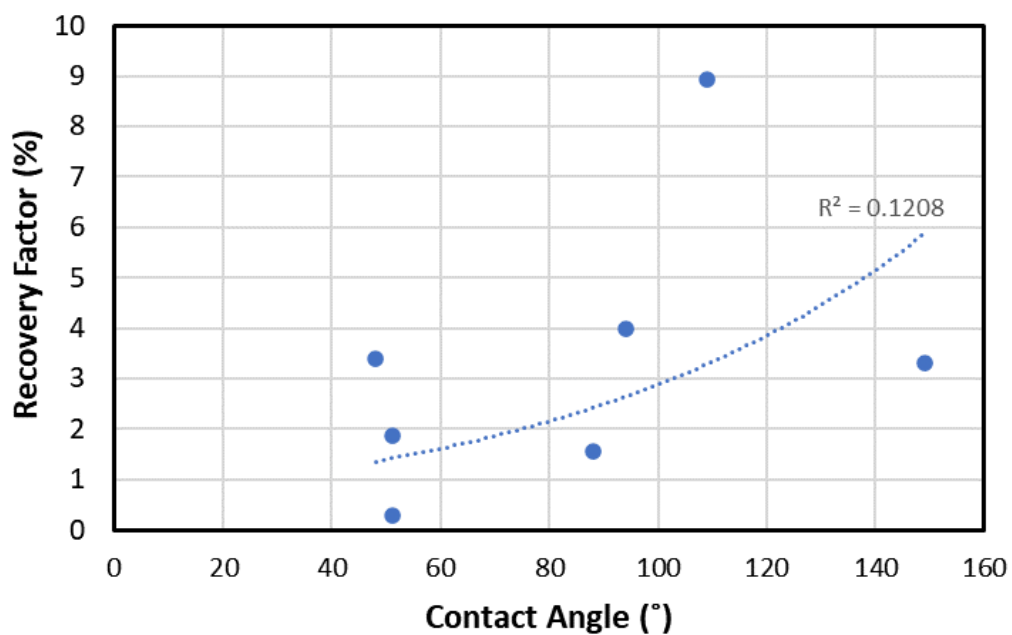


Figure 93: Correlation between contact angle and recovery factor.

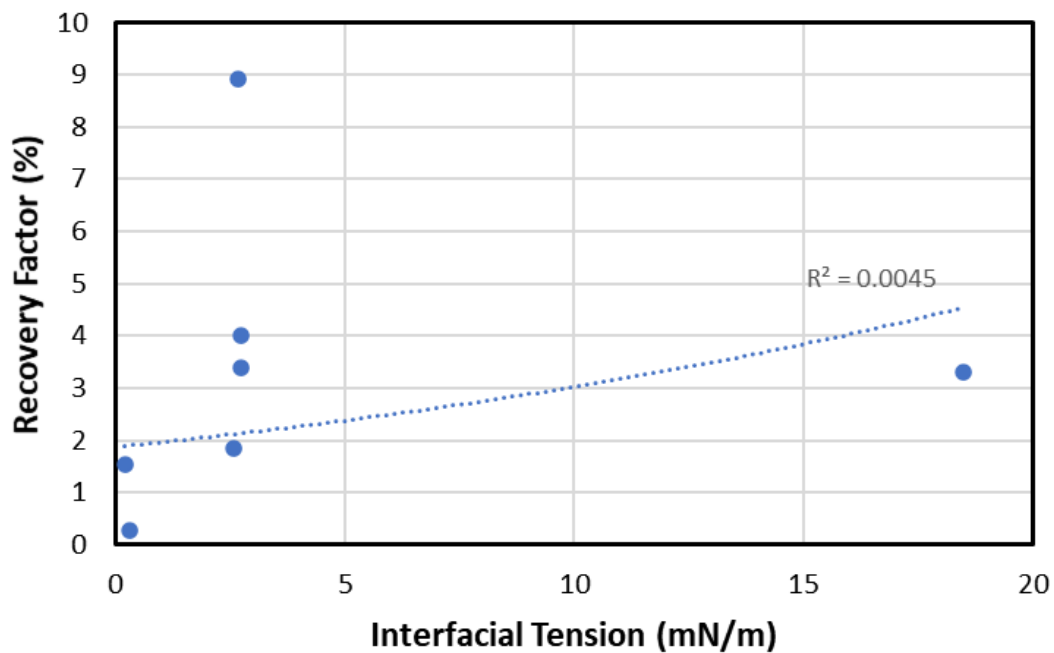
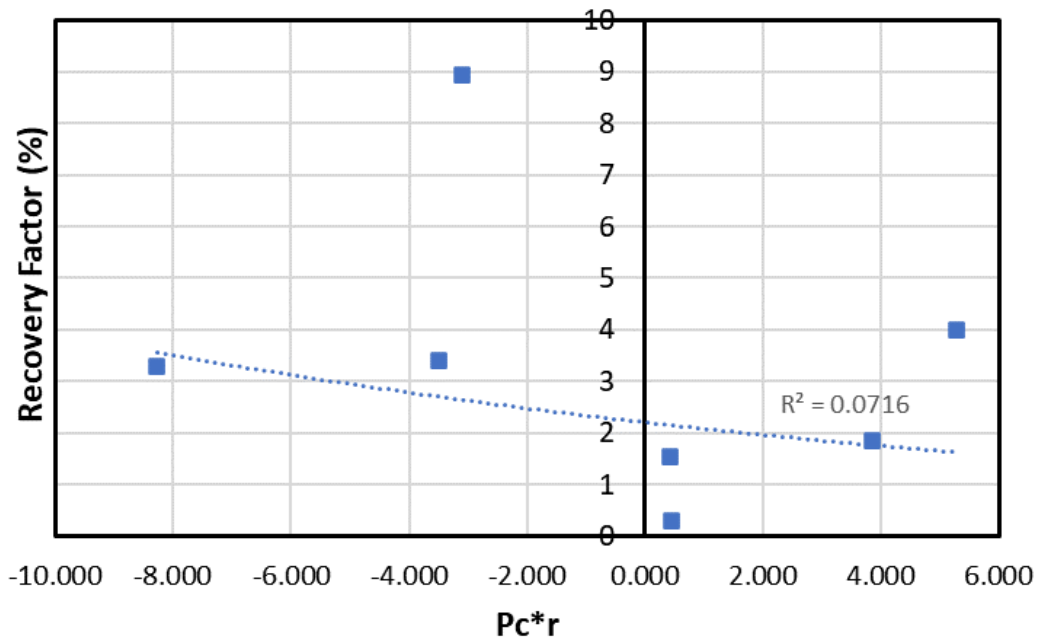
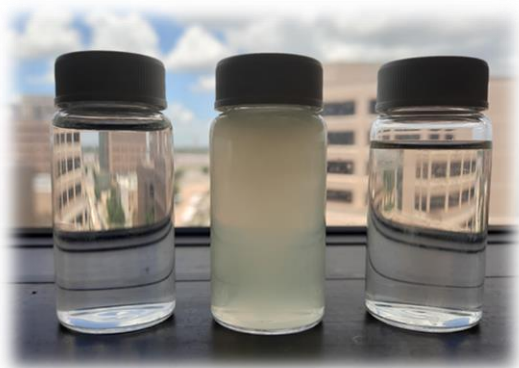


Figure 94: Correlation between interfacial tension and recovery factor.

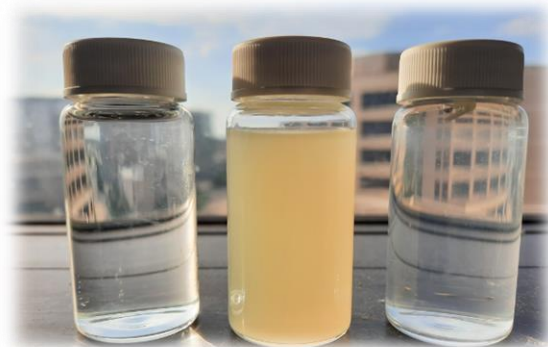


**Figure 95: Correlation between capillary pressure and recovery factor.**

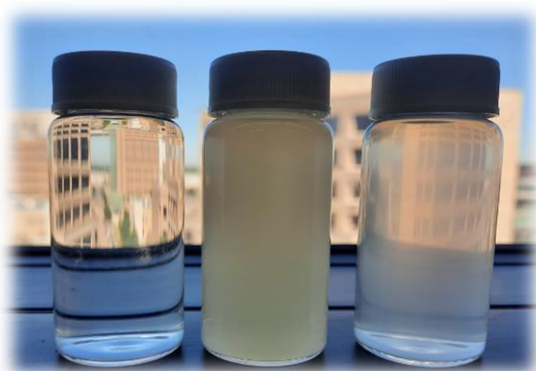
The lack of direct evidence for the driving force behind oil production was undoubtedly the result of the tight emulsions formed during the imbibition process. Surfactant samples collected from the freshly prepared solution before heating were compared to the effluent produced from the imbibition chamber. A third sample, recovered from the accumulator cell heated to reservoir temperature, was also included. The images in Figure 96 clearly show the creation of water-in-oil nano-emulsions. The ratio of surfactant-rich aqueous phase to oil in the chamber at high temperatures of 325°F.



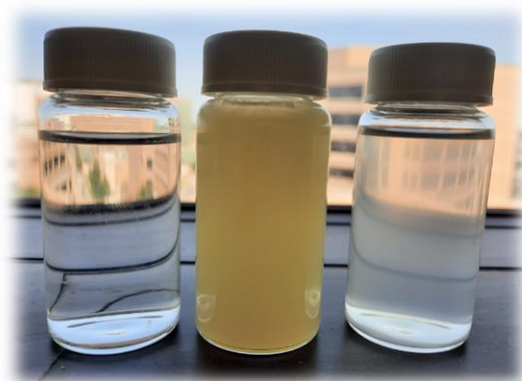
a.



b.



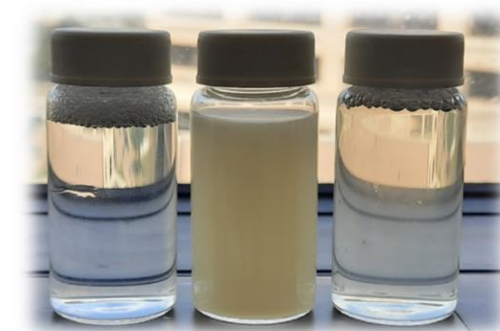
c.



d.



e.



f.

**Figure 96: Images of surfactant solutions collected during the life cycle of the HPHT SASI study. From left to right: 1. Fresh surfactant sample, 2. Effluent from imbibition cell, and 3. Sample recovered from accumulator (after heating).**

**Surfactant: a. N4+A2 (0.4 wt%), b. N4+A1+A2 (0.2 wt%), c. N4+A1+A2 (0.4 wt%), d. N4+A4+A2 (0.2 wt%), e. N4+A4+A2 (0.4 wt%), f. N4+A1+A2 (4:3:1, 0.4 wt%).**

Therefore, at the end of this study, the combination of water-wet CA with low IFT was no match for the emulsions formed using the nonionic surfactant blends. The tight nano-emulsions created significantly decreased the visible amount of oil recoverable. In addition, the wax produced was noted as undesirable as it can clog production lines and increase treatment costs in the surface facilities.

### **Computerized Tomography Scan Results**

Comparing CT images taken before and after the HPHT SASI experiments, oil production regions were identified by the increase in CT number (brighter colors), which indicates water imbibition. Figures 97-101 show 2D cross-sections at different points along the length of each core plug used. The general change in color from violet to yellow indicates an increase in water saturation and water movement into the core plug.

For samples shown in Figure 97 and Figure 98 CT imaging revealed a decrease in density as indicated by a shift to darker colors post-imbibition, contrary to what is expected after spontaneous imbibition. A plot of CT difference against production was generated by estimating the average CT numbers across each core, and then calculating the difference in pre-imbibition CT number and post-imbibition CT number. Where the difference is positive, post-imbibition CT number is lower, which is an anomaly noted in this study. As seen in Like the earlier attempts at correlating recovery, CT difference showed no visible trend.

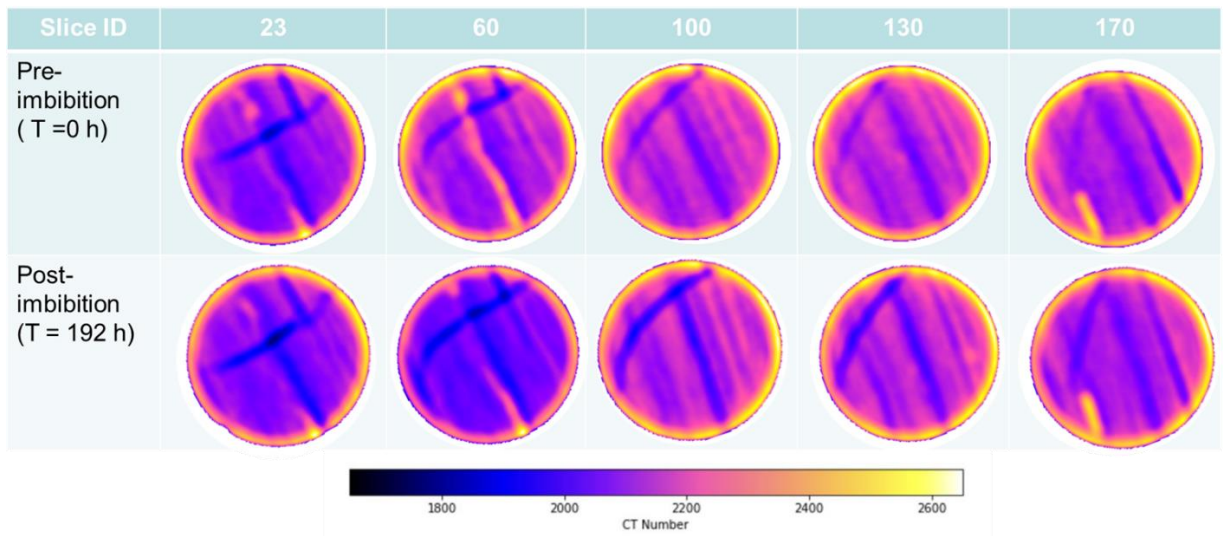


**Figure 97: CT images of core plug which imbibed surfactant N4(0.2)+A1(0.2). Post-imbibition CT numbers are lower, implying higher oil saturation which is unlikely.**

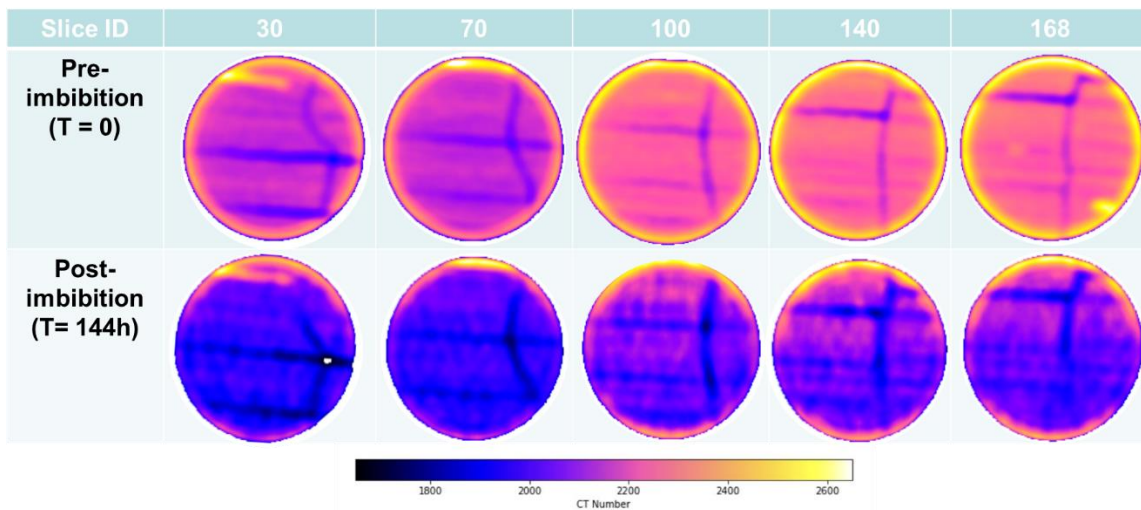


**Figure 98: CT images of core plug which imbibed surfactant N4(0.1)+A1(0.05)+A2(0.05). Post-imbibition CT numbers are lower, implying higher oil saturation which is unlikely.**

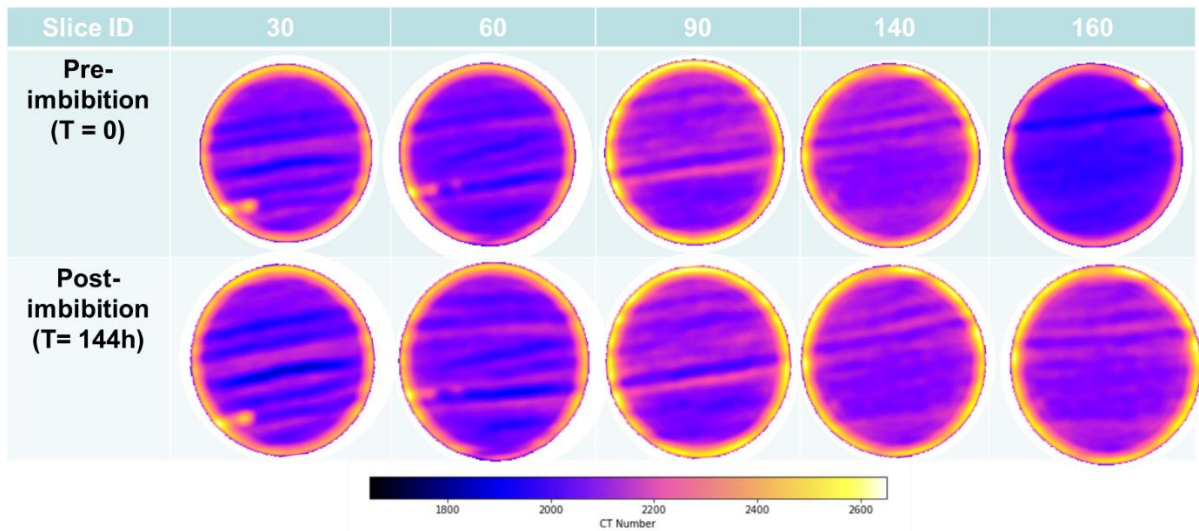


**Figure 99:** CT images of core plug which imbibed surfactant N4(0.1)+A4(0.05)+A2(0.05). Post-imbibition CT numbers are higher, implying increased water saturation.

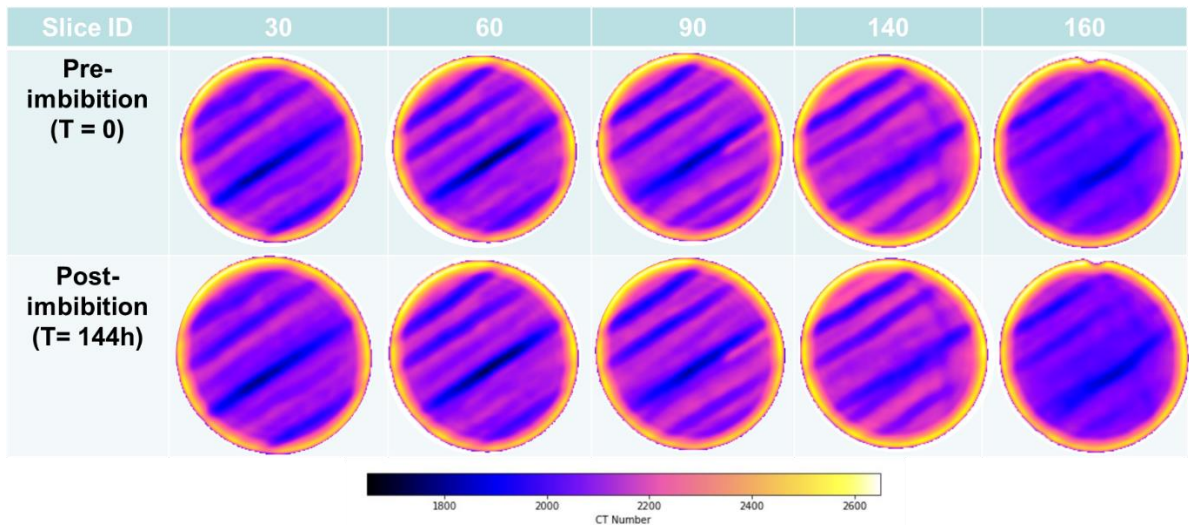


**Figure 100:** CT images of core plug which imbibed surfactant N4(0.2)+A1(0.1)+A2(0.1). Post-imbibition CT numbers were lower in a few regions, implying increased water saturation.

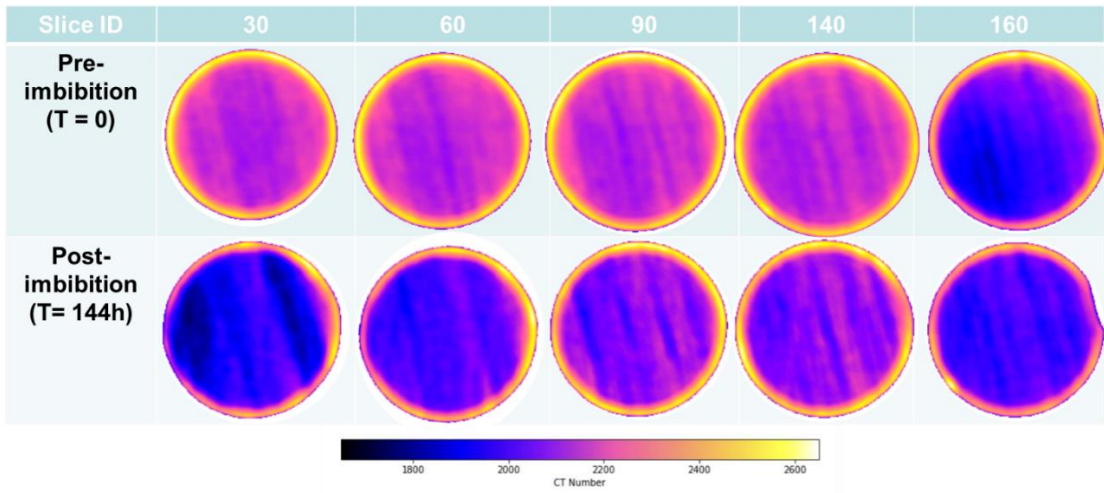


**Figure 101: CT images of core plug which imbibed surfactant N4(0.2)+A4 (0.1)+A2(0.1). Post-imbibition CT numbers are lower, implying increased oil saturation.**

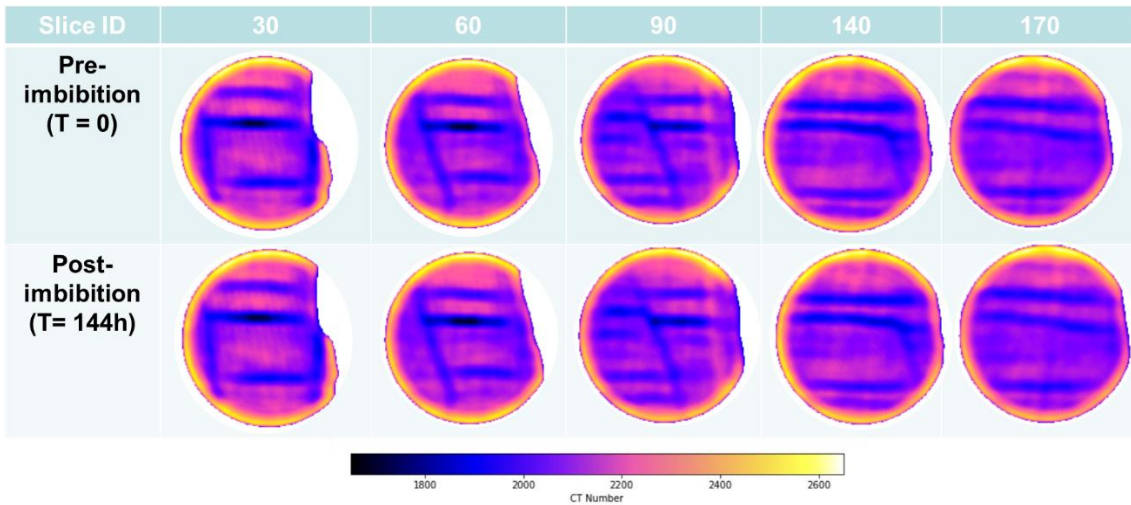


**Figure 102: CT images of core plug which imbibed surfactant N4(0.2)+A2 (0.15)+A2(0.05). Post-imbibition CT numbers appear similar indication little oil saturation.**



**Table 7: Average CT numbers for each core sample.**

	N1	N2	N3	N4	N5	N6
<b>0 HR</b>	2226.725	2180.830	2199.476	2182.433	2241.866	2096.796
<b>144 HR</b>	2213.257	2050.170	2191.200	2149.582	2093.495	2212.214
<b>Difference</b>	13.467	130.660	8.276	32.851	148.371	-115.417

Note: A1 represents the sample used with surfactant N4:A1, A2 is N4:A1:A2 (0.2 wt%), A3 is N4:A4:A2 (0.2 wt%), A4 is N4:A1:A2 (0.4 wt%), A5 is N4:A4:A2 (0.4 wt%) and A6 is N4:A1:A2 (4:3:1\_0.4 wt%).

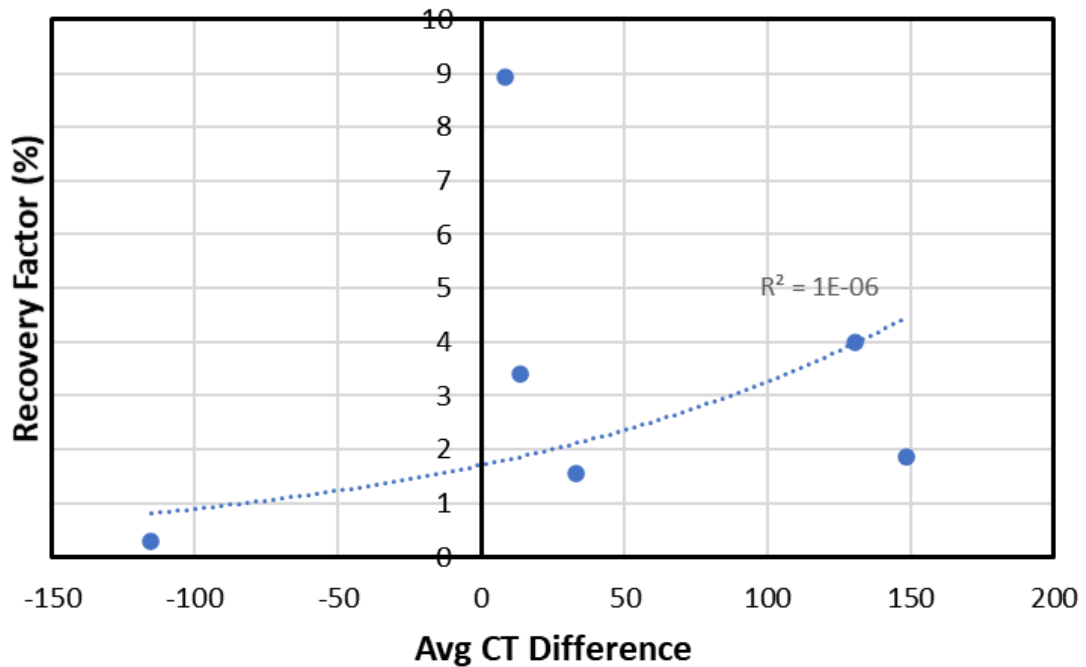


**Figure 103: Correlation between average CT number difference and recovery factor.**

## Surfactant Adsorption

As explained in the introductory part of this study, surfactants in the reservoir treatment fluid can affect fluid interaction or rock interactions. In conventional reservoirs, enhancing oil recovery focuses on increasing capillary number as IFT is reduced to low or ultra-low values. However, when dealing with unconventional reservoirs, we aim to alter wettability. Wettability alteration occurs when surfactant molecules adsorb on the rock surface. Therefore, increased surfactant adsorption on the reservoir matrix is desirable, unlike in conventional reservoirs where the surfactant adsorption means the loss of surfactant for IFT reduction.

Using a Bubble Pressure Tensiometer manufactured by Kruss, the surfactant concentration in the effluent produced during the SASI experiments was measured. Concentration curves made by dilution of the same surfactant samples were used to mimic the reduction in surfactant concentration which is expected as the surfactant is adsorbed onto the rock. By matching the surface tension of the effluent to the surfactant curves, an approximate of the amount of surfactant left in the core was obtained.

For the surfactant N4+A1 (1:1), at a total surfactant concentration of 0.4 wt%, the BPT data shown in Figure 104 revealed that the effluent produced contained approximately 0.2 wt%. This indicates that approximately half of the surfactant concentration was adsorbed during the imbibition process. Surface tension data was unclear for the surfactants at 0.2 wt%, as seen in Figure 105 and Figure 106 where readings varied with bubble age. Consequently, values across the surfactant concentration curves at 410 ms were compared to that of the effluent to determine an approximate surfactant

concentration after imbibition. N4+A1+A2 at 0.2 wt% was then determined to be at 0.14 wt%, implying an absorbed amount of 0.06 wt% of active surfactant. Similarly, the effluent of N4+A4+A2 at 0.2 wt% contained 0.08 wt% of surfactant, implying adsorption of 0.12 wt%. At a total weight percent of 0.4, the effluent of surfactant N4+A1+A2 (2:1:1) contained 0.26 wt% implying adsorption of 0.14 wt% while the effluent of N4+A4+A2 (2:1:1) contained 0.29 wt% implying adsorption of 0.11 wt%. Surfactant N1+A1+A2 (4:3:1) contained 0.175 wt% implying adsorption of 0.225 wt%.

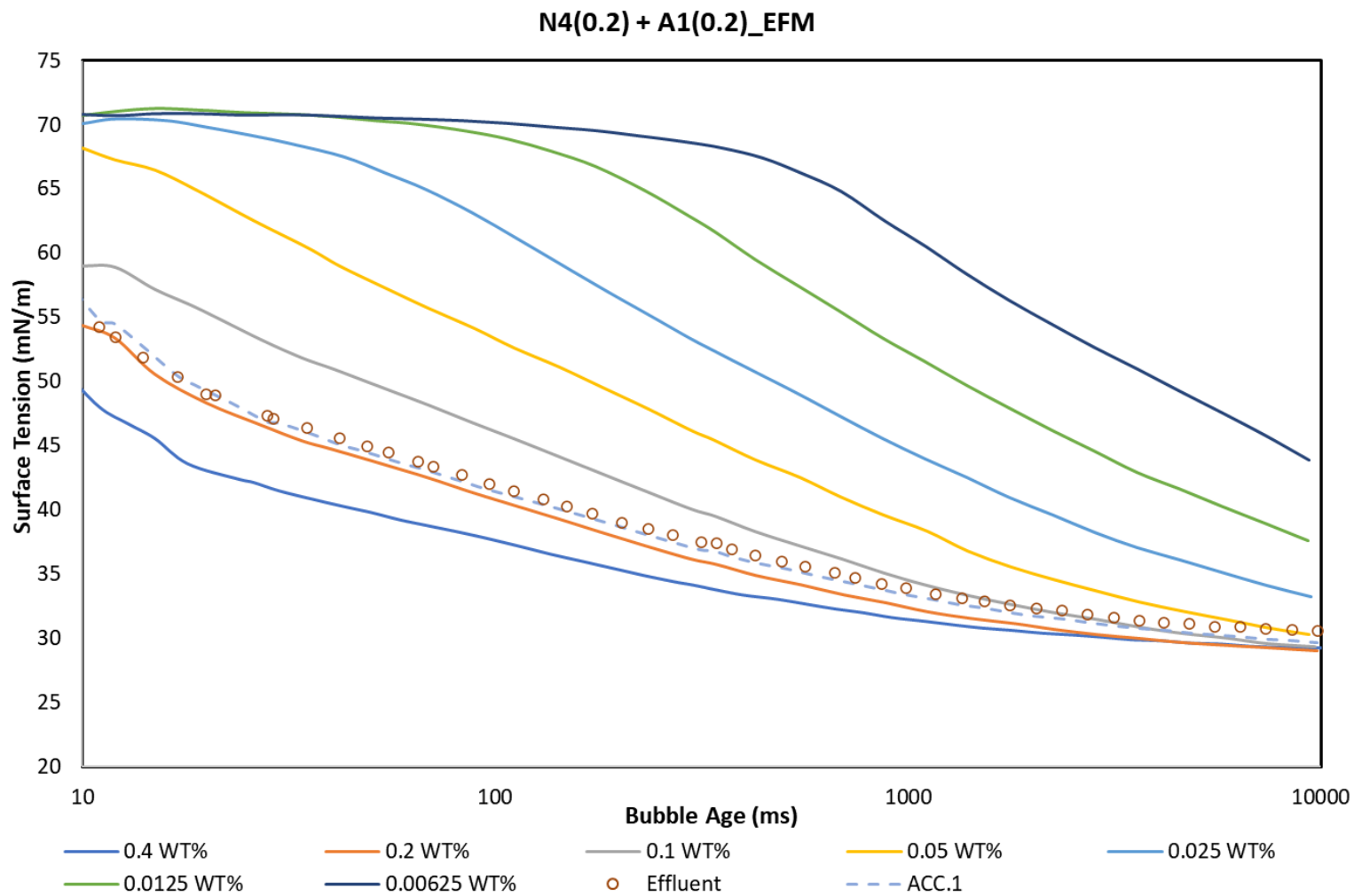


**Figure 104: Surfactant adsorption curves showing interfacial tension of effluent compared to surfactant concentrations not in contact with core plug. Note: surfactant system N4+A1 (1:1) in aqueous solution of 0.2 TDS.**

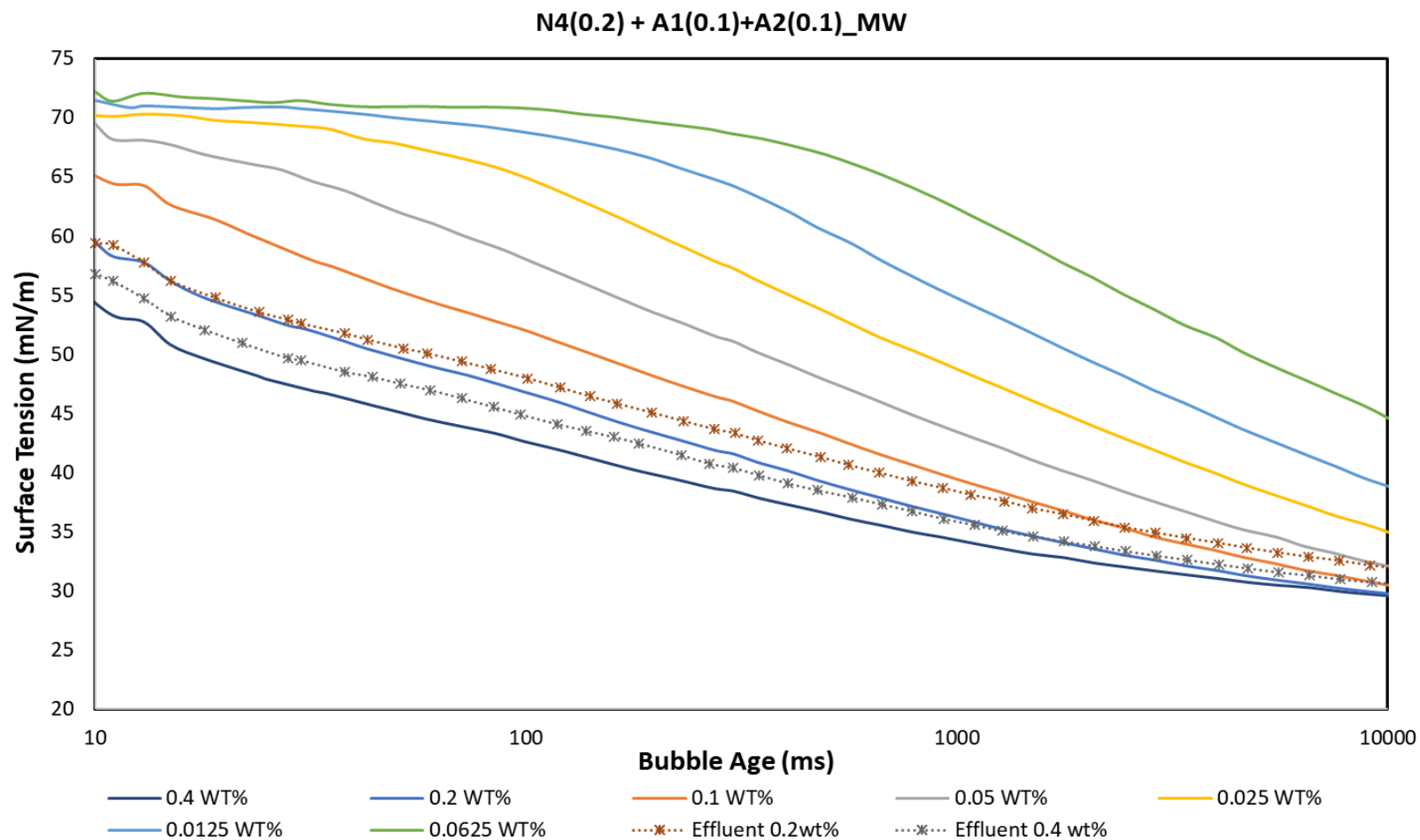


**Figure 105: Surfactant adsorption curves showing interfacial tension of the effluents from the surfactants with total wt% of 0.2 and 0.4, compared to surfactant concentrations not in contact with core plug. Note: surfactant system N4+A1+A2 (2:1:1) in aqueous solution of 0.2 TDS.**

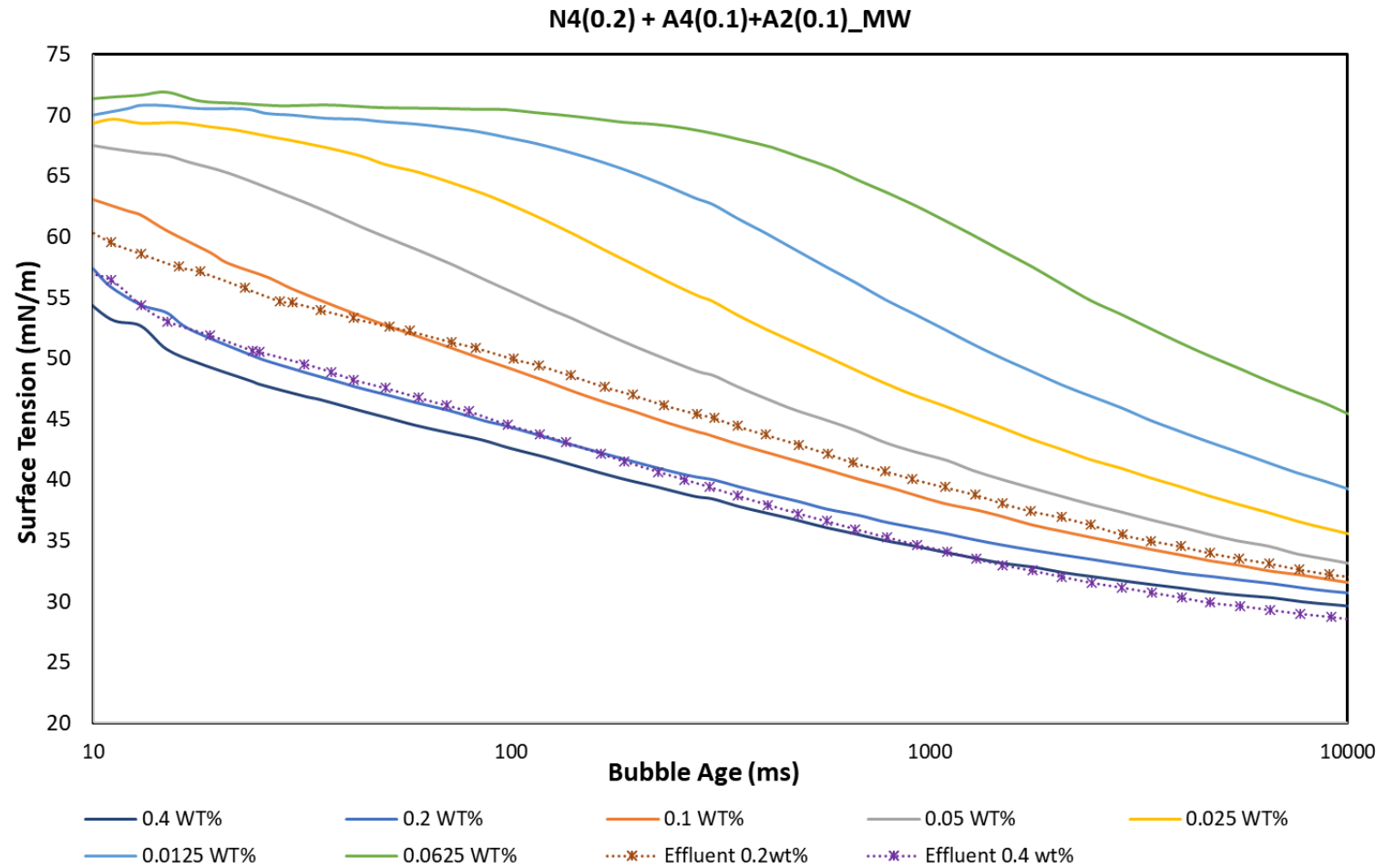


**Figure 106: Surfactant adsorption curves showing interfacial tension of the effluents from the surfactants with total wt% of 0.2 and 0.4, compared to surfactant concentrations not in contact with core plug. Note: surfactant system N4+A4+A2 (2:1:1) in aqueous solution of 0.2 TDS.**

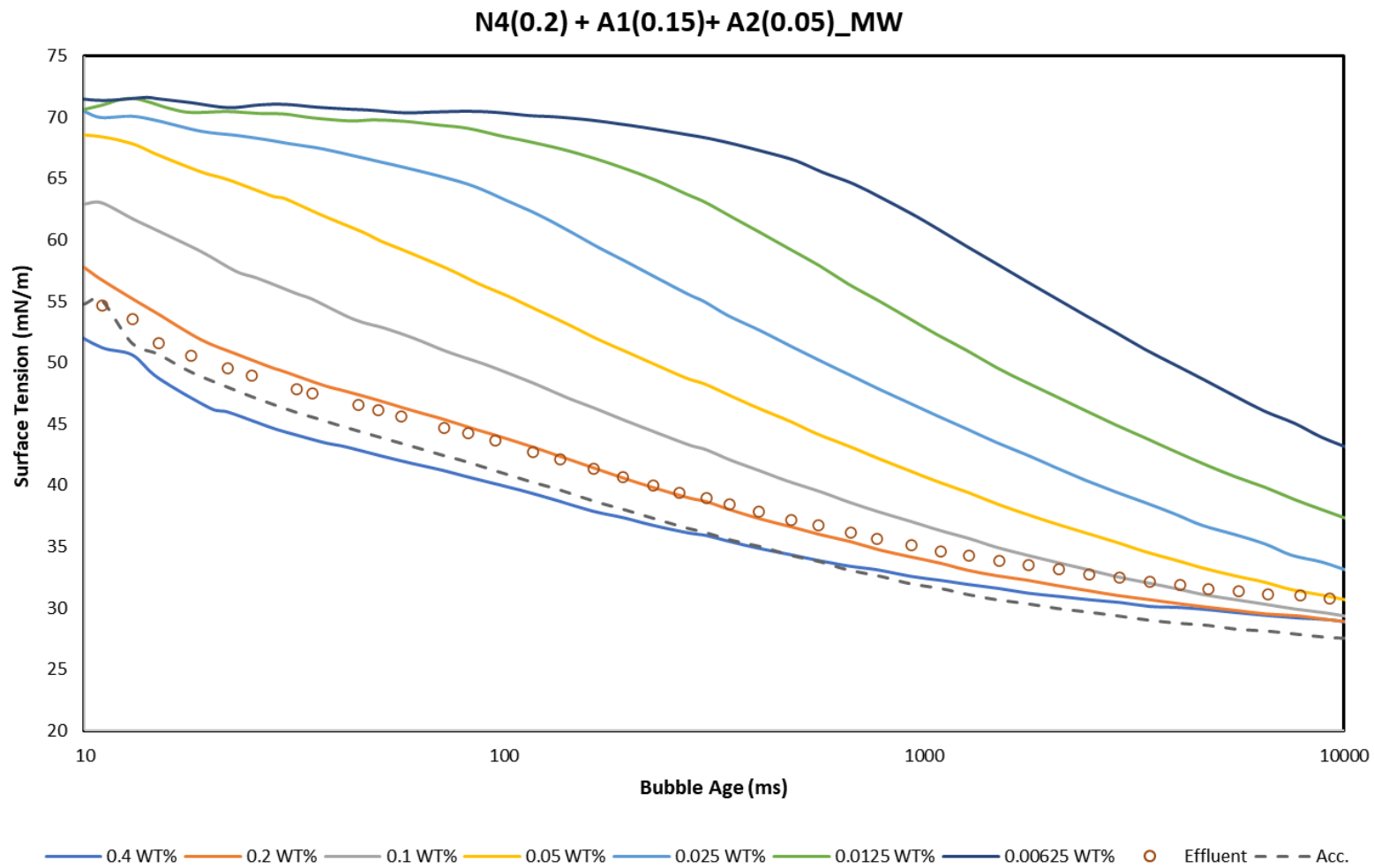


**Figure 107: Surfactant adsorption curves showing interfacial tension of the effluents from the surfactants with total wt% of 0.4 compared to surfactant concentrations not in contact with core plug. Note: surfactant system N4+A1+A2 (4:3:1) in aqueous solution of 0.2 TDS.**

## CHAPTER VII

### CONCLUSIONS

Using cloud point, contact angle, interfacial tension, and spontaneous imbibition experiments, this study into the use of nonionic surfactants and nonionic surfactant blends has been able to observe the behavior of surfactant systems in a high-temperature section of the Eagle Ford reservoir, and provide a system for enhancing oil recovery. The methodology adopted is suitable for studies in other unconventional liquids-rich reservoirs and should serve as guidance for the surfactant screening and selection process. Therefore, the main conclusions are as follows:

#### **Cloud Point**

1. Nonionic surfactants for enhanced recovery are insufficient in certain plays due to the extreme reservoir temperature, which is significantly higher than the cloud point of any single nonionic surfactant. Therefore, ionic surfactants are required as thermal stabilizers to improve nonionic solubility at higher temperatures. Nonionic application at temperatures above the cloud point should be avoided as the surfactant loses its detergency at this condition.
2. Alcohols improve the solubility of nonionic surfactants by increasing the number of hydrogen bonds formed with the aqueous phase.
3. Nonionic surfactants with shorter EO groups (more hydrophobic) show higher thermal stability when combined with ionic surfactants. Van der Waals interactions exist between the nonpolar alkyl tails. This creates a mixed surfactant system whose hydrophilicity is supported by the head groups of both nonionic and ionic surfactant molecules.
4. Increasing the concentration of ionic surfactant leads to an increase in the cloud point temperature.



5. Increasing brine salinity generally results in lower cloud point temperature. Compared to anionic co-surfactants, cationic co-surfactants were observed to perform better in high salinity brines.
6. Due to the competition for solubility amongst ionic charges, anionic surfactants A3 and A2 precipitate at high concentrations creating solutions with irreversible turbidity when the temperature of the solution is lowered.

### **Contact Angle and IFT**

1. All ULR reservoirs are initially oil-wet, as observed during the aging study. The process of restoring reservoir wettability is an essential first step in the surfactant selection process.
2. Although increasing hydrophobicity of the ionic surfactant improves cloud point, it also reduces the surfactant's wettability alteration capability. It was observed that an oil-wet surface is created with an ionic stabilizer with a longer alkyl chain length as a cosurfactant when the temperature is increased. It is believed to result from increased surfactant solubility in the bulk phase rather than adsorption at the rock surface at high temperatures.
3. The use of cationic surfactants as thermal stabilizers shows poor wettability alteration while also damaging the rock surface.
4. Anionic and zwitterionic surfactants used as thermal stabilizers show greater synergy with the nonionic surfactant, creating strongly water-wet surfaces.
5. The use of binary surfactants (nonionic + anionic) is still limited by their cloud point temperature for this reservoir with temperatures at 320°F.

6. Combination cosurfactants, one with a short hydrocarbon tail to maintain water-wet performance and a second with a longer hydrocarbon tail, as the thermal stabilizer work; to raise cloud point to temperatures above 320°F while maintaining water-wet to intermediate contact angles.
7. The use of alcohols as cosolvents helps in improving surfactant cloud point while maintaining wettability alteration potential.
8. However, increasing alcohol concentration increases contact angle as the surfactant becomes more soluble in the bulk phase and does not adsorb on the rock surface.
9. IFT is observed to decrease to ultra-low values with increasing temperature. The decrease is followed by an increase that occurs before cloud point temperature.
10. Increase in the hydrophobicity (length of the carbon tail) of the ionic cosurfactant decreases IFT. As opposed to the case of single nonionic surfactants, which increase IFT with increasing hydrophilicity (increasing EO groups).

### **Spontaneous Imbibition**

1. Surfactant N4+A4+A2 (2:1:1) at a total concentration of 0.2 wt% possesses the best performance with the highest recovery factor of 8.9% OOIP.
2. Spontaneous imbibition experiments reveal that nonionic surfactant blends are prone to emulsion formation.

3. N4+A1+A2 (2:1:1) at 0.2 wt% and N4+A4+A2 (2:1:1) at 0.4 wt% produced more waxy looking emulsions. It is believed the surfactant phase becomes soluble in the oil expelled and at room temperature the mixture coagulates.
4. Correlations between recovery factor and contact angle, interfacial tension, adsorption, or average CT number is not evident. The presence of emulsions made accurate estimation of recovery difficult; thereby impeding efforts to determine the driving factor behind imbibition and improved recovery.
5. CT images show lower density in the core plugs after imbibition. This is abnormal because imbibition of the aqueous phase is meant to increase core density as brine replaces oil in the pores.

### **Recommendations**

Having uncovered a number of interesting findings, the following recommendations are put forward to improve future studies.

1. To help simulate natural production, the spontaneous imbibition experiments should be conducted in two or three stages. The first in formation fluid to simulate natural production, the second in surfactant for EOR, and the third in formation fluid once more to simulate production post surfactant treatment.
2. Imbibition studies should be conducted at low and high-pressure conditions, similar to the contact angle studies. This may help in understanding the effect of temperature on the core effluent.

3. Adsorption analysis should be conducted on uncompromised effluents. There is need for a high-pressure cell, similar to that on the Biolin, which maintains pressure without diluting the surfactant in contact with the core.
4. Analysis of the produced oil to determine what fraction of oil is produced by the surfactant and if the surfactant is present in the oil.

## REFERENCES

- Al-Sabagh, A. M., Nasser, N. M., Migahed, M. A., & Kandil, N. G. (2011). Effect of chemical structure on the cloud point of some new nonionic surfactants based on bisphenol in relation to their surface-active properties. *Egyptian Journal of Petroleum*, 20(2), 59-66. doi:10.1016/j.ejpe.2011.06.006
- Alvarez, J. O., Neog, A., Jais, A., & Schechter, D. S. (2014). *SPE-169001-MS impact of surfactants for wettability alteration in stimulation fluids and the potential for surfactant EOR in unconventional liquid reservoirs*
- Alvarez, J. O., Saputra, I. W. R., & Schechter, D. S. (2018). The impact of surfactant imbibition and adsorption for improving oil recovery in the Wolfcamp and Eagle Ford reservoirs. *SPE Journal (Society of Petroleum Engineers (U.S.) : 1996)*, 23(6), 2103-2117. doi:10.2118/187176-PA
- Alvarez, J. O., & Schechter, D. S. (2017). Wettability alteration and spontaneous imbibition in unconventional liquid reservoirs by surfactant additives. *SPE Reservoir Evaluation & Engineering*, 20(1), 107-117. doi:10.2118/177057-PA
- Anderson, W. G.(1986c). Wettability literature survey-part 3: The effects of wettability on the electrical properties of porous media
- Anderson, W. O.(1987c). Wettability literature survey-part 6: The effects of wettability on waterflooding

- Anderson, W. G. (1987a). Wettability literature survey- part 4: Effects of wettability on capillary pressure. *Journal of Petroleum Technology*, 39(10), 1283-1300.  
doi:10.2118/15271-PA
- Anderson, W. G. (1986a). Wettability literature survey- part 1: Rock/Oil/Brine interactions and the effects of core handling on wettability
- Anderson, W. G. (1987b). Wettability literature survey- part 5: The effects of wettability on relative permeability
- Anderson, W. G. (1986b). Wettability literature, survey- part 2: Wettability measurement
- Austad, T., & Strand, S. (1996). *COLLOIDS A AND colloids and surfaces ELSEVIER* chemical flooding of oil reservoirs 4. effects of temperature and pressure on the middle phase solubilization parameters close to optimum flood conditions
- Austad, T., & Taugbol, K. (1995a). *COLLOIDS A AND colloids and surfaces ELSEVIER* chemical flooding of oil reservoirs 1. low tension polymer flood using a polymer gradient in the three-phase region
- Austad, T., & Taugbol, K. (1995b). *COLLOIDS AND SURFACES A . chemical flooding of oil reservoirs dissociative surfactant-polymer interaction with a negative effect on oil recovery*

- Bera, A., Mandal, A., Belhaj, H., & Kumar, T. (2017). Enhanced oil recovery by nonionic surfactants considering micellization, surface, and foaming properties. *Petroleum Science*, 14(2), 362-371. doi:10.1007/s12182-017-0156-3
- Borysenko, A., Clennell, B., Sedev, R., Burgar, I., Ralston, J., Raven, M., . . . Liu, K. (2009). Experimental investigations of the wettability of clays and shales. *Journal of Geophysical Research: Solid Earth*, 114(B7), B07202-n/a. doi:10.1029/2008JB005928
- Buckley, J. S. (2001). Effective wettability of minerals exposed to crude oil. *Current Opinion in Colloid & Interface Science*, 6(3), 191-196. doi:10.1016/S1359-0294(01)00083-8
- Cuiec, L. (1984) SPE 13211 Rock/crude-oil interactions and wettability: An attempt to understand their interrelation.
- Curbelo, F., Garnica, A., & Neto, E. (2013). Salinity effect in cloud point phenomena by nonionic surfactants used in enhanced oil recovery tests. *Petroleum Science and Technology*, 31(15), 1544-1552. doi:10.1080/10916466.2010.547906
- Das, S., Nguyen, Q., Patil, P. D., Yu, W., & Bonnecaze, R. T. (2018). Wettability alteration of calcite by nonionic surfactants. *Langmuir*, 34(36), 10650-10658. doi:10.1021/acs.langmuir.8b02098
- Das, S., Katiyar, A., Rohilla, N., Nguyen, Q., & Bonnecaze, R. T. (2020). Universal scaling of adsorption of nonionic surfactants on carbonates using cloud point

temperatures. *Journal of Colloid and Interface Science*, 577, 431-440.

doi:10.1016/j.jcis.2020.05.063

Das, S., Katiyar, A., Rohilla, N., Nguyen, Q., & Bonnecaze, R. T. (2020). Universal scaling of adsorption of nonionic surfactants on carbonates using cloud point temperatures. *Journal of Colloid and Interface Science*, 577, 431-440.

doi:10.1016/j.jcis.2020.05.063

Dehghanpour, H., Yassin, M. R., & Begum, M. (2016). Source rock wettability: A

Duvernay case study. Paper presented at the doi:10.15530/URTEC-2016-2461732

Retrieved from <https://www.onepetro.org/conference-paper/URTEC-2461732-MS>

Gao, Y., Neeves, K. B., He, K., Bai, B., Ma, Y., Xu, L., . . . Yin, X. (2014). Validating surfactant performance in the eagle ford shale: A correlation between the reservoir-on-a-chip approach and enhanced well productivity. Paper presented at the

doi:10.2118/169147-MS Retrieved from <https://www.onepetro.org/conference-paper/SPE-169147-MS>

Gbadamosi, A., Junin, R., Manan, M., Agi, A., & Yusuff, A. (2019). An overview of

chemical enhanced oil recovery: Recent advances and prospects. *International Nano Letters*, 9(3), 171-202. doi:10.1007/s40089-019-0272-8

Gu, T., Qin, S., & Ma, C. (1989). The effect of electrolytes on the cloud point of mixed solutions of ionic and nonionic surfactants. *Journal of Colloid and Interface*

*Science*, 127(2), 586-588. doi:10.1016/0021-9797(89)90064-7



- Gao, Z., Fan, Y., Hu, Q., Jiang, Z., Cheng, Y., & Xuan, Q. (2019). A review of shale wettability characterization using spontaneous imbibition experiments. *Marine and Petroleum Geology*, *109*, 330-338. doi:10.1016/j.marpetgeo.2019.06.035
- Haagh, M. E. J., Siretanu, I., Duits, M. H. G., & Mugele, F. (2017). Salinity-dependent contact angle alteration in oil/brine/silicate systems: The critical role of divalent cations. *Langmuir*, *33*(14), 3349-3357. doi:10.1021/acs.langmuir.6b04470
- Habibi, A., Esparza, Y., Boluk, Y., & Dehghanpour, H. (2020). Enhancing imbibition oil recovery from tight rocks by mixing nonionic surfactants. *Energy & Fuels*, *34*(10), 12301-12313. doi:10.1021/acs.energyfuels.0c02160
- Hayes, M. E., Bourrel, M., El-Emary, M. M., Schechter, R. S., & Wade, W. H. (1979). Interfacial tension and behavior of nonionic surfactants. *Society of Petroleum Engineers Journal*, *19*(6), 349-356. doi:10.2118/7581-PA
- Hu, Q., Liu, X., Gao, Z., Liu, S., Zhou, W., & Hu, W. (2015). *Pore structure and tracer migration behavior of typical american and chinese shales* Elsevier BV. doi:10.1007/s12182-015-0051-8
- Hu, Y., Sigal, R. F., Devegowda, D., Phan, A., Striolo, A., Ho, T. A., & Civan, F. (2014). Microscopic dynamics of water and hydrocarbon in shale-kerogen pores of potentially mixed wettability. *SPE Journal*, *20*(1), 112-124. doi:10.2118/167234-PA

- Huibers, P., Shah, D. Katritzky, A. (1997). Predicting surfactant cloud point from molecular structure. *Journal of Colloid and Interface Science*, 193, 132-136.
- Kulinič, V. (2015). The influence of wettability on oil recovery. *AGH Drilling, Oil, Gas*, 32(3), 493. doi:10.7494/drill.2015.32.3.493
- Li, J., Bai, D., & Chen, B. (2009). Effects of additives on the cloud points of selected nonionic linear ethoxylated alcohol surfactants. *Colloids and Surfaces. A, Physicochemical and Engineering Aspects*, 346(1), 237-243.  
doi:10.1016/j.colsurfa.2009.06.020
- Loucks, R. G., Reed, R. M., Ruppel, S. C., & Hammes, U. (2012). Spectrum of pore types and networks in mudrocks and a descriptive classification for matrix-related mudrock pores. *AAPG Bulletin*, 96(6), 1071-1098. doi:10.1306/08171111061
- Loucks, R. G., Reed, R. M., Ruppel, S. C., & Jarvie, D. M. (2009). Morphology, genesis, and distribution of nanometer-scale pores in siliceous mudstones of the Mississippian Barnett shale. *Journal of Sedimentary Research*, 79(12), 848-861.  
doi:10.2110/jsr.2009.092
- Long Term Thermal Stability of Chemical EOR Surfactants. (2018). *Spe-190361-ms*
- Milner, J., & Austad, T. (1996a). *COLLOIDS A AND colloids and surfaces ELSEVIER*  
chemical flooding of oil reservoirs 6. evaluation of the mechanism for oil expulsion by spontaneous imbibition of brine with and without surfactant in water-wet, low-permeable, chalk material

Milner, J., & Austad, T. (1996b). *COLLOIDS AND SURFACES ELSEVIER*

chemical flooding of oil reservoirs 7. oil expulsion by spontaneous imbibition of brine with and without surfactant in mixed-wet, low permeability chalk material 1

Mirchi, V., Saraji, S., Akbarabadi, M., Goual, L., & Piri, M. (2017). A systematic study on the impact of surfactant chain length on dynamic interfacial properties in porous media: Implications for enhanced oil recovery. *Industrial & Engineering Chemistry Research*, 56(46), 13677-13695. doi:10.1021/acs.iecr.7b02623

Mirchi, V., Saraji, S., Goual, L., & Piri, M. (2015). Dynamic interfacial tension and wettability of shale in the presence of surfactants at reservoir conditions. *Fuel* (Guildford), 148, 127-138. doi:10.1016/j.fuel.2015.01.077

Moreau, P., Hocine, S., Cuenca, A., Magnan, A., & Tay, A. (2016). An extensive study of the thermal stability of anionic chemical EOR surfactants - part 1 stability in aqueous solutions. Paper presented at the doi:10.2523/IPTC-18974-MS Retrieved from <https://www.onepetro.org/conference-paper/IPTC-18974-MS>

Morsy, S., Gomma, A., Hughes, B., & Sheng, J. J. (2014). *SPE-168985-MS improvement of eagle ford shale formation's water imbibition by mineral dissolution and wettability alteration*

Mazen Ahmed Muherei, & Radzuan Junin. (2008). Mixing effect of anionic and nonionic surfactants on micellization, adsorption and partitioning of nonionic

surfactant *Canadian Center of Science and Education*. Retrieved from <https://agris.fao.org/agris-search/search.do?recordID=#61;AV20120168797>

Nasr-El-Din, H. A., Alotaibi, M. B., & Nasralla, R. A. (2011). Wettability studies using low-salinity water in sandstone reservoirs. *SPE Reservoir Evaluation & Engineering*, 14(6), 713-725. doi:10.2118/149942-PA

Puerto, M. C., & Reed, R. L. (Jan 01, 1982). Three-parameter representation of surfactant-oil-brine interaction. Paper presented at the SPE/DOE 10678 Retrieved from <https://www.osti.gov/biblio/6222287>

Puerto, M., Hirasaki, G. J., & Miller, C. A. (2012). SPE, Shell global solutions international B. V. Surfactant Systems for EOR in High-Temperature, High-Salinity Environments.

Roshan, H., Al-Yaseri, A. Z., Sarmadivaleh, M., & Iglauer, S. (2016). On wettability of shale rocks. *Journal of Colloid and Interface Science*, 475, 104-111. doi:10.1016/j.jcis.2016.04.041

Roshan, H., Ehsani, S., Marjo, C. E., Andersen, M. S., & Acworth, R. I. (2015). Mechanisms of water adsorption into partially saturated fractured shales: An experimental study. *Fuel*, 159, 628-637. doi:10.1016/j.fuel.2015.07.015

Sadaghiana, A. S., & Khan, A. (1991). Clouding of a nonionic surfactant: The effect of added surfactants on the cloud point. *Journal of Colloid and Interface Science*, 144(1), 191-200. doi:10.1016/0021-9797(91)90250-C

Salager, J. (2002) Laboratory of Formulation, Interfaces Rheology and Processes

Universidad De Los Andes Facultad De Ingenieria Escuela De Ingenieria Quimica

Mérida-Venezuela Versión # 2 \*\*\*\*\* FIRP Booklet # E300-A Surfactants

Types and Uses FIRP Booklet # E300-A In English

Salehi, M., Johnson, S. J., & Liang, J. (2008). Mechanistic study of wettability alteration

using surfactants with applications in naturally fractured

reservoirs. *Langmuir*, 24(24), 14099-14107. doi:10.1021/la802464u

Saraji, S., Goual, L., Mirchi, V., & Piri, M. (2014). Dynamic interfacial tensions and

contact angles of surfactant-in-brine/oil/shale systems: Implications to enhanced oil

recovery in shale oil reservoirs. Paper presented at the doi:10.2118/169171-MS

Retrieved from <https://www.onepetro.org/conference-paper/SPE-169171-MS>

Schramm, L. L., Mannhardt, K., & Novosad, J. J. (1991). Electrokinetic properties of

reservoir rock particles. *Colloids and Surfaces*, 55, 309-331. doi:10.1016/0166-

6622(91)80102-T

ShamsiJazeyi, H., Verduzco, R., & Hirasaki, G. J. (2014). Reducing adsorption of

anionic surfactant for enhanced oil recovery: Part I. competitive adsorption

mechanism. *Colloids and Surfaces A: Physicochemical and Engineering*

*Aspects*, 453, 162-167. doi:10.1016/j.colsurfa.2013.10.042

Sharma, K. S., Patil, S. R., & Rakshit, A. K. (2003). Study of the cloud point of C12E<sub>n</sub>

nonionic surfactants: Effect of additives *Elsevier BV*. doi:10.1016/s0927-

7757(03)00012-8

- Sheng, J. J. (2013). Comparison of the effects of wettability alteration and IFT reduction on oil recovery in carbonate reservoirs. *Asia-Pacific Journal of Chemical Engineering*, 8(1), 154-161. doi:10.1002/apj.1640
- Sheng, J. J. (2015). Status of surfactant EOR technology. *Petroleum*, 1(2), 97-105. doi:10.1016/j.petlm.2015.07.003
- Siddiqui, M. A. Q., Ali, S., Fei, H., & Roshan, H. (2018). Current understanding of shale wettability: A review on contact angle measurements. *Earth-Science Reviews*, 181, roshan1-11. doi:10.1016/j.earscirev.2018.04.002
- Siddiqui, M. A. Q., Chen, X., Iglauer, S., & Roshan, H. (2019). A multiscale study on shale wettability: Spontaneous imbibition versus contact angle. *Water Resources Research*, 55(6), 5012-5032. doi:10.1029/2019WR024893
- Singh, R., & Miller, J. (2020) *SPE-200856-MS synergistic surfactant blends for wettability alteration in Wolfcamp and eagle ford shale for improved oil recovery*
- Sondergeld, C., Rai, C., & Tinni, A. (2017). Pore connectivity between different wettability systems in organic-rich shales. *SPE Reservoir Evaluation & Engineering*, 20(4), 1020-1027. doi:10.2118/185948-PA
- Souayah, M., Al-Maamari, R. S., Karimi, M., & Aoudia, M. (2021). Wettability alteration and oil recovery by surfactant-assisted low salinity water in carbonate rock: The impact of nonionic/anionic surfactants. *Journal of Petroleum Science & Engineering*, 197 doi:10.1016/j.petrol.2020.108108

- Standnes, D. C., & Austad, T. (2000a). Wettability alteration in chalk: 1. preparation of core material and oil properties. *Journal of Petroleum Science & Engineering*, 28(3), 111-121. doi:10.1016/S0920-4105(00)00083-8
- Standnes, D. C., & Austad, T. (2000b). Wettability alteration in chalk: 2. mechanism for wettability alteration from oil-wet to water-wet using surfactants. *Journal of Petroleum Science & Engineering*, 28(3), 123-143. doi:10.1016/S0920-4105(00)00084-X
- Takahashi, S., & Kovscek, A. R. (2010). Spontaneous countercurrent imbibition and forced displacement characteristics of low-permeability, siliceous shale rocks. *Journal of Petroleum Science & Engineering*, 71(1), 47-55. doi:10.1016/j.petrol.2010.01.003
- Taugbol, K., Ly, T. V., & Austad, T. (1995). *COLLOIDS AND A SURFACES . chemical flooding of oil reservoirs dissociative surfactant-polymer interaction with a positive effect on oil recovery*
- Tinni, A., Sondergeld, C., & Rai, C. (2017). Pore connectivity between different wettability systems in organic-rich shales. *SPE Reservoir Evaluation & Engineering*, 20(4), 1020-1027. doi:10.2118/185948-PA
- Wang, D., Butler, R., Seright, R., & Zhang, J. (2012). Wettability survey in Bakken shale with surfactant-formulation imbibition. *SPE Reservoir Evaluation & Engineering*, 15(6), 695-705. doi:10.2118/153853-PA

- Wang, Y., Hou, B., Cao, X., Zhang, J., Song, X., Ding, M., & Chen, W. (2018). Interaction between polymer and anionic/nonionic surfactants and its mechanism of enhanced oil recovery. *Journal of Dispersion Science and Technology*, 39(8), 1178-1184. doi:10.1080/01932691.2017.1386112
- Ward, J. S., Morrow, N. R., & Lim, H. T. (1986). Effect of crude-oil-induced wettability changes on oil recovery. *SPE Formation Evaluation*, 1(1), 89-103. doi:10.2118/13215-PA
- Wilson, D., Poindexter, L., & Nguyen, T. (2019) *SPE-193595-MS role of surfactant structures on surfactant-rock adsorption in various rock types*
- Xie, S., Brady, P., Pooryousefy, E., Zhou, D., Liu, Y., & Saeedi, A. (2017). The low salinity effect at high temperatures. doi:10.1016/j.fuel.2017.03.088
- Zhang, R., & Somasundaran, P. (2006). Advances in adsorption of surfactants and their mixtures at solid/solution interfaces. *Advances in Colloid and Interface Science*, 123, 213-229. doi:10.1016/j.cis.2006.07.004
- Zhong, J., Wang, P., Zhang, Y., Yan, Y., Hu, S., & Zhang, J. (2013). Adsorption mechanism of oil components on water-wet mineral surface: A molecular dynamics simulation study. *Energy (Oxford)*, 59, 295-300. doi:10.1016/j.energy.2013.07.016